2013

Genome-Wide Angiotensin Ii Regulated Microrna Expression Profiling ; A Smooth Muscle-Specific Microrna Signature

Jacqueline R. Kemp
Cleveland State University

GENOME-WIDE ANGIOTENSIN II REGULATED MICRORNA EXPRESSION PROFILING: A SMOOTH MUSCLE-SPECIFIC MICRORNA SIGNATURE

JACQUELINE R. KEMP

Bachelor of Science in Biology

John Carroll University

June, 2002

Master of Science in Biology

John Carroll University

August, 2008

Submitted in partial fulfillment of requirement for the degree

DOCTOR OF PHILOSOPHY IN REGULATORY BIOLOGY

at the

CLEVELAND STATE UNIVERSITY

MAY 2013

This dissertation has been approved for

the Department of Biological, Geological, and Environmental Sciences

and for the College of Graduate Studies of Cleveland State University by

_____ Date: _____

Sadashiva S. Karnik, Ph.D., CCF-LRI

Major Advisor

_____ Date: _____

Anton A. Komar, Ph.D., CSU-BGES

Advisory Committee Member

_____ Date: _____

Barsanjit Mazumder, Ph.D., CSU-BGES

Advisory Committee Member

_____ Date: _____

Christine S. Moravec, Ph.D., CCF-LRI

Advisory Committee Member

_____ Date: _____

Girish Shukla, Ph.D., CSU-BGES

Internal Examiner

_____ Date: _____

Edward F. Plow, Ph.D., CCF-LRI

External Examiner

Dedicated to my brother, whose love and encouragement is a constant source of inspiration.

ACKNOWLEDGEMENTS

One of the greatest pleasures of finishing my degree is being given the opportunity to thank those individuals who had a significant impact on my growth and development as a scientist. First and foremost, I would like to extend my sincerest gratitude to my advisor, Dr. Sadashiva Karnik. His constant encouragement and vast knowledge instilled confidence in me throughout my pre-doctoral training. Dr. Karnik's patience and understanding is honorable and his passion for science is contagious. To have been trained by such a distinguished scientist early in my career is gratifying. I am privileged to say that over the past four years, Dr. Karnik has been more than a teacher and a mentor; he has been a friend.

I would also like to thank the members of my Advisory Committee. Dr. Anton A. Komar, Dr. Barsanjit Mazumder, and Dr. Christine S. Moravec were instrumental in the progression of my work. Even though I've had just two committee meetings with them as a whole, their time was invaluable and their ideas were extremely insightful. I would especially like to thank Dr. Moravec, who has always shown a keen interest in my progress and growth.

I would like to thank an additional faculty member of the Department of Molecular Cardiology at CCF who has contributed to my professional development. Dr. Sathyamangala Naga Prasad was always supportive and provided useful advice during each stage of my project and during preparation for my Ph.D. candidacy examination.

In addition, it is imperative that I extend my gratitude to scientists throughout the LRI and CCF. Dr. Peter Faber and the Genomics Core for microarray miRNA expression profiling, Jeanie Jie Na in Quantitative Health Sciences for microarray data processing and statistical analyses, and Dr. Judy Drazba and Dr. John Peters from the Imaging Core for assistance with confocal, phase-contrast, and live cell microscopy. The efforts of each of these individuals allowed my research endeavors to progress in a very sophisticated manner.

Without the camaraderie of the past and present members of the Karnik lab, I would not have thrived. Contributions from each person were influential in sharpening my thinking and expanding my knowledge of various aspects of biology. I would like to take this opportunity to warmly thank Russell Desnoyer, for his willingness to assist me and for his steady reassurance throughout my research. I would also like to graciously acknowledge Dr. Hamiyet Unal, Dr. Kalyan Tirupula, Dr. Rajanapathi Jagannathan, Dr. Arunachal Chatterjee, and Zaira Palomino-Jara for their support and words of advice. Lastly, I must thank Dr. Anushree Bhatnagar and Dr. Hong Yue, whose willingness to guide me in the early stages of my training helped to build my interest in this exploration. Anushree always helped me to look at the 'big picture' in science and taught me many valuable techniques. Both, Anushree and Hong have become dear friends.

Financial support was provided by an assistantship from the Department of Biological, Geological, and Environmental Sciences, Cleveland State University and NIH RO1 grants to Dr. Karnik.

A special thank you goes to Dr. Cyrilla H. Wideman and Dr. Helen M. Murphy, whose enthusiasm for science and constant guidance during my undergraduate and Masters training at John Carroll University pointed me toward a career in research. I was constantly encouraged to aim higher under their supervision and for that I owe my eternal gratitude. Their friendship is something I will always cherish.

I would like to express my love and gratitude to my immediate and extended family for their constant care, prayers, and affection. I would like to thank my father, who is always supportive of my decisions and provides the best dose of humor in times of need. I would also like to recognize my brother, David, for his nurturing advice and unfaltering protection. Words cannot express the appreciation I have for my biggest advocate, my mother. She raised me to be a woman with goals and to have the strength and drive to pursue those goals. Her confidence in me was always enough to walk me through the most difficult times. My life would be inconsequential without her love. Finally, I would like to acknowledge my best friend, Bradley, who gives me the most colorful life imaginable. I will be forever grateful for his compassion, unconditional love, and encouragement to chase my dreams.

GENOME-WIDE ANGIOTENSIN II REGULATED MIRNA EXPRESSION PROFILING: A SMOOTH MUSCLE-SPECIFIC MIRNA SIGNATURE

JACQUELINE R. KEMP

ABSTRACT

Renin-angiotensin system (RAS) activation and phenotypic modulation of vascular smooth muscle cells (VSMCs) are common characteristics associated with human diseases, such as pulmonary hypertension, atherosclerosis and stroke. While elevation of the RAS hormone product, angiotensin II (AngII) is a well-established risk in these diseases; the mechanism of activation of RAS and modulation of VSMC phenotype by AngII is vague, suggesting that novel global regulators may mediate the risk by AngII. MicroRNAs (miRNAs) represent one such class of potential global regulators. MiRNAs are small (~22 nt), endogenous, non-coding RNAs that act as post-transcriptional regulators of physiological processes. MiRNAs primarily function by binding to complementary target sites in the 3'-untranslated regions (3'-UTR) of mRNAs, causing translational repression and/or mRNA destabilization.

To elucidate the global miRNA expression profile following chronic Angiotensin II Type 1 Receptor (AT_1R) activation by AngII, we performed microarray analysis in 23 biological and technical replicates derived from humans, rats and mice. We

pharmacologically distinguished the AT_1R-regulated miRNA profiles by comparing technical replicates treated with the specific AT_1R-blocker, losartan and biological replicates following chronic AT_2R activation by AngII. Thirty-two miRNAs are AngII-regulated universally. Most other miRNAs are regulated in a treatment- or species-specific manner. A few miRNAs are unique to specific cell types.

We have previously shown that a single miRNA can have multiple targets, potentially providing simultaneous regulation of the genes involved in a physiological pathway and accounting for a complex phenotype, such as human heart failure (JBC 284: 27487-27499). In the current study, we explored the extent to which AngII/AT_1R-regulated miRNAs contribute to maintenance of RAS homeostasis and phenotypic modulation of VSMCs. A distinct AngII-regulated miRNA expression pattern emerged in the human and rat VSM cell lines in the profiling experiment, which was validated in our independent samples. Of the 17 miRNAs comprising the VSMC expression pattern, we selected miR-483 as a representative candidate for further study because of its location within the genome and its ability to potentially target multiple components of RAS. In addition, we show evidence that suggests muscle cell-specific expression of miR-483. We incorporated a miR-483 expression cassette into two distinct cell lines as a means to determine post-transcriptional inhibition of specific RAS component gene expression. The functionality of miR-483, in terms of modulating the cellular phenotype, was assessed in a wound-healing assay. Overall, miR-483 regulates both RAS and AngII-activated migration; specifically in VSMCs. Our results further suggest that following inhibition of several AT_1R-activated kinases, the AngII-regulated MEK1 kinase signaling

cascade most effectively mediates the steady state pool of miRNAs, which includes downregulation of mir-483. In this context, JAK2 inhibition is somewhat effective. This results in activation of RAS and switching of the VSMC phenotype associated with pathological states *in vivo*, such as hypertension. Further insight into these mechanisms will be valuable for a greater understanding of AngII biology. In the context of determining the full capacity of RAS as an intrinsic regulatory system, AngII-regulated miRNAs will likely have a strong influence on cardiovascular disease.

TABLE OF CONTENTS

Page

ABSTRACT……viii

NOMENCLATURE……..……xv

LIST OF TABLES…….…..xvii

LIST OF FIGURES……....xviii

CHAPTER I: INTRODUCTION

1.1 The Renin-Angiotensin System……..…….1

1.1.1 The Circulating Axis of RAS.....1

1.1.2 Role of G-Protein Coupled Receptors in Mediating RAS Effects.....5

1.1.3 AngII-induced Pleiotropic Signaling Events: The AngII Receptors.....9

1.1.3.1 The AT_2R……..……...9

1.1.3.2 Significance of the AT_1R……..…13

1.1.4 Consequences of AT_1R Signal Transduction: Tissue RAS Over Activity.....16

1.1.5 Effectiveness of Drugs Targeting the RAS.....20

1.2 Regulation and Characteristics of Vascular Smooth Muscle Cells.....22

1.2.1 The Vascular Smooth Muscle Cell and Its Function…….....22

1.2.2 Modulation of VSMC Phenotype……..……23

1.2.3 AngII-mediated Vascular Damage.....27

1.3 Characteristics of micro-RNAs……..……30

1.3.1 Discovery of miRNAs.....30

1.3.2 Biogenesis and Function of miRNAs.....32

1.3.3 MiRNAs in Human Health and Disease…..……..35

1.3.4 Therapeutic Potential of miRNAs.....37

1.3.5 MiRNAs Targeting RAS Components…..……40

1.3.6 AngII Regulation of Small Ribonucleic Acids.....42

1.4 Significance of Current Work.....43

CHAPTER II: MATERIAL AND METHODS

2.1 Construction of Plasmids.....48

2.2 Cell Culture Maintenance and Transfection.....60

2.3 FACS Analysis.....64

2.4 Immunocytochemistry……..…….66

2.5 Ligand Treatment…….……..68

2.6 Samples for miRNA Profiling…….……..68

2.7 Cardiac Tissue Harvest…….……..…71

2.8 RNA Isolation…….…….…..72

2.9 RNA Processing and Profiling……..…….75

2.10 Statistical Analysis of miRNA Microarray Data……...76

2.11 RT-qPCR Analysis……77

2.12 RNA Solution Hybridization…….....83

2.13 Pharmacological Kinase Inhibition……88

2.14 Protein Isolation and Western Immunoblotting…….....88

2.15 Analysis of ERK1/2 and STAT3 Phosphorylation……89

2.16 MiRNA Target Prediction…….....89

2.17 Luciferase Reporter Assay…….....90

2.18 Analysis of Endogenous RAS Components……..94

2.19 Wound Healing Assay……...94

2.20 Statistical Analysis……97

CHAPTER III: GLOBAL MIRNA EXPRESSION PROFILING

3.1 Introduction……98

3.2 Distinct AngII-regulated miRNA Expression Profiles……..99

3.3 AT_1R Specificity of miRNA Expression…….....114

CHAPTER IV: ANGII-REGULATED MIRNAS

4.1 Introduction……...118

4.2 MiRNAs Regulated Universally by AngII……...119

4.3 MiRNA Signature in Human and Rat VSMCs…….....122

CHAPTER V: REGULATION OF MIRNAS BY ANGII

5.1 Introduction…….131

5.2 Validation of VSMC miRNAs by RT-qPCR……..131

5.3 Modulation of the AngII-regulated VSMC miRNA Pool……..135

CHAPTER VI: MIR-483-3P: A NOVEL ANGII-REGULATED MIRNA

6.1 Introduction……142

6.2 Selection of miR-483-3p for Analysis……...144

CHAPTER VII: EXPRESSION AND FUNCTIONAL ROLE OF MIR-483-3P

7.1 Introduction……154

7.2 Validation of miR-483-3p……....154

7.3 Muscle Cell Lineage Expression of miR-483-3p……158

7.4 Functionality of miR-483-3p……..161

CHAPTER VIII: MODULATION OF VSMC PHENOTYPE

8.1 Introduction……170

8.2 Effects of miR-483-3p on VSMC Migration……172

CHAPTER IX: FUTURE DIRECTIONS

9.1 Comprehensive Description of miR-483-3p……..175

CHAPTER X: DISCUSSION

10.1 The Implications of Genome-wide MiRNA Profiling in Response to AngII……180

10.2 Specificity of MiRNA Expression……181

10.3 A SMC-specific MiRNA Signature……..183

10.4 Regulation of the AngII-induced MiRNA Pool……184

10.5 MiR-483-3p is a Novel AngII-regulated MiRNA……186

10.6 Regulation of the RAS by miR-483-3p……187

10.7 Modulation of VSMC Phenotype……189

10.8 Final Remarks……189

CHAPTER XI: FUTURE DIRECTIONS

11.1 Introduction……192

11.2 Complete Transcriptional Characterization……193

BIBLIOGRAPHY……..195

NOMENCLATURE

3'-UTR, 3'-Untranslated Region

ACE-1, Angiotensin Converting Enzyme 1

ACE-2, Angiotensin Converting Enzyme 2

AGT, Angiotensinogen

AGTR1, Angiotensin II Type 1 Receptor gene

AGTR2, Angiotensin II Type II Receptor gene

ANG I, Angiotensin I

ANGII, Angiotensin II

ARB, Angiotensin Receptor Blocker

AT_1R, Angiotensin II Type 1 Receptor

AT_2R, Angiotensin II Type 2 Receptor

BSA, Bovine Serum Albumin

cAMP, Cyclic Adenosine Monophosphate

CVD, Cardiovascular Disease

DAG, Diacylglycerol

DMEM, Dulbecco's Modified Eagle's Medium

ECM, Extracellular Matrix

ERK, Extracellular Signal Regulated Kinase

GDP, Guanosine Diphosphate

GPCR, G-Protein Coupled Receptor

GTP, Guanosine Triphosphate

HASMC, Human Aortic Smooth Muscle Cell

HF, Heart Failure

IP_3, Inositol Triphosphate

JAK2, Janus Kinase 2

MAPK, Mitogen Activated Protein Kinase

MEK1, Mitogen Activated Protein Kinase Kinase 1

MIR/MIRNA, microRNA

NT, Non-transgenic

PBS, Phosphate Buffered Saline

PCR, Polymerase Chain Reaction

PLC, Phospholipase C

RAS, Renin-Angiotensin System

RASMC, Rat Aortic Smooth Muscle Cell

RT-qPCR, Real Time Quantitative Polymerase Chain Reaction

SDS-PAGE, Sodium Dodecyl Sulfate Polyacrylamide Gel Electrophoresis

SMC, Smooth Muscle Cell

STAT3, Signal Transducer and Activated of Transcription 3

TG, Transgenic

VSMC, Vascular Smooth Muscle Cell

LIST OF TABLES

Page

Table I.I. Differential effects of AngII stimulation of the AT_1 and AT_2 receptors……12

Table I.II. Genes associated with a particular SMC phenotype..……..…….26

Table II.I. Primers used for 3'-UTR amplification……..……..……55

Table II.II. Characteristics of biological and technical replicates utilized in the microarray analysis…….……...…..70

Table II.III. MiRNA-specific primers…….…….….81

Table II.IV. Oligonucleotide primers for mRNA quantitation……..……82

Table III.I. AngII responsive miRNAs in transgenic mouse hearts (C57BL/6)……..…104

Table III.II. AngII responsive miRNAs in transgenic mouse hearts (C3H)……...105

Table III.III. AngII responsive miRNAs in primary HASMC culture……106

Table III.IV. AngII responsive miRNAs in HL-1-AT_1R cell line…..…….107

Table III.V. AngII responsive miRNAs in HEK-AT_1R kidney cell line……..……...107

Table III.VI. AngII responsive miRNAs in immortalized RASM cell line…..……...109

Table III.VII. AngII responsive miRNAs in RASMC-AT_1R cell line…..……..110

Table III.VIII. Human miRNA clusters differentially regulated upon AngII treatment……..112

Table III.IX. Novel miRNAs regulated in response to AT_1R activation by AngII..…...113

Table IV.I. AngII-responsive miRNAs across AT_1R overexpressing model system…..121

Table IV.II. Genomic characteristics of VSMC-specific miRNAs..……..128

Table IV.III. Involvement of VSMC-specific miRNAs in various tissues and disease states…….....……...……..130

LIST OF FIGURES

Page

Figure 1.1. The classical circulating axis of RAS……..……..3

Figure 1.2. Additional RAS components……..……...4

Figure 1.3. Prototypical GPCR activation……..…….8

Figure 1.4. Major AT_1R signal transduction pathways……..……15

Figure 1.5. Effects of tissue RAS over activity……..……...17

Figure 1.6. Characteristics of contractile and synthetic SMCs……..……25

Figure 1.7. Canonical pathway of miRNA biogenesis and modes of action……..…...34

Figure 1.8. Effects of AngII on VSMCs……..……..46

Figure 2.1. Subcloning of HA-AT_1R gene in pcDNA3.1 expression vector……..…...49

Figure 2.2. MiRNA insert for expression construct…..…….……52

Figure 2.3. MiR-483 in pRNA U6.1 expression vector.…….……...53

Figure 2.4. Cloning of 3'-UTRs in psiCHECK-2 expression vector…….…….……...56

Figure 2.5. Nucleotide sequences of 3'-UTRs…….…….…….58

Figure 2.6. FACS analysis of transfected RASMCs……..……65

Figure 2.7. Expression of HA-AT_1R and HA-AT_2R in RASMCs……..……...67

Figure 2.8. Agarose gel fractionation of RNA samples for microarray..……...74

Figure 2.9. miScript principle……..……..80

Figure 2.10. Detection of short RNA molecules by solution hybridization……..……86

Figure 2.11. Principle of luciferase gene expression……..……...92

Figure 2.12. Wound-healing principle and analysis……..……96

Figure 3.1. Measure of AT_1R activation and inhibition……..…….100

Figure 3.2. Heat map depicting miRNA expression across AngII activated samples….103

Figure 3.3. Venn diagrams of miRNAs altered in response to AngII treatment..……...115

Figure 4.1. Pairwise plot of sample comparisons…..……..123

Figure 4.2. Characteristics of VSMC-specific miRNAs……..……125

Figure 5.1. RT-qPCR validation of VSMC miRNAs……..……133

Figure 5.2. Inhibition of AngII-mediated ERK1/2 and STAT3 phosphorylation..……..136

Figure 5.3. Effect of kinase inhibition, iMEK1 and iJAK2, on miRNA levels..…...…..138

Figure 5.4. Mechanism of AngII-induced miRNA regulation……..…...140

Figure 6.1. Volcano plot of VSMC-specific miRNAs……..……..…….145

Figure 6.2. MiR-483-3p target prediction……..……..147

Figure 6.3. IGF2 abundance in VSMCs after AngII treatment……..…..149

Figure 6.4. MiR-483 encoded in intron 2 of IGF2……..…….152

Figure 6.5. MiR-483-3p expression is favored over miR-483-5p expression…….....153

Figure 7.1. Detection of miR-483-3p by solution hybridization……..……...156

Figure 7.2. Quantitation of miR-483-3p by RT-qPCR……..……..157

Figure 7.3. Basal miR-483-3p expression across various cell lines……..……..159

Figure 7.4. MiR-483-3p is undetectable in HEK-AT_1R cells……..……160

Figure 7.5. Stably expressing miR-483-3p in HEK-293T cells…..……162

Figure 7.6. Stably expressing miR-483-3p in RASMC and RASMC-AT_1R cells……..163

Figure 7.7. MiR-483-3p targets components of tissue RAS……..……..165

Figure 7.8. MiR-483-3p alters expression of endogenous AGT and ACE-1……..….166

Figure 7.9. Effect of MEK1 inhibition on endogenous AGT and ACE-1……..…….168

Figure 8.1. Effect of miR-483-3p on VSMC phenotypic switching…..……..171

Figure 8.2. MiR-483-3p decreases AngII-mediated cell migration…..……...173

Figure 9.1. Lentiviral expression system……..……...178

Figure 9.2. Genetic murine models constructed to exhibit increased blood pressure..…179

CHAPTER I

INTRODUCTION

1.1 The Renin-Angiotensin System (RAS)

1.1.1 The Circulating Axis of RAS

The Renin-Angiotensin System (RAS) has been a key target for the management of cardiac and vascular abnormalities since its discovery and has been found to be increasingly complex. RAS is an elaborate endocrine system that globally regulates numerous physiological processes, such as blood pressure maintenance, electrolyte/volume homeostasis, vascular tone, facilitation of catecholamine release (e.g., epinephrine and norepinephrine) from the brain and aldosterone release from the adrenal gland. Increasing evidence has pointed to a role for Angiotensin II (AngII), the major bioactive product of RAS, in disease states (Aplin et al., 2008, Taubman, 2003, Forbes, 2011). AngII has the capability to induce numerous intracellular signaling events that can ultimately lead to global gene expression changes and pathological conditions, including hypertension, heart failure (HF), renal and inflammatory diseases (Teerlink, 1996).

The classical, circulating axis of RAS is activated in response to decreased plasma sodium and fluid volume, resulting in the secretion of renin from the juxtaglomerular cells of the kidney. The enzyme renin releases the N-terminal decapeptide angiotensin I (Ang I) from a liver-produced serpin, angiotensinogen (AGT), by proteolytic cleavage. Angiotensin converting enzyme-1 (ACE-1), abundant in the endothelial lumen of the pulmonary microvasculature, hydrolyzes the C-terminal dipeptide to produce the octapeptide hormone, AngII (Figure 1.1) (Lavoie and Sigmund, 2003, Teerlink, 1996). AngII then interacts with specific receptors on the plasma membrane to elicit a cellular response. The physiological importance of AngII cannot be overstated. The biological result of circulating AngII is widespread and diverse, giving the system an endocrine characteristic. Notably, AngII is also formed by an alternative pathway, in which chymase, a serine protease highly expressed in the heart, vasculature, and kidney in humans, is capable of local AngII production from its precursor Ang I (Forbes, 2011).

AngII has a short half-life in circulation; therefore, the peptide hormone is readily cleaved by amino- and carboxy- peptidases, resulting in production of additional angiotensin peptides (e.g., Ang III, Ang^{3-8}, Ang IV, Ang^{1-7}) (Figure 1.2) (Forbes, 2011). Each of the angiotensin metabolites exerts biological effects, some of which are distinct from the functions of AngII (Lavoie and Sigmund, 2003).

Figure 1.1. The classical circulating axis of RAS. Decreased blood pressure stimulates the release of renin from the kidney. Renin cleaves angiotensinogen to produce Ang I, which is in turn cleaved by ACE-1 to produce AngII. AngII is the major bioactive product of RAS, regulating blood pressure through vasoconstriction and stimulation of aldosterone and vasopressin release. AngII is capable of giving rise to pathological conditions such as cardiac and vascular hypertrophy and end-organ damage.

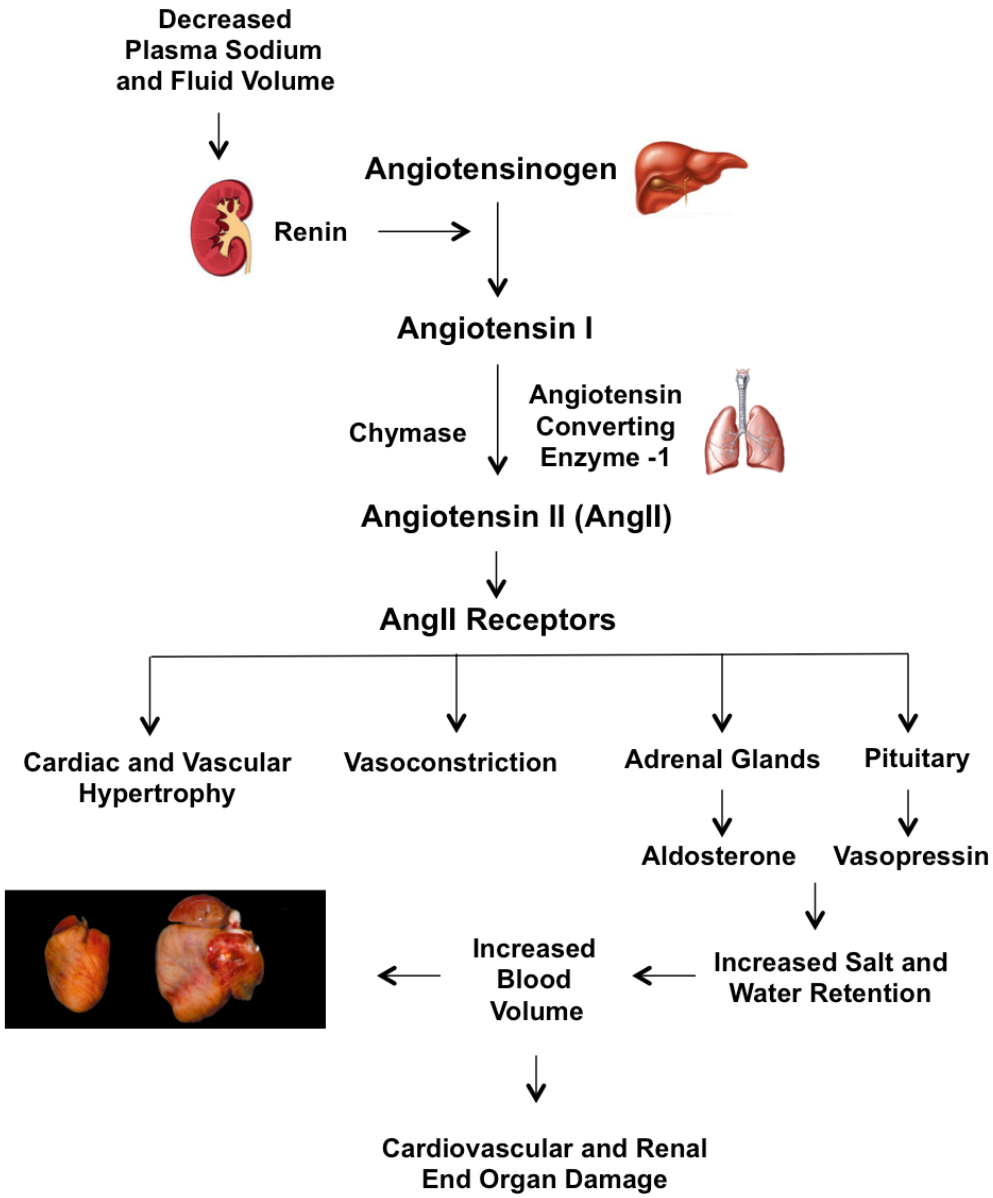

Figure 1.2. Additional RAS components. The peptide hormone, AngII can be readily cleaved, resulting in the production of additional angiotensin peptides (shown in red). The angiotensin peptides exert distinct biological effects. Adapted from (Hunyady and Catt, 2006).

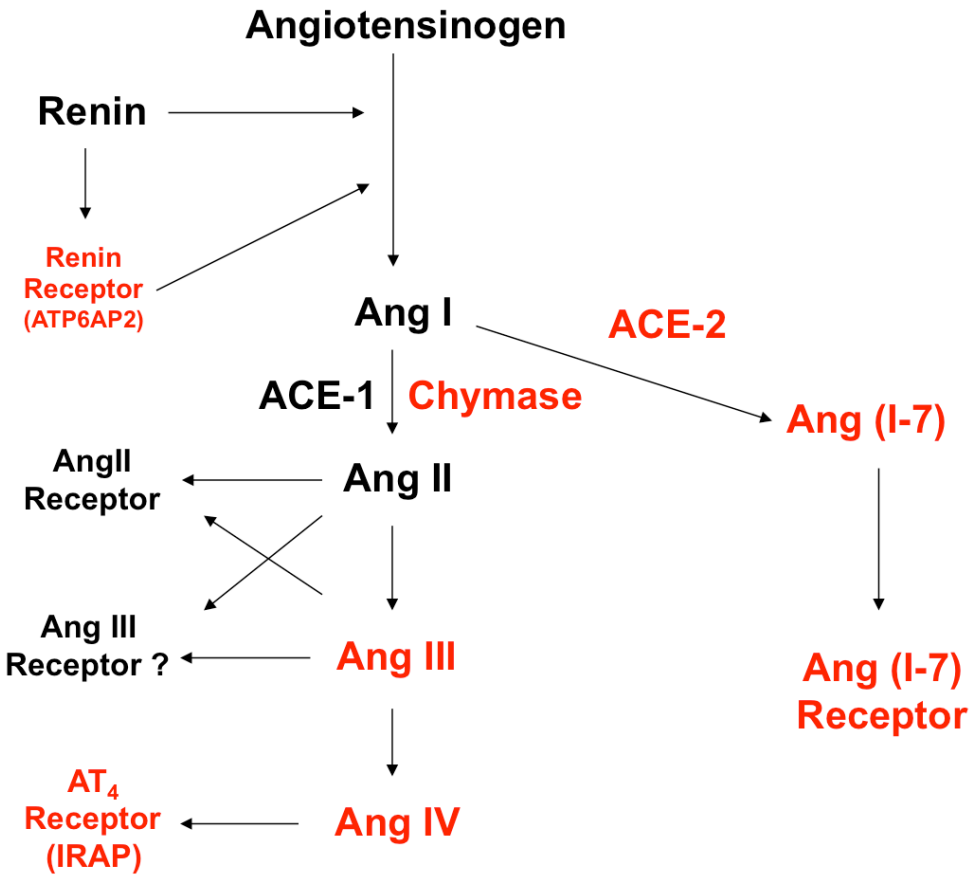

For example, a homolog of ACE-1, ACE-2, was discovered and shown to degrade AngII, yielding Ang^{1-7} and leading to activation of a second major axis of RAS, the ACE-2/Ang^{1-7}/Ang^{1-7} Receptor axis (Zhang et al., 2010, Santos et al., 2003). This axis has been proposed to have a vasoprotective role in pathophysiology of the cardiovascular, renal, pulmonary, and central nervous systems and is considered counter-regulatory to the classical circulating axis (Zhang et al., 2010, Santos et al., 2003). Furthermore, a protein has recently been discovered, which binds and activates renin in tissues, the renin receptor. The physiological role of these new RAS components is not completely resolved, but they may exert considerable impact on local AngII generation and effect mediation in tissues (Bader et al., 2001).

1.1.2 Role of G-Protein Coupled Receptors (GPCRs) in Mediating RAS Effects

AngII affects various cell systems by binding to seven-transmembrane, cell surface, GPCRs (Mehta and Griendling, 2007). GPCRs constitute a vast integral membrane protein family that encompasses a wide-range of functions; therefore, they are divided into classes, of which the rhodopsin-like family accounts for nearly 85% of the GPCR genes (Rosenbaum et al., 2009). The AngII receptors are included within the rhodopsin-like family and are a member of the subgroup of peptide receptors. The characteristic feature of the rhodopsin family is the presence of conserved amino acid sequences that suggest common structural features and activation mechanisms.

GPCRs are the largest family of cell surface receptors, having a major role in signal transduction. They mediate responses to extracellular ligands by binding,

facilitating a conformational change in the receptor, and activating intracellular heterotrimeric G-proteins (Karnik et al., 2003, Rosenbaum et al., 2009). The GPCR activates the intracellular G-protein by facilitating the exchange of bound GDP for GTP. In so doing, the G-protein's α subunit, together with the GTP, can dissociate from the β and γ subunits to elicit activation of effectors such as adenylyl cyclase and phospholipases, which in turn changes the levels of intracellular second messengers, such as calcium and cAMP (Figure 1.3) (Pierce et al., 2002). In addition to the canonical signaling events initiated by G-protein signaling, studies have also shown alternative signaling pathways that are related to diverse functions of these receptors. GPCRs, for example, can also signal in a G-protein-independent manner, which leads to activation of mitogen activated protein kinases (MAPKs) (Miura et al., 2004). Numerous G proteins exist, including $G_{\alpha s}$, $G_{\alpha i/o}$, $G_{\alpha q/11}$, and $G_{\alpha 12/13}$. Each of these G proteins causes distinct functional consequences within the cell, due to the varying subunits present (Karnik et al., 2003, Rosenbaum et al., 2009).

A common feature of GPCRs is that they exhibit a degree of basal activity in the absence of an agonist, which can be reduced in the presence of an inverse agonist. Agonists are ligands that fully activate the receptor beyond the basal level. Conversely, antagonists compete with other ligands without affecting the basal activity (Kobilka, 2007). GPCRs transmit extracellular signals across the cell membrane as a response to a wide variety of ligands, including hormones, ions, neurotransmitters, proteins/peptides, fatty acids, small molecules, and physical stimuli such as light, smell, taste, and

mechanical stretch (Rosenbaum et al., 2009). Thus, GPCRs are extremely relevant in cell signaling, pharmacology, physiology, and pathophysiology.

Due to their involvement in many biological functions, GPCRs are also extremely important in drug discovery. Nearly 50% of all modern human therapeutics is targeted to only a few GPCRs. Understanding the full capacity of GPCR signaling in physiology and pathophysiology is a critical aspect of receptor biology.

Figure 1.3. Prototypical GPCR activation. Upon activation of a GPCR, the GDP of the G-protein is exchanged with GTP, resulting in dissociation of the α and βγ subunits of the heterotrimeric protein. The dissociated subunits further activate intracellular downstream effectors, which in turn alter the levels of second messengers.

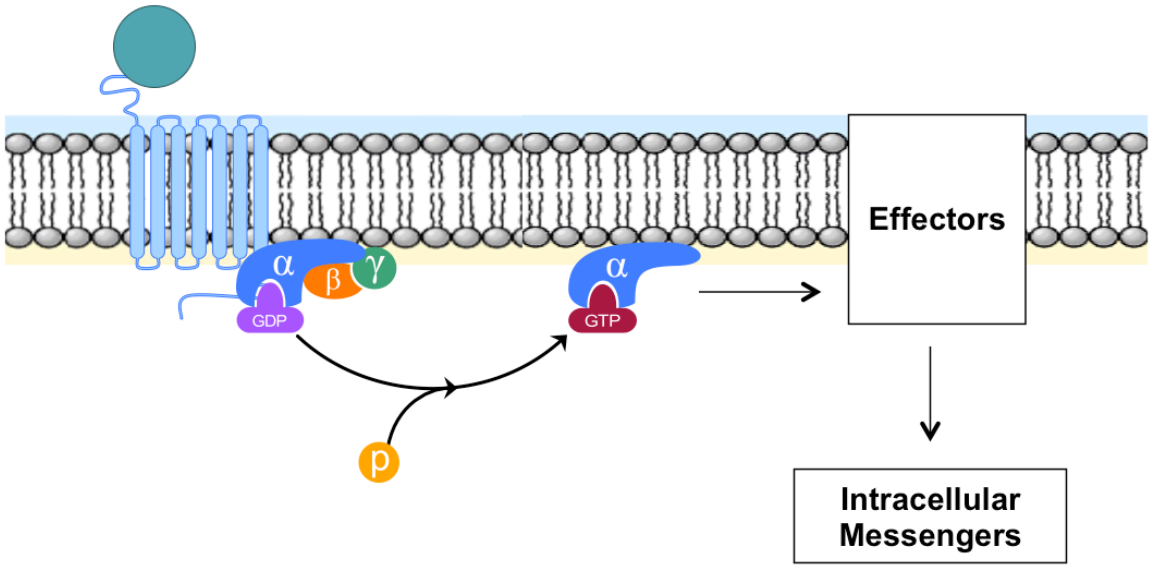

1.1.3 AngII-induced Pleiotropic Signaling Events: The AngII Receptors

AngII functions as a master regulator of cardiovascular and renal system homeostasis. As its name implies, the net effect of AngII action is a potent constriction of vessels in most vascular beds (Aplin et al., 2008, Taubman, 2003, Touyz and Schiffrin, 2000). In recent years, AngII has been shown to play a pivotal role in mediating cell proliferation and/or apoptosis and fibrosis through activation of intracellular signaling molecules in a variety of cell types, including cardiac myocytes, fibroblasts, renal mesangial and epithelial cells, endothelial cells (ECs), and vascular smooth muscle cells (VSMCs) (Bell and Madri, 1990, Kim and Iwao, 2000, Lijnen and Petrov, 1999, Ohtsu et al., 2006).

AngII elicits many diverse physiological effects in various tissues due to 1) its ability to bind to different receptor subtypes; 2) receptor coupling to distinct second messenger pathways; and 3) tissue specificity of the receptor subtypes (Berk, 2003). Cellular responses to AngII are dependent on two pharmacologically distinct GPCR subtypes, the Angiotensin II Type 1 Receptor (AT_1R) and the Angiotensin II Type 2 Receptor (AT_2R), both of which have similar affinity for the agonist, AngII (Aplin et al., 2008, de Gasparo et al., 2000, Hunyady and Catt, 2006, Miura and Karnik, 1999).

1.1.3.1 The AT_2R

The AT_2 receptor subtype shares approximately 34% sequence homology with the AT_1R, but unlike its RAS counterpart, the precise role of the AT_2R is debatable. The gene for the AT_2R is located on the X chromosome within exon 3 of the AGTR2 gene

and is approximately 50 Kb. While the signaling mechanisms induced by activation of the AT_2R remain poorly understood, it is known that the type 2 receptor is abundantly expressed in the developing fetus, owing to a role in physiological development. The AT_2R is expressed at low levels in the normal adult cardiovascular system, but it may increase in density in tissues under pathological conditions, in which inflammation and tissue remodeling occur (e.g., myocardial infarction, hypertension, atherosclerosis, diabetes mellitus, neointima formation after vascular injury) (Lemarie and Schiffrin, 2010, Booz and Baker, 1996). The proposed increase in AT_2R expression during pathology can be viewed as fetal gene-reactivation, which is a prominent feature of the disease state of the cardiovascular system (Paul et al., 2006).

Many studies have suggested that the AT_2R is constitutively active and does not require binding of AngII to induce intracellular signaling cascades. For example, Miura and Karnik found that overexpression of the AT_2R alone determined whether cultured fibroblasts, epithelial, or VSMCs underwent apoptosis in the absence of AngII (Miura and Karnik, 2000). The AT_2R has been implicated in cardiovascular disease as a beneficial moiety due to its proposed vasodilatory role, ability to inhibit cell growth, induce apoptosis, and inhibit activation of mitogen activated protein kinases (MAPKs) – functions that appear to counterbalance the actions of the AT_1R (Table I.I) (Miura et al., 2010, Berk, 2003). Three main events have been described for the function of the AT_2R in signal transduction: 1) phosphatase activation causing protein dephosphorylation; 2) activation of the bradykinin/nitric oxide/cGMP pathway; and 3) stimulation of phospholipase A_2 and release of arachidonic acid (Blume et al., 2001, Matsubara, 1998).

The AT_2R-selective antagonists, PD123319 and PD123177, are capable of inhibiting these signaling events by displacing the receptor's agonist (Gallinat et al., 2000, Verdonk et al., 2012).

Table I.I. Differential effects of AngII stimulation of the AT_1 and AT_2 receptors. Adapted from (Silverstein and Ram, 2005).

AT_1 Receptor Stimulation
Increased vasoconstriction
Increased cardiac contractility and hypertrophy
Increased vascular smooth muscle proliferation
Increased extracellular matrix production
Increased tubular sodium reabsorption
Increased synthesis and secretion of aldosterone
Increased secretion of vasopressin
Increased noradrenergic activity
Cell growth and proliferation
AT_2 Receptor Stimulation
Regulation of:
Cell growth and proliferation
Cell differentiation
Extracellular matrix composition
Left-ventricular remodeling
Fetal tissue development
Apoptosis
Vasodilation
Antiproliferation
Increased neuronal regeneration

1.1.3.2 Significance of the AT_1R

The human AT_1R (hAT_1R) is ubiquitously expressed in the cardiovascular system and mediates the major cardiovascular effects of AngII (Dinh et al., 2001) (de Gasparo et al., 2000). The gene for the hAT_1R (AGTR1) is approximately 50 Kb in size and located within exon 5 on chromosome 3 in the genome (de Gasparo et al., 2000, Elton and Martin, 2007). A prototypical GPCR, the AT_1R has been characterized by molecular cloning, mutagenesis, and molecular pharmacology studies to be functionally activated upon high-affinity AngII binding and shown to rapidly undergo desensitization and internalization (Elton and Martin, 2007).

Under normal conditions, AngII activated AT_1R generates acute responses by coupling to the Gq-PLC pathway, leading to production of the second messengers, inositol 1,4,5-triphosphate (IP_3) and diacylglycerol (DAG). Production of IP_3 and DAG leads to Ca^{2+} mobilization and activation of protein kinase C (PKC), respectively (Mehta and Griendling, 2007, Hunyady and Catt, 2006). AT_1R activation is associated with a rapid increase in tyrosine phosphorylation of various signaling molecules (Yin et al., 2003). Phosphorylation leads to induction of growth-promoting signals such as mitogen-activated protein kinase (MAPK)/extracellular signal-related kinase (ERK), phosphatidylinositol 3-kinase/Akt, and JAK-STAT signaling (Saito and Berk, 2002). These cytoplasmic signaling cascades ultimately propagate to the nucleus upon chronic AT_1R activation. In the nucleus, gene expression is either induced or repressed by distinct transcription factors (e.g., NFAT, MEF2, GATA, and STAT), following binding to response elements in the promoters of genes (Figure 1.4) (Hunyady and Catt, 2006,

Saito and Berk, 2002, Friddle et al., 2000). Additionally, Gβγ, through interaction with histones and transcription factors, modulates transcription in response to AT_1R activation in cells (Bhatnagar et al., 2013). The pleiotropic signaling events that occur in response to AngII and result in changes in gene expression of a set of AngII responsive genes are ultimately responsible for phenotypic modulation of target cells (Hunyady and Catt, 2006).

Figure 1.4. Major AT_1R signal transduction pathways. Binding of AngII to the AT_1R activates the Gq-coupled signaling pathway, leading to activation of PLC, which results in mobilization of Ca^{2+}. AT_1R activation leads to phosphorylation of multiple signaling pathways and induction of growth-promoting signals.

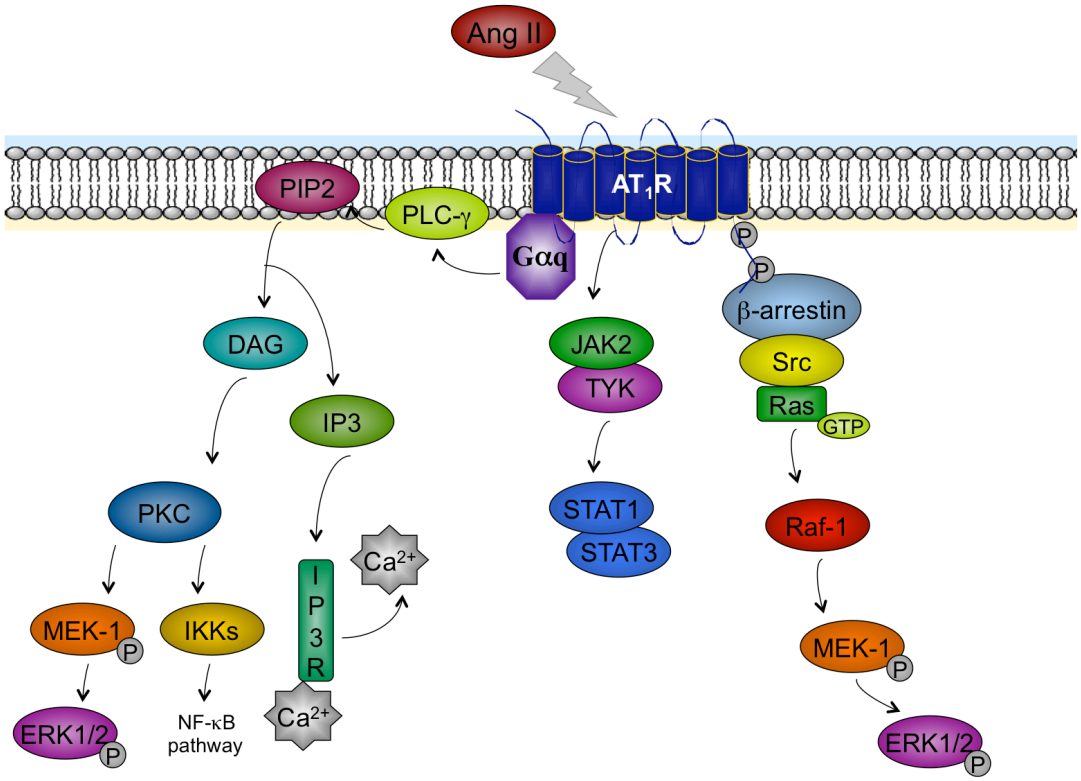

1.1.4 Consequences of AT_1R Signal Transduction: Tissue RAS Over Activity

In addition to systemic RAS, the components of RAS with the exception of renin are also expressed at variable levels throughout tissues, including the brain, heart, vasculature, pancreas, adipocytes and kidneys, allowing for local production of AngII peptides (Bader et al., 2001, Paul et al., 2006). Tissue RAS regulates long-term and chronic responses to locally produced AngII in these tissues, thus, implicating AngII in the progression of development and growth, regulation of metabolic pathways, learning and memory. Importantly, tissue RAS primarily functions independently of circulating RAS; therefore, it has a critical role in pathophysiological conditions, acting as a paracrine or autocrine system (Bader et al., 2001, Nakashima et al., 2006). These conditions include inflammation, oxidative stress, hypertension, thrombosis, end-stage renal disease, coronary artery disease, cardiovascular hypertrophy and HF (Figure 1.6) (Daugherty and Cassis, 2004, Margulies et al., 2009, Mehta and Griendling, 2007). As a result, fine control mechanisms regulating the effectiveness of tissue RAS is a major research frontier.

Figure 1.5. Effects of tissue RAS over activity. The components of RAS are expressed at variable levels through many major tissue types. This leads to local production of AngII and progression of pathophysiological conditions.

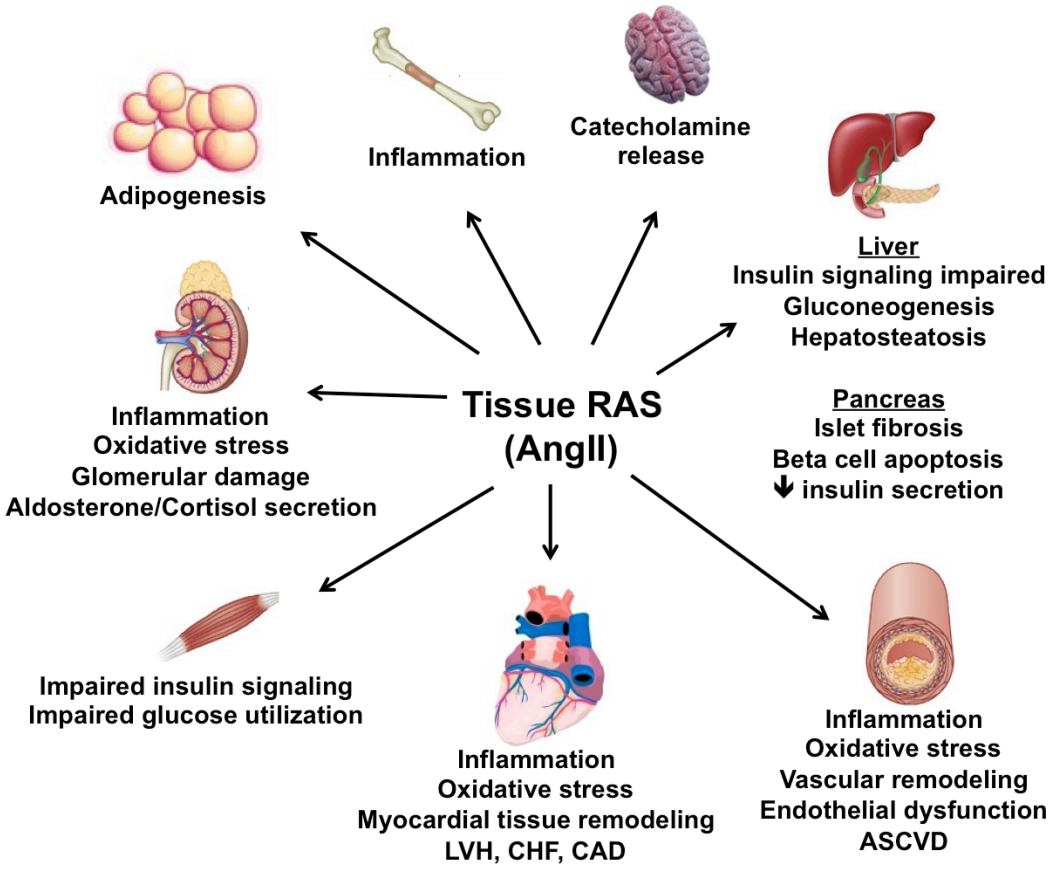

Genomic and proteomic advances have established that GPCRs regulate global gene expression programs, leading to processes such as differentiation, proliferation, and apoptosis in a variety of cell types (Karnik et al., 2003, Rosenbaum et al., 2009). Two main cell types directly and adversely affected by an increase in local AngII action are VSMCs and ECs due to the high density of AT_1 receptors present within these cells. Ultimately, tissue RAS contributes to the maintenance of cardiovascular homeostasis by the impact on vessel function mediated through the AT_1R. Extensive research into the precise signal transduction mechanisms that are critical for modulation of EC and VSMC phenotype and function are important to fully characterize the molecular effects of AngII. In particular, animal models as well as cellular studies have sought to examine the effects of AngII as a mediator of the development of vascular diseases.

Cardiac fibroblasts and myocytes are additional cell types that express AT_1 receptors. AngII was found to exhibit growth-promoting effects in the heart more than 30 years ago. Furthermore, in the heart, these effects were thought to be most relevant by inducing hypertrophy and fibrosis (Bader and Ganten, 2008). The results of animal studies, including the angiotensin type 1 receptor gene (*Agtr1*)-null mice (Oliverio et al., 1998), tissue targeted AT_1R transgenic (TG) mice (Paradis, 2000), and gain of function AT_1R mutant knock-in mice (Billet et al., 2007), indicate that the AT_1R mediates hypertrophic and proliferative effects of AngII. The AT_1R is an AngII-activated growth promoter in tissues and indeed overexpression of AT_1R correlates with a higher risk for cardiac hypertrophy, vascular thickening and ultimately tissue fibrosis. A hallmark of pathogenesis of human cardiovascular disease (CVD) is the overexpression of the AT_1R

and most CVDs respond favorably to therapy with AT_1R-selective drugs (Aplin et al., 2008).

It has become increasingly clear that tissue RAS is not an isolated entity, but can interact with circulating RAS as well as other peptide systems on multiple levels. In response to either systemically or locally generated AngII, the AT_1R mediates the contractile response of VSMCs by PLC-dependent mechanisms leading to an increase in intracellular calcium. It also functions indirectly, by stimulating the synthesis of other vasoconstrictors. At the cellular level, the endothelium dysfunction that occurs in response to AngII is primarily due to an increase in adhesion, migration, and proliferation of ECs. In the presence of AngII, there is increased expression of the vasoconstrictor, endothelin, which can act to potentiate the action of PDGF (Rossi et al., 1999). Moreover, using an animal model overexpressing the AT_1 receptor only in endothelial cells, Ramchandran et al. demonstrated that AngII also acts as a vasodilator, when interacting with the AT_1R on these cells (Ramchandran et al., 2006). AngII promoted tissue factor and initiator of coagulation expression, both of which could lead to a coagulant property of AngII (Taubman, 2003, Touyz and Schiffrin, 2000).

The global mRNA expression regulated by the AT_1R (transcriptome) is a persistent response of AT_1R signaling that is widely studied in both physiological and pathological settings. That is, if the activity of the AT_1R is not properly regulated, AngII stimulus becomes chronic and can damage the tissue, as well as contribute to lasting cardiovascular disorders. The long-term research aim in this area is to elucidate how normal gene regulatory mechanisms are altered in response to over activity of the RAS in

different pathological settings. Typical transcriptional regulatory mechanisms are significantly altered in the experimental models. In a recent study, Yue *et al.* discovered that chronic AT_1R activation mediates gene expression through U-STAT3 by a mechanism distinct from that of physiological regulator phospho-STAT3. This accounts for a dual role of STAT3 in regulating physiological and pathological gene expression programs (Yue et al., 2010). Yue *et al.* discovered nuclear accumulation of unphosphorylated STAT3 (U-STAT3) which activates "renegade" transcription of genes such as osteopontin (OPN), connective tissue growth factor (CTGF), regulator of G protein signaling 2 (RGS2), and alpha-1 skeletal muscle actin, leading to hypertrophy and HF in mice (Yue et al., 2010). This study suggested that chronic AngII/AT_1R signaling might alter the structure and dynamics of chromatin in target cell nuclei, such that latent regulatory sites on promoters of genes may be rendered potent for promoting overexpression (Yue et al., 2010).

Ultimately, the physiological role of this local system is the maintenance of homeostasis at the tissue level. The local generation of AngII has been demonstrated for all tissues relevant for cardiovascular control (Bader and Ganten, 2008). Tissue RAS plays an important role in conveying and amplifying the effects of circulating AngII, thereby modulating cardiovascular parameters and mostly accelerating the pathogenesis of cardiovascular diseases. Overall, tissue RAS forms the basis for the understanding of the extraordinary therapeutic efficiency of drugs inhibiting the RAS.

1.1.5 Effectiveness of Drugs Targeting the RAS

The RAS has been a therapeutic target for cardiovascular diseases for decades. Drugs targeting significant components of circulating RAS, such as ACE inhibitors and antagonists for the AT_1 receptor can effectively lower blood pressure and RAS-induced pathologies. Very recently, inhibitors of the enzyme renin were also approved for clinical use (Staessen et al., 2006). The efficiency of these drugs is partially based on the fact that they not only inhibit the classical RAS in the circulation, but also local RAS in tissues (Bader and Ganten, 2008).

ACE inhibitors compete with Ang I binding, preventing AngII formation mediated by ACE-1 in the circulation and tissues (Doulton et al., 2005). The beneficial effects of these pharmacologically distinct agents extend to the nonhemodynamic functions of RAS, which suggests that RAS blockade is an overall effective means for organ protection, not merely for blood pressure reduction. These therapeutic agents have been used in the treatment of renal, cardiovascular, and cerebrovascular diseases, showing that RAS has a global biological effect within the body (Doulton et al., 2005, Miura et al., 2011).

An additional treatment option for controlling RAS is the use of AT_1R-selective drugs (i.e., AT_1R blockers [ARBs]), which halt or reverse the pathological vascular remodeling and cardiac dysfunction that occur in response to over activity of AngII at the molecular level (Aplin et al., 2008, Burnier, 2001, Miura et al., 2011). This suggests that the AT_1R contributes to phenotypic changes at the cellular level *in vivo* (de Gasparo et al., 2000, Hunyady and Catt, 2006). ARBs, a widely used class of anti-hypertensive

drugs, are well tolerated with fewer side effects than ACE inhibitors. Irrespective of whether AngII is generated systemically or by non-ACE mediated pathways, ARBs specifically block AngII binding to the AT_1R, and thereby target AT_1R-regulated gene expression changes (Miura et al., 2011). Several ARBs available for the treatment of RAS associated disorders are losartan and candesartan, for treatment of hypertension and hypertrophy, irbesartan, for treatment of diabetic nephropathy, and valsartan, for treatment of heart failure in people who cannot tolerate ACE inhibitors (Silverstein and Ram, 2005).

1.2 Regulation and Characteristics of Vascular Smooth Muscle Cells

1.2.1 The Vascular Smooth Muscle Cell (VSMC) and Its Function

Lying within the tunica media of blood vessels, smooth muscle cells (SMCs) are essential for accurate performance of the vasculature. By contraction and relaxation, these specialized cells alter the luminal diameter, which allows blood vessels to maintain a homeostatic blood pressure (Rensen et al., 2007). VSMCs are innervated primarily by the sympathetic nervous system through adrenergic receptors. Activation of α-adrenergic receptors causes vasoconstriction, while activation of β-adrenergic receptors causes vasodilation. In addition, within seconds to minutes of binding to AT_1Rs, AngII causes Ca^{2+} mobilization from the sarcoplasmic reticulum and promotes the interaction of actin and myosin filaments to allow for contraction of cells. Excessive vasoconstriction leads to hypertension, whereas excessive vasodilation leads to hypotension. Notably, due to

their function of carrying blood away from the heart to all other organs and tissues, arteries have a great deal more smooth muscle than veins.

VSMCs perform additional functions, which become important during physiological conditions, or following vascular injury. In these cases, VSMCs will synthesize increased amounts of extracellular matrix (ECM) components and exhibit increased rates of migration and proliferation. Due to these characteristics, VSMCs are a prime candidate for both short-term regulation of vessel diameter, and also for long-term adaptation, involving vessel remodeling and changes in cell number (Rensen et al., 2007, Gabbiani et al., 1981).

1.2.2 Modulation of VSMC Phenotype

The different functions that VSMCs exert are translated into distinct morphologies, expression of SMC-specific genes, and varying degrees of proliferative and migratory potential (Rensen et al., 2007). When the prime function of a VSMC is contraction, the cytoplasm is filled with myofilaments, and when it is repair (synthesis of matrix and/or cell division), the morphology changes to fit the altered functional demand (Figure 1.5). Contractile SMCs are elongated, spindle-shaped cells with many contractile filaments throughout the cytoplasm of the cell. Synthetic SMCs exhibit cobblestone morphology and contain a high number of organelles necessary for protein synthesis.

VSMCs undergo reversible phenotypic switching from a quiescent, contractile phenotype, in which cells have a unique repertoire of filamentous proteins (e.g., α-

smooth muscle actin and smooth muscle-myosin heavy chain), agonist-specific receptors and signaling molecules necessary for contraction to a synthetic state where cells exhibit poor contractibility, changes in lipid metabolism and high production of ECM components (Bell and Madri, 1990). In general, synthetic SMCs exhibit higher migratory potential and proliferative rates than contractile SMCs. SMCs with different phenotypes typically express varying levels of marker proteins, rather than completely different marker proteins (Table I.II.) (Rensen et al., 2007).

Figure 1.6. Characteristics of contractile and synthetic SMCs. Contractile SMCs are elongated, spindle-shaped cells, whereas synthetic SMCs are less elongated and have cobblestone morphology. From (Rensen et al., 2007).

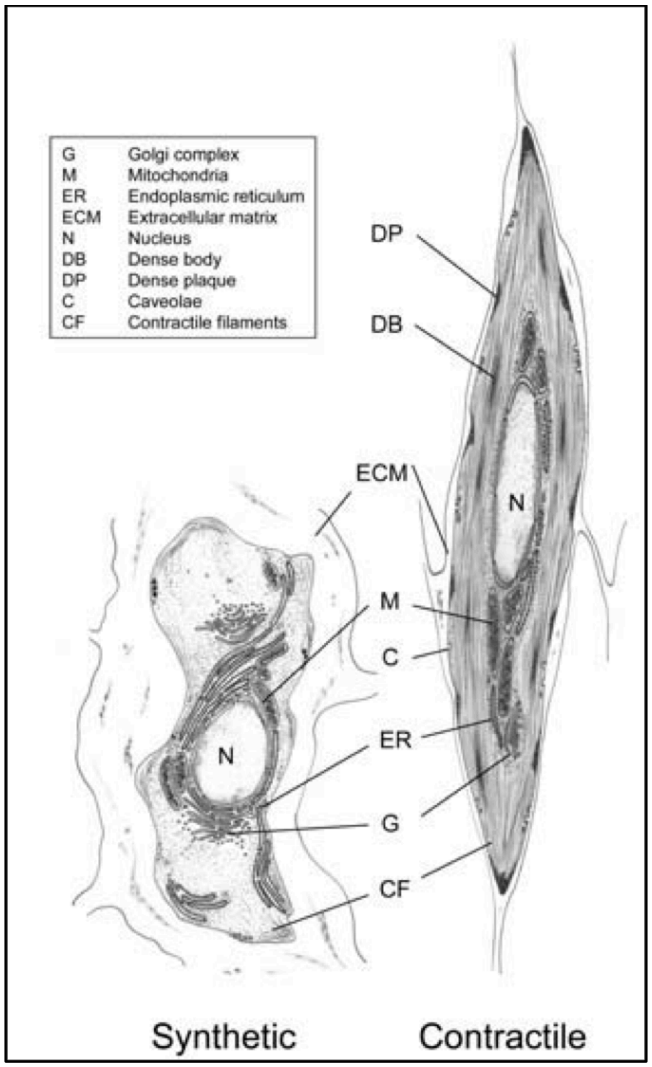

Table I.II. Genes associated with a particular SMC phenotype.

Marker Protein	Phenotype Specificity
α1 integrin, β1 integrin, α7 integrin, Myocardin, N-/T-cadherin	C > S
α-SMA, γ-SMA	C > S
Desmin	C > S
SM22α	C > S
ACLP, APEG-1, CRP-2	C
SM-calponin, h-caldesmon, meta-vinculin	C > S, C, C > S
SM-MHC, Smoothelin	C > S, C
CRBP-1, Smemb	S > C
PDGF-A, ICAM-1, MGP	S
I-caldesmon	S
OPN	S > C
Collagen I, Moesin, Collagenase IV, Connexin43, MMP isoforms, Syndecan-1/-4	S > C

Currently, two marker proteins that provide the best definition of a mature contractile SMC phenotype are SM-MHC and smoothelin. In humans and rodents, respectively, Smemb/non-muscle MHC isoform-B and CRBP-1 represent suitable synthetic SMC markers, since these proteins are quickly and markedly upregulated in proliferating SMCs (Rensen et al., 2007).

The remarkable ability of VSMCs to shuttle between phenotypes is not unique to this cell type. However, modulation of the VSMC phenotype is the best example of this physiological phenomenon due to the ability of the cell to constantly maintain its contractile capability. This is because there are many intermediates between the two extreme ends of VSMC morphology (i.e., synthetic and contractile states) that can occur. When a fibroblast, for example, undergoes differentiation and switches to a myofibroblast, the process is irreversible (Misra et al., 2010). That is, the myofibroblast cannot switch back to a fibroblast or the synthetic phenotype.

AngII affects virtually all vascular cells (e.g., endothelial cells, SMCs, fibroblasts, monocytes/macrophages, and cardiac myocytes), and thus, is critical in disease development. Changes in the phenotype and morphology of these cells, variable gene expression, and enhanced responsiveness to stimuli lead to vascular pathology.

1.2.3 AngII-mediated Vascular Damage

As a growth factor, AngII regulates VSMC survival, growth, and hypertrophy. In particular, activation of RAS is a highly effective and selective stimulus for the

differentiation of quiescent VSMCs into the metabolically active, proliferative and migratory phenotype (Ohtsu et al., 2006, Touyz and Schiffrin, 2000, Bell and Madri, 1990). Evidence points to AngII being directly involved in pathological disease states, which are related to VSMC growth and vessel wall integrity, such as hypertension, atherosclerosis, diabetes, cardiac remodeling, asthma, aneurysm formation, and inflammatory responses to vessel injury (Daugherty and Cassis, 2004, Kim and Iwao, 2000, Hunyady and Catt, 2006).

AT_1 receptors are highly abundant in VSMCs. AngII is known to promote its effects in VSMCs by acting directly through the AT_1R, indirectly through the release of other factors, and possibly through cross-talk with intracellular signaling pathways of other growth factors (Touyz and Schiffrin, 2000).

Besides VSMC contraction, AT_1R-mediated pathways also activate various downstream proteins that further enhance growth, adhesion, and migration related signaling. Upon induction of intracellular signaling cascades in VSMCs, AngII activates the AT_1R and consequently various protein kinases (e.g., receptor or non-receptor tyrosine kinases). Cellular protein synthesis and metabolism, transport, volume regulation, gene expression, and growth all depend on MAPKs (Mehta and Griendling, 2007). AngII mediates cell survival via p38/MAPKAPK-2, and PDK 1/Akt. Cell growth and hypertrophy are mediated by AngII-mediated MAP kinases (e.g., p38MAPK, ERK1/2 and JNK, and the JAK/STAT pathway), which all lead to changes in transcription of cellular proteins. Epidermal growth factor receptor (EGFR), platelet derived growth

factor receptor (PDGFR), c-Src, and FAK are additional protein kinases that can be activated by AngII in VSMCs (Daugherty and Cassis, 2004, Taubman, 2003).

AngII is also known to generate intracellular reactive oxygen species (ROS) in VSMCs via a NADH/NADPH oxidase-dependent means, where ROS play a role in further activation and modulation of the above mentioned signaling cascades (Harrison et al., 2003, Irani, 2000). ROS mediate signaling in pathways causing hypertension and vessel inflammation. AngII promotes production of chemokines (IL-8, osteopontin, MCP-1), cytokines (IL-6, IL-12, TNFα), adhesion molecules (ICAM-1, VCAM-1, selectins, integrins), metalloproteinases, and growth factors (VEGF, TGFβ, PDGF, CTGF), all of which contribute to cell migration and enhanced extracellular matrix production, ultimately leading to inflammation, fibrosis and/or cell proliferation (Ruiz-Ortega et al., 2001, Touyz and Schiffrin, 2000). In addition, early studies demonstrated that AngII is capable of inducing the proto-oncogenes *c-Fos, c-Jun,* and *c-Myc*, which encode transcription factors that act as cell growth and differentiation mediators (Taubman, 2003). Overall, through increased activation of the factors mentioned above, AngII mediates vascular damage (Daugherty and Cassis, 2004, Irani, 2000).

The effects that AngII has on the vasculature are similar to those events that it modulates in cardiac myocytes, fibroblasts and renal epithelial cells; whereby, the hormone induces changes in protein production and activation of various intracellular signaling cascades (Kim and Iwao, 2000). Overall, these alterations lead to vessel

remodeling and ultimately, cardiovascular diseases (Kim and Iwao, 2000, Friddle et al., 2000).

1.3 Characteristics of micro-RNAs (miRNAs)

1.3.1 MiRNA Discovery

In 1993 Victor Ambros, Rosalind Lee, and Rhonda Feinbaum reported that they had discovered single-stranded non-protein-coding regulatory RNA molecules in the model organism *C. elegans* (Lee et al., 1993) . Previous research revealed that the *lin-4* gene was responsible for the repression of the protein LIN-14 during larval development of the worm; however, the mechanism for control of LIN-14 remained unknown. Ambros and colleagues found that *lin-4*, unexpectedly, did not encode a regulatory protein, but gave rise to small RNA molecules, 22 and 61 nucleotides in length, which were called lin-4S (short) and lin-4L (long). Sequence analysis showed that lin-4S was part of lin-4L, in which lin-4L was predicted to form a stem-loop structure with lin-4S contained in the 5' arm. It was discovered that lin-4S was partially complementary to several sequences in the 3'-untranslated region (3'-UTR) of the messenger RNA encoding the LIN-14 protein (Lee et al., 1993); therefore, Ambros and colleagues hypothesized that *lin-4* could regulate LIN-14 through binding of lin-4S to the *lin-14* transcript in a type of antisense RNA mechanism. In 2000, the Ruvkun lab characterized another *C. elegans* small RNA regulatory molecule, let-7. Let-7 was conserved in many species, including vertebrates (Reinhart et al., 2000). These discoveries confirmed that a class of small RNAs with conserved sequences and functions existed. These molecules are now known

as microRNAs (miRNAs).

MiRNAs were not recognized as a distinct class of regulators with conserved functions until the early 2000s. In 2006, Andrew Z. Fire and Craig C. Mello won the Nobel Prize for their work on RNA interference (RNAi) in *C. elegans*, which describes gene silencing by double-stranded RNA, (Fire et al., 1998) exactly what the Ambros and Ruvkun labs observed. RNAi is the activated product when double-stranded RNA duplex molecules exist in the cell. The RNAi, forming specific protein complexes activates biochemical machinery, which degrades those mRNA molecules that carry a silencing code identical to that of the double-stranded RNA. When such mRNA molecules disappear, the corresponding gene is silenced and no protein is made. RNAi is used to regulate gene expression in the cells of humans as well as worms. Interestingly, miRNAs can also form a double-stranded structure with RNAi, the translational silencing complex to block protein synthesis, lowering the expression of that particular gene.

Since the first report, the miRNA field has grown tremendously, becoming an integral component of how researchers view gene expression regulation. To date, miRNA research has revealed multiple roles in transcript degradation and translational suppression and possible involvement in transcriptional and translational activation (Vasudevan et al., 2007, Buchan and Parker, 2007). MiRNAs have been linked to post-transcriptional regulation of at least 60% of protein encoding genes, modulating virtually all biological processes, including differentiation, proliferation, and organ development (Bartel, 2009, Fabian et al., 2010). More than one-thousand miRNAs have been

annotated in human, rat and mouse genomes, of which expressed miRNAs are generally found in a tissue specific manner (Lagos-Quintana et al., 2002).

1.3.2 Biogenesis and Function of miRNAs

Genes that encode for miRNAs are distributed across chromosomes either individually, or in clusters, in which two or more miRNA genes are transcribed from physically adjacent miRNA genes. Usually miRNA clusters consist of two or three genes, however, larger miRNA clusters exist. For example, the miR-17-92 cluster is found on human chromosome 13 and is composed of six miRNAs. This miRNA cluster is involved in cellular processes, ranging from tumor formation to the development of heart, lungs, and immune system (Zhang et al., 2012). Whether expressed individually or in conjunction with additional miRNAs, these small, non-coding RNAs have a significant biological impact.

The majority of genes for animal miRNAs, positioned along intronic or intergenic regions of the genome, are initially transcribed by RNA polymerase II and to a lesser extent by RNA polymerase III into a several hundred-nucleotide long stem-loop primary miRNA (pri-miRNA). Pri-miRNAs are enzymatically processed to be endogenous regulators, first in the nucleus as ~70 nucleotide long precursor miRNA (pre-miR) hairpins by the enzyme Drosha and its obligate partner DGCR8. DGCR8 recognizes the double-stranded RNA and then associates with Drosha to form the "microprocessor" complex. A single pri-miRNA may contain from one to six miRNA precursors. The pre-miRNA is shuttled into the cytosol via Exportin-5/Ran-GTP where it is further processed.

Cytoplasmic processing occurs by the RNase III enzyme Dicer complexed with different RNA-binding/modifying proteins (e.g., TRBP). The activity of Dicer yields an imperfect miRNA:miRNA* duplex. Generally, only one strand of the duplex is functional. Selected on the basis of its thermodynamic instability, the single-stranded, guide RNA (miRNA) of approximately 18-25 nucleotides will be incorporated into a ribonucleoprotein complex. The complementary passenger strand (miRNA*) is typically degraded. The core component of the ribonucleoprotein (miRNP) complex is a member of Argonaute protein family (Ago1 to Ago4) (Figure 1.7) (Bartel, 2009, Shukla et al., 2011, Winter et al., 2009, Bartel, 2004). The Ago protein will orient the mature miRNA with its target mRNA, ultimately causing regulation of translation or stability of target mRNAs.

Mechanistically, miRNAs have a cis-acting regulatory function to post-transcriptionally modulate at least 60% of protein encoding genes (Bartel, 2009), with which they form imperfect hybrids, with the target sites in the 3'-UTR of mRNAs (Fabian et al., 2010). The miRNA-mRNA hybrids are directed to mRNA cleavage, translational repression, or mRNA deadenylation. MiRNAs are capable of directing cleavage of endogenous and artificial substrates, containing highly complementary binding sequences; however, the majority of interactions between miRNA and mRNAs in animals are only partially complementary, and thus, translational inhibition predominates (Hutvagner and Zamore, 2002). It has been speculated that miRNAs suppress translation by inhibiting the processes of initiation or elongation.

Figure 1.7. Canonical pathway of miRNA biogenesis and modes of action. Canonical miRNA maturation includes the production of the pri-miRNA by RNA polymerase II or III and cleavage by the microprocessor complex Drosha–DGCR8 in the nucleus. The pre-miRNA hairpin is exported from the nucleus by Exportin-5–Ran-GTP. In the cytoplasm, Dicer and TRBP cleave the pre-miRNA to its mature length. The functional strand of the mature miRNA is loaded with Ago2 proteins into the RISC, where it guides RISC to silence target mRNAs through mRNA cleavage, translational repression or deadenylation, whereas the passenger strand (black) is degraded. From (Fazi and Nervi, 2008).

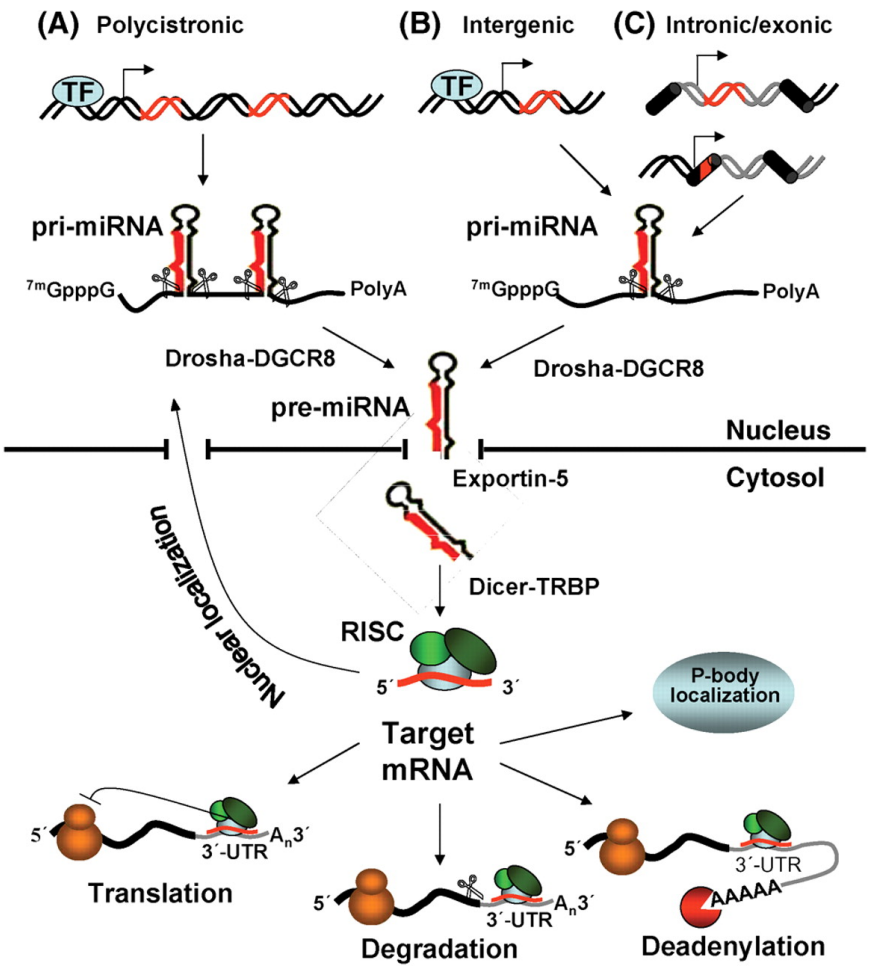

A single miRNA can regulate multiple mRNAs to varying degrees; in addition, a single mRNA can be targeted by multiple miRNAs. A miRNA, miRNA cluster, or members of a miRNA family tend to target multiple mRNA transcripts within common cellular response pathways (e.g. proliferation, apoptosis, angiogenesis, or fibrosis). Because of this function, miRNAs are considered to be essential for protein quality control and homeostasis and when misregulated, can result in developmental defects and disease (Bartel, 2009, Fabian et al., 2010).

1.3.3 MiRNAs in Human Health and Disease

An important distinction between disease and healthy states in tissue homeostasis resides in the regulatory networks that distinguish these states. As the miRNA field grows, there is increasing recognition that miRNA networks are often associated with tissue dysfunction. Because of their global function, miRNAs are vital regulators of homeostatic protein levels and when deregulated, can alter developmental fate and physiological processes (Shukla et al., 2011, Bartel, 2009). Many researchers have reported links between altered miRNA homeostasis and pathological conditions, such as cancer, psychiatric and neurological diseases, cardiovascular disease, and autoimmune disease. MiRNA deficiencies or excesses have been correlated with a number of clinically important diseases.

Dysregulation of miRNA expression in cancer has suggested that miRNAs can act as oncogenes ("oncomiRs"), by decreasing expression of tumor-suppressor genes or as tumor-suppressors, by targeting oncogenic mRNA for translational silencing (Esquela-

Kerscher and Slack, 2006). Mirs-17-92 and miR-21 have been identified as oncomiRs and are linked to regulators of the cell cycle to promote proliferation. (Nana-Sinkam and Croce, 2011, Pandit et al., 2011). An example of a tumor suppressor miRNA is let-7. When overexpressed, this miRNA has been shown to inhibit tumor development and growth (Nana-Sinkam and Croce, 2011). To add to the complexity, the cell and tissue context of miRNA expression can be critical to understanding the overall pathobiology of cancer. For example, miR-31 seems to be pro-oncogenic in lung cancer, but protective in breast cancer. In addition, an observed increase in miR-3 occurs in lung cancer cell lines and knockdown reduces cellular growth and colony formation (Liu et al., 2011).

Specific and global alteration of miRNA expression profiles has been shown in heart and kidney, two main organs that are pathophysiologically affected by AngII (Bhatt et al., 2011, Elton et al., 2010, Ikeda and Pu, 2010, Scalbert and Bril, 2008, Small and Olson, 2011). In the kidney, collagen production during diabetic nephropathy (miRs-192, -216a, and -217), fibrosis, (miR-21, and miR families -29, and -200), acute kidney injury (miRs-132, -362, -379, -668, and -687), polycystic kidney disease (miRs-15a and -17), kidney cancer (miRs-210, -155, -185, -21, 483-3p, and -562), and hypertensive kidney sclerosis (miRs-200a-b, -141, -429, -205, and -192) exhibit altered expression of miRNAs (Li et al., 2010).

Regulation of cardiac structure and function by miRNAs can also have deleterious implications. Recent studies have established essential roles for miRs in cardiac development and cardiac health. For example, cardiac cell fate decisions (miR-1-2),

hyperplasia (miR-1-2), hypertrophy (miR-1, -133, -21, -23a, -24, -195, -199a, 208, -214), apoptosis (miR-1, -133), contraction (miR-208), electrical conductance (miR-1-2, -133, -208), and cardiomyocyte fibrosis (miR-21, -29) can be strongly modulated by miRNAs. In addition, early studies implicate specific miRNAs as contributors to vascular disease (e.g., miR-155, -143, -145, -21, 126) (Dorn, 2011, van Rooij et al., 2008).

In a previous study, we have shown an altered miRNA expression profile in dilated cardiomyopathic human hearts. MiRs-1, -29b, -7, and -378 were downregulated in end-stage dilated cardiomyopathy; whereas, miRs-214, -342, -125b, and -181b were upregulated. The altered miRNAs target gene networks (e.g., NFκB) that account for compensatory remodeling in human HF. These novel studies suggest that mRNA and miRNA profiles, together, contribute to AT_1R biology in health and disease (Naga Prasad et al., 2009, Naga Prasad and Karnik, 2010). It is unknown, however, miRNAs that are involved in AngII and ARB mediated vascular pathologies, which is a major drawback to fully understanding the signaling pathways mediated by RAS.

1.3.4 Therapeutic Potential of miRNAs

It is well established that miRNAs act as negative regulators of gene expression via various mechanisms. Because individual miRNA often regulate the expression of multiple target genes with related functions, modulating the expression of a single miRNA can, in theory, influence an entire gene network and thereby modify complex disease phenotypes. Thus, molecules that alter the function or abundance of specific miRNAs represent a new strategy for treating human disease.

The molecular mechanism by which miRNAs regulate gene expression is still not fully understood, nor is the complete repertoire of mRNAs targeted by each miRNA known. However, continual advances in the field points to effective strategies for modulating expression of miRNAs, allowing them to have therapeutic potential. MiRs-155 (inflammation), -122 (Hepatitis C virus), -208 (cardiac remodeling), -21 (fibrosis, -92a (neoangiogenesis), -33 (metabolic disease), -103/107 (metabolism), -15 family (cardiac regeneration and injury) are multiple examples of instances where controlling expression of the miRNA would show therapeutic promise (van Rooij et al., 2012).

To understand the roles of miRNAs in biological systems, it is important to be able to artificially increase or decrease their function or abundance. Expression of exogenous small RNAs in cells is possible through transient or stable transfection or viral transduction of a pri-miRNA transgene, pre-miRNA, or mature miRNA/miRNA*. MiRNAs can also be targeted for inhibition by using antisense oligonucleotides, which will bind miRNAs and prevent them from interacting with mRNA target genes (i.e., antagomirs) (van Rooij et al., 2012). Studies have examined various chemical modifications of antagomirs to improve their *in vitro* and *in vivo* stability and to improve their *in vivo* delivery. Modifications include, 2′-*O*-methoxyethyl, 2′-fluoro and 2′, 4′-methylene (locked nucleic acids (LNAs)), which have greater affinity to bind and inhibit miRNAs and are more resistant to degradation (Broderick and Zamore, 2011).

Delivery of therapeutic miRNAs to its target tissue is a challenge. Anything with a diameter larger than 5nm, including therapeutic RNAs, cannot cross the capillary endothelium and will remain in circulation until filtered by the kidneys. Therefore, local delivery increases its bioavailability in target tissues and minimizes uptake in non-target tissues. Local delivery is, unfortunately, limited to the eye, skin, mucous membranes and tumors. Alternatively, systemic delivery into the bloodstream is challenged by the immune response of the body. In some cases, where direct delivery is not possible, nucleic acids can be encapsulated in lipids, forming vesicles (e.g., PEGylated liposomes, lipidoids and biodegradable polymers) and enhancing intracellular delivery (Broderick and Zamore, 2011). The advantage of using lipid delivery is that these lipid particles can be tailored to 1) enable fusion with the cytoplasmic, endosomal or nuclear membrane and 2) promote endosomal release once inside the cell.

In the anti-miRNA therapeutics field, numerous clinical trials are being actively pursued, particularly for those miRNAs mentioned above. The pharmacokinetics (fate of the drug in the body), pharmacodynamics (time course and nature of pharmacological effects), and absorption, distribution, metabolism, and excretion of the delivered antagomirs are critical aspects that are taken into account when moving from the bench to a clinical trial. In addition, the toxicity of the agent must be addressed to determine the most effective dose and dose regimen that is safe and free of unwanted side effects (van Rooij et al., 2012).

A significant drawback to miRNA-targeted therapies is the extreme potential for off-target-effects. Although a miRNA might target related genes, the fact still remains that a single miRNA can target many genes and the genes that are targeted are cell type–dependent, meaning that many genes can be unintentionally turned off and cause additional deleterious outcomes (van Rooij et al., 2012). There are a lot of unknowns surrounding the mode of action of the different antagomirs; however, the interest surrounding miRNAs as novel therapeutic entities is tremendous and the anticipated success of these early forerunners will likely spur the search for additional miRNA therapeutic targets.

1.3.5 Regulation of RAS Components by miRNAs

Variations in the genotype of many of the RAS components (e.g., AGT, ACE1, AT_1R) are associated with altered activity and function and may have significant clinical implications (Pontremoli et al., 2000). For example, a wide range of known stimuli can regulate AT_1R expression at the transcriptional level (e.g., NO, peroxisome proliferator-activated receptor (PPAR)-γ suppress receptor density, while IL-6, glucocorticoids, and insulin-like growth factor cause upregulation) (Elton and Martin, 2007). In recent years, several studies have investigated the ability of miRNAs to regulate AT_1R expression and expression of other GPCRs. From regulated expression of β2-adrenergic receptors by let-7f to controlling AT_1R density by various miRNAs binding to either the 3'UTR or a region of the protein-coding portion of the gene, miRNAs have a powerful function in controlling receptor expression, and thereby function within the cell (Wang et al., 2011, Elton et al., 2010).

Recently, it has been demonstrated that miR-155 regulates the expression of the AT_1R. In human lung fibroblasts, miR-155 translationally repressed the expression of AT_1R and the inhibition of miRNA expression by anti-miR-155 or by transforming growth factor-β1 (TGF-β1) treatment substantially increased AT_1R protein levels, which may have a role in the treatment of blood pressure (Martin et al., 2007b, Martin et al., 2007a). MiR-155 has been shown to interact with the silent polymorphism (+1166A/C) of the human AT_1R gene in ECs and VSMCs. Martin and colleagues showed that when the +1166C-allele polymorphism is present in the 3'UTR of the gene, the ability of miR-155 to interact with the cis-regulatory site is decreased, leading to translational repression of the AT_1R (Martin et al., 2007b). The same group showed, for the first time, that miRNAs (i.e., miR-132) could also bind to sequence recognition sites harbored in the coding region of the hAT_1R mRNA and suppress its translation (Elton, 2008). Furthermore, miR-802 in the GI tract specifically, has been shown to regulate AT_1R expression through binding to the 3'UTR of the AGTR1 gene. In the absence of this miRNA, researchers observed increased hAT_1R levels and $AngII/AT_1R$ signaling (Sansom et al., 2010). MiRNAs have also been shown to regulate additional components of RAS. Specifically, rats experiencing nonpathological left ventricular hypertrophy induced by exercise had altered expression of specific miRNAs targeting RAS genes. MiR-27a and -27b targeting ACE were increased and miR-143 targeting ACE2 was decreased in the heart (Fernandes et al., 2011). Finally, Boettger et al. demonstrated that miR-145, which is enriched in mouse VSMCs, targets mouse ACE1 mRNA, leading to thinning of the arterial tunica media in the absence of the miRNA (Boettger et al., 2009). The miR-145 deficient mice had a decrease in the number of contractile VSMCs and an

increase in the number of proliferative VSMCs, which gave rise to a defect in AngII-induced contractility and blood pressure maintenance (Elia et al., 2009). These examples show the potent ability of small RNAs to have a widespread effect on overall AT_1R signal transduction and function through changing mRNA expression of RAS components.

1.3.6 AngII Regulation of Small Ribonucleic Acids

Establishing AngII/AT_1R activation as a broad cellular agonist has provided the foundation to undertake further comprehensive analyses of AngII effects on gene expression induction. Understanding the role of AngII regulated small ribonucleic acids (RNAs) is an area of interest that will provide additional insight into the ability of AngII to modulate physiological and pathological phenotypes. GPCR regulated miRNA (miRNome) expression, particularly AT_1R regulated miRNA expression, is an area of mounting interest to researchers. The consequence of an important regulatory system, such as RAS, modulating miRNA gene expression has not been extensively studied, but promises to have a significant impact on the field of AngII biology. Specifically, miRNAs that are involved in AngII and ARB mediated vascular pathologies are not known, which is a major drawback to fully understanding the signaling pathways mediated by RAS.

Recent work by Jeppesen and colleagues shows that cardiac fibroblasts and HEK293N cells overexpressing the AT_1R have a differential miRNA profile in response to AngII/AT_1R activation, compared to control cells (Jeppesen et al., 2011). In a Gq/11-

dependent manner, miR-29b, -129-3p, -132, -132* and -212 were upregulated in their system, suggesting a possible role for these miRNAs in AngII mediated cardiovascular biology (Jeppesen et al., 2011). This study has shown that the AT_1R is an ideal model system for exploring the GPCR regulated miRNome. Additionally, researchers have shown that circulating levels of vascular and inflammation-associated miRNAs are significantly downregulated in patients with coronary artery disease, which is an important aspect of AngII biology (Fichtlscherer et al., 2010). Determining the AT_1R regulated miRNome and its effect on the pleiotropic signaling events of the AngII/AT_1R interactions will introduce a distinct regulatory axis into RAS as a whole.

4.1 Significance of Current Work

In both physiological and pathological settings, if the activity of AngII as a broad cellular agonist is not properly regulated, AngII stimulus becomes chronic and can damage the tissue, as well as contribute to lasting cardiovascular disorders (Mehta and Griendling, 2007). It's well established that activation of the AT_1R by AngII leads to an increase in protein coding genes and protein expression. A novel are of research is the pursuit of understanding the regulation of expression and processing of miRNAs, which is stringently controlled within a cell. The role of miRNAs must be a critical aspect of effectiveness of vital hormones such as AngII. The miRNAs may also be involved in modulation of beneficial tissue response to treatment of cardiovascular pathologies using blockade of RAS. This aspect of AngII biology has not been studied, but acquisition of knowledge of AngII modulating miRNA gene expression promises to have a significant impact on the field.

Increasing evidence points to the realization that the AT_1R-mediated gene expression models in various tissues and disease states are incomplete without the accompanying miRNA profile. In this study, we documented the global AngII-regulated miRNA expression profile for various model systems of human, mouse and rat origin. The biological and technical replicates included cardiac tissue, cardiac myocytes, VSMCs and epithelial cells. Our goal was to observe the established equilibrium of the miRNA pool that would persist following chronic AngII treatment in each model as a means to ultimately observe a common AngII responsive miRNA signature. We pharmacologically distinguished the AT_1R-regulated miRNA profiles by comparing technical replicates treated with the specific AT_1R-blocker, losartan and biological replicates following chronic AT_2R activation by AngII. We observed 32 miRNAs that were universally regulated by AngII. Most other miRNAs were regulated in a treatment- or species-specific manner. In addition, a few miRNAs were unique to specific cell types.

In the current study, we also explored the extent to which AngII/AT_1R-regulated miRNAs contribute to maintenance of RAS homeostasis and phenotypic modulation of VSMCs, which are an important cell type that can be adversely affected by a local increase in AngII action. The balance between VSMC phenotypes depends on the expression of different intracellular proteins, secretion of cytokines and chemokines, and deposition of ECM components (Figure 1.8) (Ruiz-Ortega et al., 2001, Daugherty and Cassis, 2004, Touyz and Schiffrin, 2000). Understanding the role that miRNAs may play

in the regulation of AngII-induced VSMC phenotypic alterations will be an important aspect for determining the full capacity of AngII/AT_1R activation on vascular diseases.

Figure 1.8. Effects of AngII on VMSCs. It has been well established that upon stimulation with AngII, the AT_1R becomes activated leading to an increase in protein coding genes and protein expression. Receptor activation ultimately manifests as a specific VSMC phenotype due to a host of alterations, including changes in gene expression, the secretion of cytokines and chemokines, and increased protein and ECM synthesis. Whether the effect AngII has on VSMCs is mediated through miRNA expression and regulation is unknown.

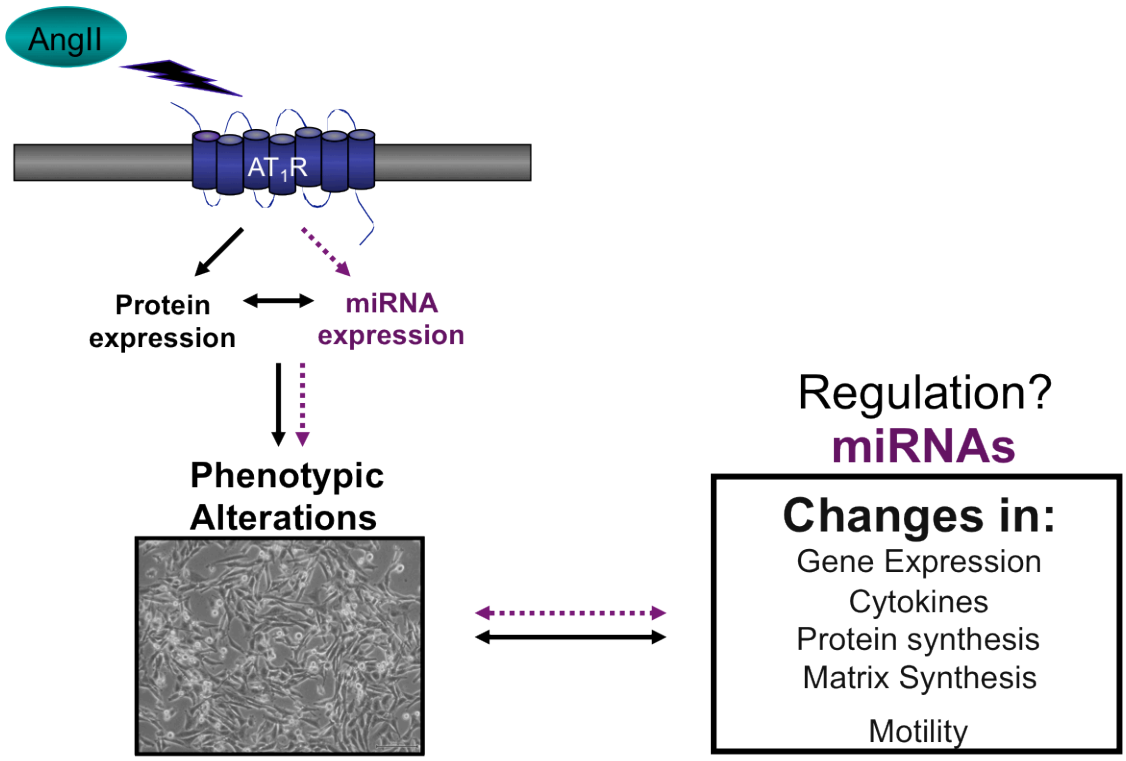

A distinct AngII-regulated miRNA expression pattern emerged in the human and rat VSM cell lines in the profiling experiment, which was validated in our independent samples. Of the 17 miRNAs comprising the VSMC expression pattern, we selected miR-483 as a representative candidate for further study because of its location within the genome and its ability to potentially target multiple components of RAS. Overall, we show evidence that indicates muscle cell-specific expression of miR-483 and regulation of tissue RAS and AngII-mediated migration by miR-483; specifically in VSMCs. Our results further suggest that the AngII-regulated MEK1 kinase signaling cascade most effectively mediates the steady state pool of miRNAs, which includes downregulation of mir-483. This results in activation of RAS and switching of the VSMC phenotype associated with pathological states *in vivo*, such as hypertension.

Our findings are significant in the context of determining the full capacity of RAS as an intrinsic regulatory system. AngII-regulated miRNAs will likely have a strong influence on cardiovascular and renal disease states. Further, understanding their expression and regulation could be applied to other biological systems in which ligand-induced GPCR activation or inhibition induces changes in gene expression and formation of pathologies.

CHAPTER II

MATERIALS AND METHODS

2.1 Construction of Plasmids

The hemaglutinin (HA)-tagged AT_1R gene was subcloned into the shuttle expression vector, pcDNA3.1 (+) (Life Technologies, NY, USA), which contains unique *Eco*R1 and *Not*1 restriction sites (Figure 2.1 A). An *Eco*R1 restriction site on the 5' end and a *Not*1 restriction site on the 3' end flank the synthetic rat AT_1R gene. HA-AT_1R was previously sequenced and cloned into the pMT3 expression vector; therefore, the gene was removed for subcloning using the appropriate restriction enzymes. The digest was fractionated on a 1% agarose gel and isolated by QIAquick Gel Extraction Kit (Cat. No. 28704; QIAGEN, Valencia, CA, USA). The insert was ligated into the pcDNA3.1 (+) expression cassette (Figure 2.1 B). The HA-tagged AT_2R gene was cloned into pcDNA 3.1 (+), previously.

Figure 2.1. **Subcloning of HA-AT_1R gene in pcDNA3.1 expression vector. A)** Schematic representation of pcDNA3.1 cloning vector. P_{CMV}, cytomegalovirus promoter; T7, promoter/priming site; *Eco*R1-*Not*1, cloning sites for expression, BGH pA, polyadenylation sequence; SV40, origin of replication; SV40 pA, early polyadenylation signal; Neo^R, neomycin resistance gene; pUC, origin of replication; Amp^R, ampicillin resistance gene. **B)** Schematic representation of subcloning HA-AT_1R gene into pcDNA3.1 (+) vector.

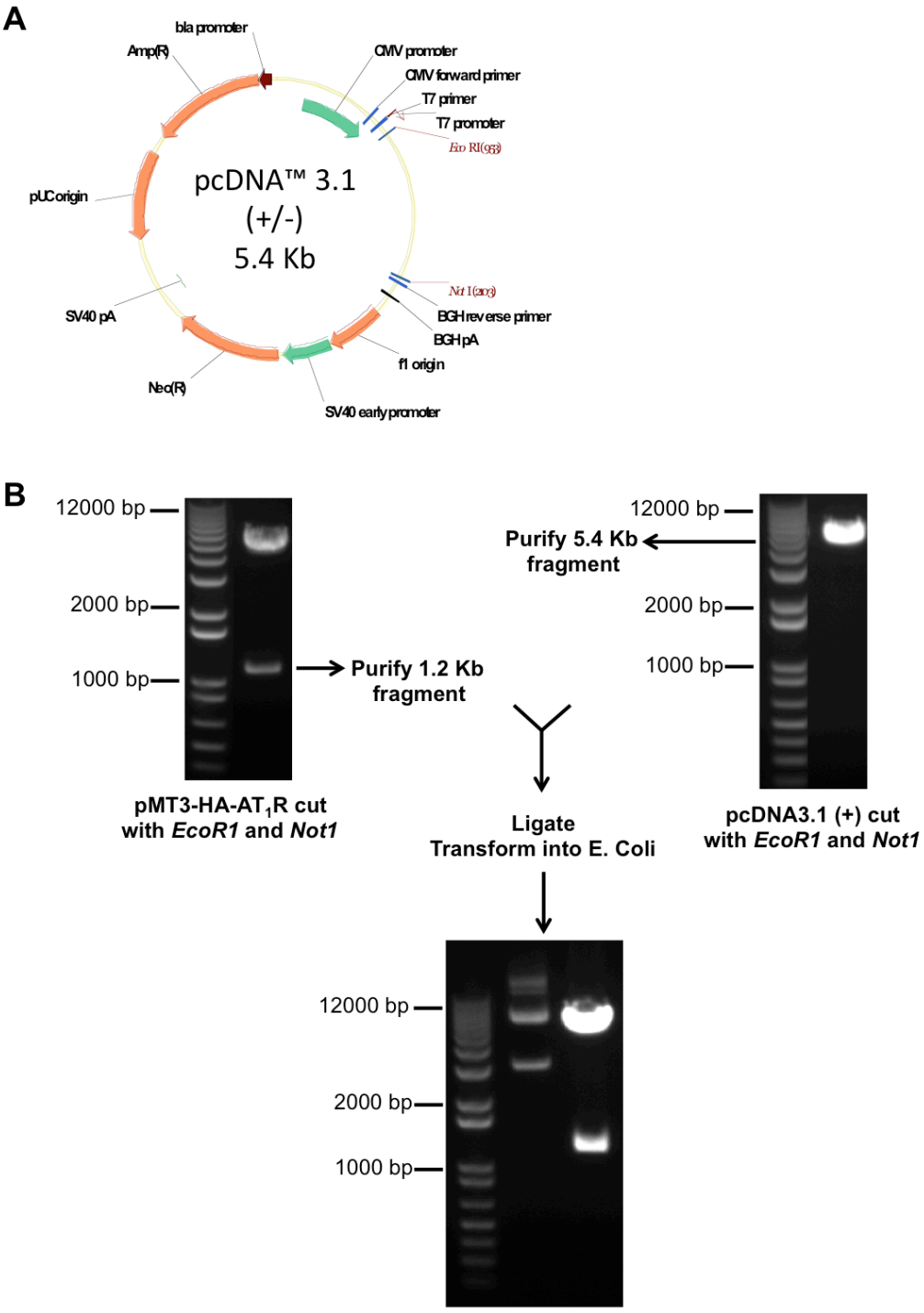
A
bla promoter
Amp(R)
CMV promoter
CMV forward primer
T7 primer
T7 promoter
Eco RI(933)
pcDNA™ 3.1
(+/-)
5.4 Kb
pUC origin
Not I(2103)
BGH reverse primer
BGH pA
f1 origin
SV40 pA
Neo(R)
SV40 early promoter
B
12000 bp
2000 bp
1000 bp
Purify 1.2 Kb fragment
pMT3-HA-AT1R cut with EcoR1 and Not1
Purify 5.4 Kb fragment
pcDNA3.1 (+) cut with EcoR1 and Not1
Ligate
Transform into E. Coli

Pre-miR-483 was designed to have a completely complementary hairpin sequence and to be oriented in the 3'→5' direction to allow for optimal expression of miR-483-3p in mammalian cells (Figure 2.2).

The 76-nucleotide sequence was synthesized and cloned into the expression vector pRNA U-6.1/Hygro by GenScript (Figure 2.3 A) (GenScript, NJ, USA) ad provided as mini-prep DNA. Upon receipt, the pRNA U6.1-miR483 construct was transformed into competent FB10B cells. The plasmid was isolated using the GenElute HP Plasmid Maxiprep Kit (Cat. No. NA0300; Sigma-Aldrich, MO, USA) (Figure 2.3 B).

The 3'-UTRs of human AGT, ACE-1, ACE-2, and AGTR2 were generated using polymerase chain reaction (PCR) amplification and cloned into the psiCHECK™-2 dual luciferase reporter expression vector, which contains unique *Xho1* and *Not1* restriction sites (Figure 2.3 A) (Cat. No. C8021; Promega, WI, USA). Genomic DNA was isolated from human kidney epithelial (HEK) cells using the DNeasy Blood and Tissue Kit (Cat. No. 69506; QIAGEN) and served as the DNA template for each individual PCR reaction. Sense and antisense primers were designed to be complementary to each 3'-UTR sequence and harbor nucleotide changes to incorporate restriction sites specific for *Xho*1 and *Not*1 enzymes (Table II.I.).

Figure 2.2. MiRNA insert for expression construct. The insert sequence was designed for expression of miR-483-3p in mammalian cells. Magenta, *BamHI* restriction site; teal, purine for transcription initiation; yellow, sense (miR-483-3p); green, loop; red, antisense (mir-483-5p); purple, termination signal; aqua, *HindIII* restriction site.

MiR-483 Hairpin Nucleotide Sequence

GGATCCCGTCACTCCTCTCCTCCCGTCTTTTGATATCCGAAGACGGGAGGAGAGGAGTG
ATTTTTTCCAAAAGCTT

Figure 2.3. MiR-483 in pRNA U6.1 expression vector. A) Schematic representation of pRNA U6.1/Hygro cloning vector. U6, promoter; T7, primer; *Bam*H1-*Hind*III, cloning sites for expression; SV40, origin of replication; Hygromycin, resistance gene; pUC, origin of replication; Ampicillin, resistance gene. **B)** Schematic representation of isolating plasmid DNA for transfection.

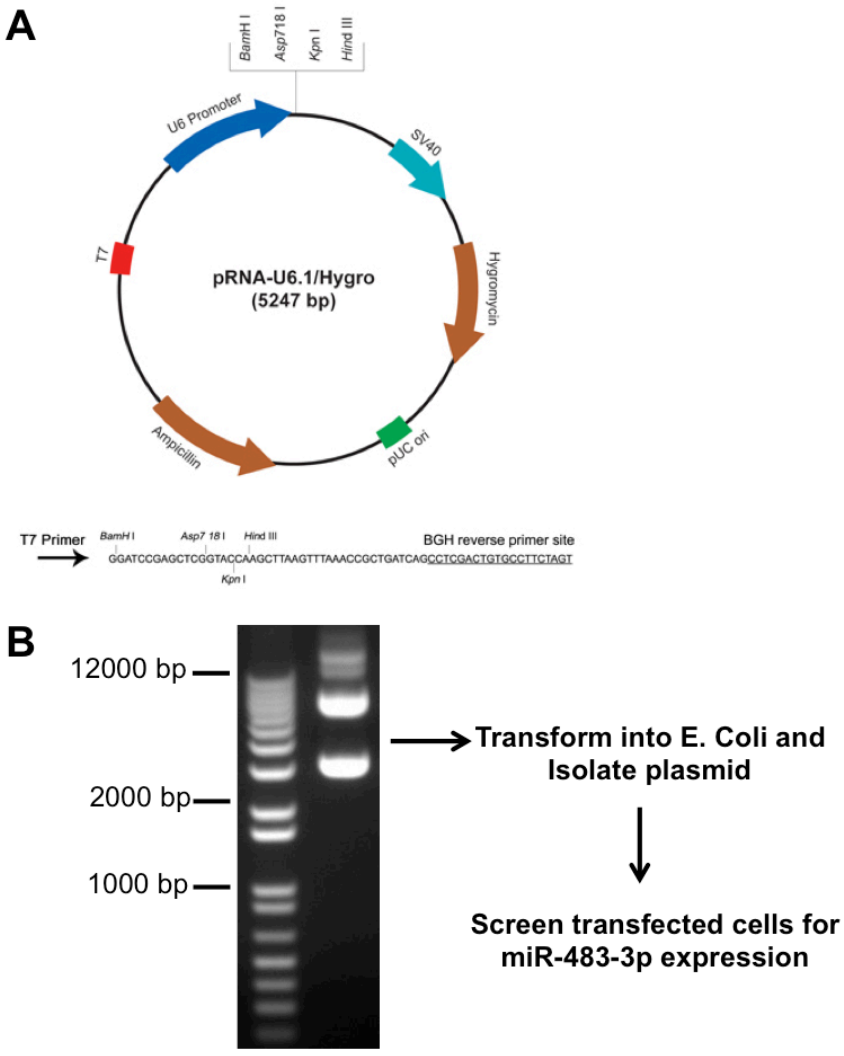

The 3'-UTR of each gene was PCR amplified in the presence of FailSafe enzyme (Cat. No. FS99060; Epicentre Biotechnologies, WI, USA) using 10pmol/µl of sense and 10pmol/µl antisense primer. The parameters used for the PCR reaction were an initial denaturing step of 5 min at 95°C followed by 30 cycles of 94°C for 1 min, 55°C for 1 min, and 72°C for 1.5 min and then a final extension at 72°C for 10min. The PCR products were fractionated on a 1% agarose gel and isolated using QIAquick Gel Extraction Kit (QIAGEN), digested with *Xho*1 and *Not*1, and purified with QIAquick PCR purification Kit (Cat. No. 28104; QIAGEN). The purified products were ligated into psiCHECK-2 and transformed into competent FB10B cells. The plasmids were isolated using the GenElute HP Plasmid Maxiprep Kit (Sigma-Aldrich) (Figure 2.3 B). The sequence of each 3'-UTR construct was verified using automated DNA sequencing (Figure 2.4).

Table II.I. Primers used for 3'-UTR amplification. Green, G clamp; aqua, *Xho*1 restriction site; red, stop codon; magenta, *Not*1 restriction site.

Primer	Sequence (5' → 3')	bp	%GC	TM
AGT sense	GGGGCTCGAGTGAGGCCAGGGCCCCAGAACACAG	34	71	86
AGT antisense	GGGGGCGGCCGCGGAGGCTTATTGTGGCAAGAC	33	70	87
ACE-1 sense	GGGGCTCGAGTGAGGTGACCCGGCTGGGTCGGCC	34	77	89
ACE-1 antisense	GGGGGCGGCCGCGGGAGGGCAGGACCTTTAATTG	34	71	88
ACE-2 sense	GGGGCTCGAGTAGAAAAATCTATGTTTTTCCTC	33	42	70
ACE-2 antisense	GGGGGCGGCCGCGAGTGTGTAAATCTAGCATTTATTG	37	54	81
AGTR2 sense	GGGGCTCGAGTTACGTGAGAGCAAAATGCATG	32	53	77
AGTR2 antisense	GGGGGCGGCCGCCTTCCAATTAAAAATTTTATTTATATG	39	41	77

Figure 2.4. Cloning of 3'-UTRs in psiCHECK-2 expression vector. A) Schematic representation of psiCHECK-2 cloning vector. HSV-TK, promoter; *hluc*+, Firefly luciferase gene; SV40, late poly (A) signal; Amp^R, ampicillin resistance gene; SV40, early enhancer/promoter; T7, promoter; *hRluc,* Renilla luciferase gene; *Not*1-*Xho*1, cloning sites for expression; Synthetic poly (A). **B)** Schematic representation of subcloning HA-AT_1R gene into pcDNA3.1 (+) vector.

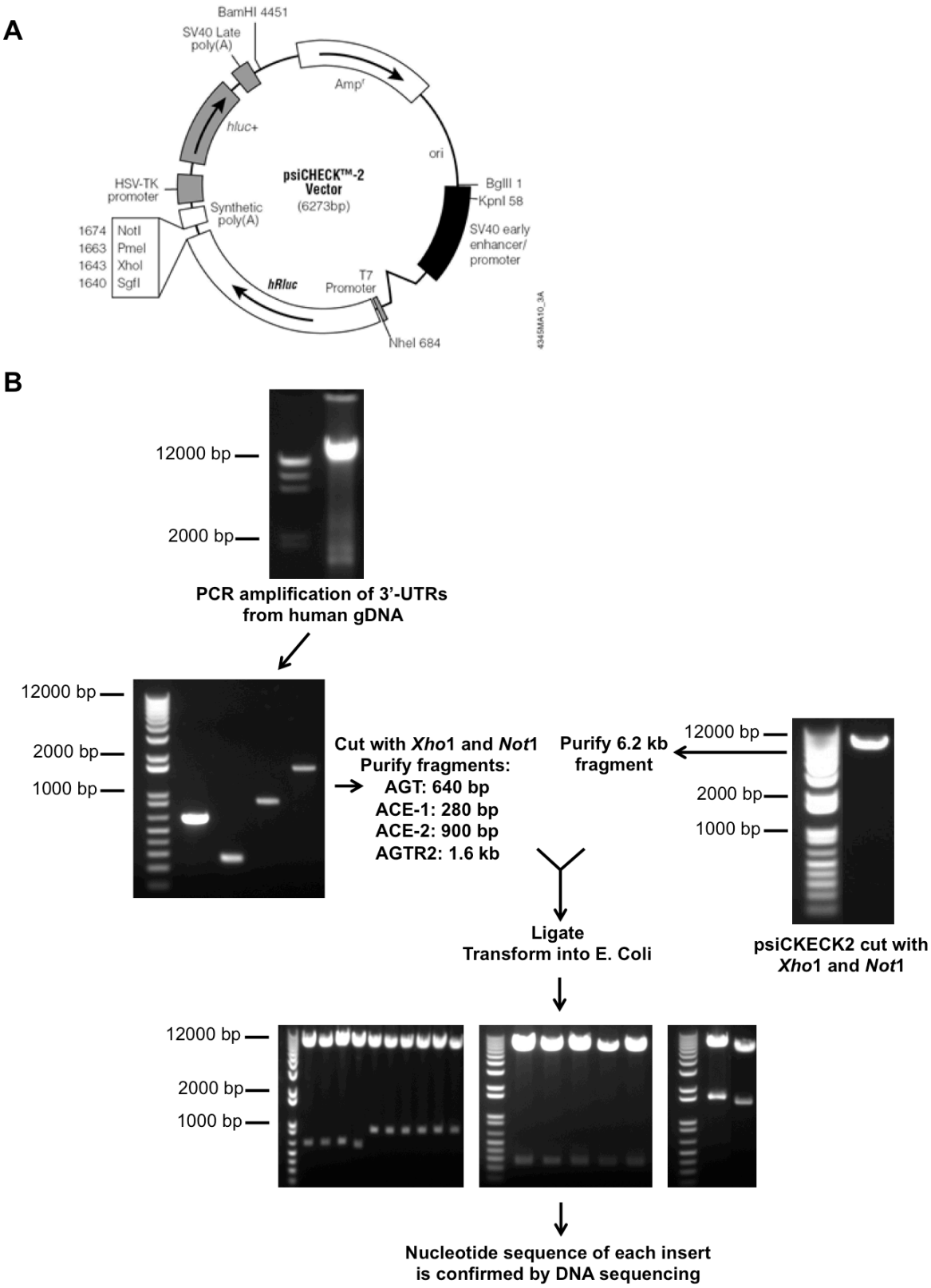
A
BamHI 4451
SV40 Late poly(A)
Amp^r
hluc+
ori
psiCHECK™-2 Vector (6273bp)
HSV-TK promoter
Synthetic poly(A)
BglII 1
KpnI 58
SV40 early enhancer/ promoter
1674 NotI
1663 PmeI
1643 XhoI
1640 SgfI
hRluc
T7 Promoter
NheI 684
B
12000 bp
2000 bp
PCR amplification of 3'-UTRs from human gDNA
12000 bp
2000 bp
1000 bp
Cut with Xho1 and Not1
Purify fragments:
AGT: 640 bp
ACE-1: 280 bp
ACE-2: 900 bp
AGTR2: 1.6 kb
Purify 6.2 kb fragment
12000 bp
2000 bp
1000 bp
psiCKECK2 cut with Xho1 and Not1
Ligate
Transform into E. Coli
12000 bp
2000 bp
1000 bp
Nucleotide sequence of each insert is confirmed by DNA sequencing

Figure 2.5. Nucleotide Sequences of 3'-UTRs. The 3'-UTR sequence of AGT, ACE-1, ACE-2, and AGTR2 was verified by automated DNA sequencing. Aqua, *Xho*1 restriction site; red, stop codon; green, miR-483-3p native binding site; magenta, *Not*1 restriction site.

AGT 3'-UTR Nucleotide Sequence

CTCGAGTGAGGCCAGGGCCCCAGAACACAGTGCCTGGCAAGGCCTCTGCCCCTGGCCTT
TGAGGCAAAGGCCAGCAGCAGATAACAACCCCGGACAAATCAGCGATGTGTCACCCCCA
GTCTCCCACCTTTTCTTCTAATGAGTCGACTTTGAGCTGGAAAGCAGCCGTTTCTCCTT
GGTCTAAGTGTGCTGCATGGAGTGAGCAGTAGAAGCCTGCAGCGGCACAAATGCACCTC
CCAGTTTGCTGGGTTTATTTTAGAGAATGGGGGTGGGGAGGCAAGAACCAGTGTTTAGC
GCGGGACTACTGTTCCAAAAAGAATTCCAACCGACCAGCTTGTTTGTGAAACAAAAAAG
TGTTCCCTTTTCAAGTTGAGAACAAAAATTGGGTTTTAAAATTAAAGTATACATTTTTG
CATTGCCTTCGGTTTGTATTTAGTGTCTTGAATGTAAGAACATGACCTCCGTGTAGTGT
CTGTAATACCTTAGTTTTTTCCACAGATGCTTGTGATTTTTGAACAATACGTGAAAGAT
GCAAGCACCTGAATTTCTGTTTGAATGCGGAACCATAGCTGGTTATTTCTCCCTTGTGT
TAGTAATAAACGTCTTGCCACAATAAGCCTCCAAAAAAAAGCGGCCGC

ACE-1 3'-UTR Nucleotide Sequence

CTCGAGTGACCCGGCTGGGTCGGCCCTGCCCAAGGGCCTCCCACCAGAGACTGGGATGG
GAACACTGGTGGGCAGCTGAGGACACACCCCACACCCCAGCCCACCCTGCTCCTCCTGC
CCTGTCCCTGTCCCCCTCCCCTCCCAGTCCTCCAGACCACCAGCCGCCCCAGCCCCTTC
TCCCAGCACACGGCTGCCTGACACTGAGCCCCACCTCTCCAAGTCTCTCTGTGAATACA
ATTAAAGGTCCTGCCCTCCCGCGGCCGC

ACE-2 3'UTR Nucleotide Sequence

CTCGAGTAGAAAAATCTATGTTTTTCCTCTTGAGGTGATTTTGTTGTATGTAAATGTTA
ATTTCATGGTATAGAAAATATAAGATGATAAAGATATCATTAAATGTCAAAACTATGAC
TCTGTTCAGAAAAAAAATTGTCCAAAGACAACATGGCCAAGGAGAGAGCATCTTCATTG
ACATTGCTTTCAGTATTTATTTCTGTCTCTGGATTTGACTTCTGTTCTGTTTCTTAATA
AGGATTTTGTATTAGAGTATATTAGGGAAAGTGTGTATTTGGTCTCACAGGCTGTTCAG
GGATAATCTAAATGTAAATGTCTGTTGAATTTCTGAAGTTGAAAACAAGGATATATCAT
TGGAGCAAGTGTTGGATCTTGTATGGAATATGGATGGATCACTTGTAAGGACAGTGCCT
GGGAACTGGTGTAGCTGCAAGGATTGAGAATGGCATGCATTAGCTCACTTTCATTTAAT
CCATTGTCAAGGATGACATGCTTTCTTCACAGTAACTCAGTTCAAGTACTATGGTGATT
TGCCTACAGTGATGTTTGGAATCGATCATGCTTTCTTCAAGGTGACAGGTCTAAAGAGA

GAAGAATCCAGGGAACAGGTAGAGGACATTGCTTTTTCACTTCCAAGGTGCTTGATCAA
CATCTCCCTGACAACACAAAACTAGAGCCAGGGGCCTCCGTGAACTCCCAGAGCATGCC
TGATAGAAACTCATTTCTACTGTTCTCTAACTGTGGAGTGAATGGAAATTCCAACTGTA
TGTTCACCCTCTGAAGTGGGTACCCAGTCTCTTAAATCTTTTGTATTTGCTCACAGTGT
TTGAGCAGTGCTGAGCACAAAGCAGACACTCAATAAATGCTAGATTTACACACTCAAAA
AAAAAAAAGCGGCCGC

AGTR2 3'UTR Nucleotide Sequence

CTCGAGTTACGTGAGAGCAAAATGCATGTAATCAACATGGCTACTTGCTTTGAGGCTCA
CCAGAATTATTTTTAAGTGGTTTTAATAAAATAATAAAATTTCCCCTAATCTTTTCTGA
ATCTTCTGAAACCAAATGTAACTATGTTTTATCGTCCAGTGACTTTCAGGAATTGCCCA
TTGTTTTTCTGATATGTTTGTACAAGATTGTCATTAGTGAGACATATTTACAACCTAGA
AGTAACTGGTGATATATCTCAAATTGTAATTAATAATAGATTGTGAATAATGATTTGGG
GATTCAGATTTCTCTTTGAAACATGCTTGTGTTTCTTAGTGGGGTTTTATATCCATTTT
TATCAGGATTTCCTCTTGAACCAGAACCAGTCTTTCAACTCATTGCATCATTTACAAGA
CAACATTGTAAGAGAGATGAGCACTTCTAAGTTGAGTATATTATAATAGATTAGTACTG
GATTATTCAGGCTTTAGGCATATGCTTCTTTAAAAAAGCTATAAATTATATTCCTCTTG
CATTTCACTTGAGTGGAGGTTTATAGTTAATCTATAACTACATATTGAATAGGGCTAGG
AATATAGATTAAATCATACTCCTATGCTTTAGCTTATTTTTACAGTTATAGAAAGCAAG
ATGTACTATAACATAGAATTGCAATCTATAATATTTGTGTGTTCACTAAACTCTGAATA
AGCACTTTTTAAAAAACTTTCTACTCATTTTAATGATTGTTTAAAGGTTTCTATTTTCT
CTGATACTTTTTTGAAATCAGTAAACACTGTGTATTGTTGTAAAATGTAAAGGTCACTT
TTCACATCCTTGACTTTTTAGATGTGCTGCTTTGATATATAGGACATTGATTTGATTTT
TATTATTAATGCTTTGGTTCTGGGTTGTTTCCTAAAATATCTGGGTGGCTTAAAAAAAA
CTCTTTAACTTGTAATAAACCCTTAACTGGCATAGGAAATGGTATCCAGAATGGAATTT
TGCTACATGGGGTCTGGGTGGGGGCAAAGAGACCCAGTCAATTACATGTTTGGTACCAA
GAAAGGAACCTGTCAGGGCAGTACAATGTGACTTTGAAAATATATACCGTGGGGGTAGT
TTTACCCTATATCTATAAACACTGTTTGTTCCAGAATCTGTATGATTCTATGGAGCTAT
TTTAAACCAATTGCAGGTCTAGATACCTCCTTCTCAGCACTATTAAAGCTCCTAAGTTA
GAGGAGTGCCTAAAACTGAGTTACCTAAAGTTTACTTACATTAAAGTATGAATATTAAT
TTTAGAAATTTGAGACTTTATTCTGTACCAGCCCTGTATAATAACAGGTTATCTAGGAC
CTTCCTCTGAGGTAGGTCTAAATACTGATCTCTGAGGCGGAACTAACGTTTTGGGGACT
CAGCATCTCTGCCAGGTTCCAGGATTATAGACAGAAGAGTCCTGTCATACCACTTTCTG
GAAAAGTCCTAATTTCATGTAATCCTTTTATTTTCAATAAAAACAAATAGCTAAATGTA
TAACCAACTATGATGTTATGTTTTCAATAATTTTGTAAAACAGCTCATATAAATAAAAT
TTTTAATTGGAAGAAAAAAAAAGCGGCCGC

2.2 Cell Culture Maintenance and Transfection

For expression of HA-AT_1R and HA-AT_2R in mammalian VSMCs, we used the rat aortic smooth muscle cell (RASMC) line, which was obtained from American Type Culture Collection (Cat. No. CRL-2018; ATCC, VA, USA). This cell line has been transformed with the large T antigen of SV40 (SV40-LT), which immortalizes the cell line and prevents them from dedifferentiating in culture. Importantly, these VSMCs maintain the characteristics common to primary SMC cultures. RASMCs were grown in 100-mm culture dishes to approximately 40-50% confluency and transfected by Lipofectamine® Transfection Reagent (Cat. No. 18324; Life Technologies), according to the manufacturer's instructions. Briefly, 60 μl of Lipofectamine was added into 1.5 mL of OPTI-MEM reduced serum media and incubated for 5 min. Twenty-four micrograms of plasmid DNA (HA-AT1R or HA-AT2R) was added to an additional 1.5 mL of OPTI-MEM and the two mixtures were combined and incubated for 20 min at room temperature. The mixture was then added into the culture medium. Twenty-four hours following transfection, the medium was removed and medium containing 200 μg/ml of geneticin was added. Receptor expression was confirmed by Fluorescence Activated Cell Sorting (FACS) Analysis, which is described in 2.3. The RASMC cell lines stably expressing HA-AT_1R and HA-AT_2R were established by geneticin selection (700 μg/ml).

The human embryonic kidney, HEK-293 clonal cell lines stably expressing HA-AT_1R (5.1 pmol/mg) and HA-AT_2R (5 pmol/mg) were established by geneticin selection (600 μg/ml) as described previously (31). The primary human aortic smooth muscle cells (HASMC, a gift from A. Majors, Department of Pathobiology, Lerner Research Institute

(LRI), Cleveland Clinic (CCF)) (Majors et al., 2002) were used between passage number 3 and 6. The AT_1R-expressing (0.9 pmol/mg) mouse atrial cardiomyocyte clonal line (HL-1-AT_1R) was established by geneticin selection (800 μg/ml) of HL-1 cells (White et al., 2004).

For expression of miR-483-3p, we used the RASMC, RASMC-AT_1R, and HEK-293T cell lines. The HEK-293T cell line is highly transfectable and has been transformed with the temperature sensitive SV40 T-antigen (Cat. No. CRL-11268; ATCC). Expression of miR-483-3p was carried out using the Amaxa Nucleofector™ Technology (Lonza, NJ, USA). The Nucleofector technology is a novel transfection technology especially designed for the needs of primary cells and difficult-to-transfect cell lines. It is a non-viral method, which is based on a unique combination of electrical parameters and cell-type specific solutions to allow DNA to directly enter the nucleus. This procedure was performed according to the manufacturer's instructions. Briefly, cells were trypsinized and counted using an automated cell counter (Cellometer; Nexcelom, MA, USA). Approximately 2 x 10^6 cells were suspended in Nucleofection Solution L (RASMCs and RASMCs-AT1R) (Lonza) or 1X phosphate buffered saline (PBS) (HEK-293T). Two micrograms of plasmid DNA was added to the suspension and the mixture was placed into a cuvette. The cuvette was placed into the Nucleofector and the appropriate program was started (RASMCs – program 33, HEK-293T cells – program 29). Post-nucleofection, 500 μl of medium was added to the cuvette and then pipetted gently into a 6-well culture dish. Approximately 72 hours post-nucleofection, the cells were passaged into a 100-mm culture dish, containing culture medium supplemented with

hygromycin. Clones were picked and expression of miR-483-3p was analyzed by RNA solution hybridization, which is described in 2.12. For each cell line utilized, a vector control was also made, which was hygromycin resistant.

A panel of cell lines was used to monitor miR-483-3p expression in various cell types. These cells included RASMC, RASMC-AT_1R, primary rabbit aortic smooth muscle cells (RASMC, a gift from Edward F. Plow, Department of Molecular Cardiology, LRI-CCF), rat thoracic aortic smooth muscle cells (A7R5; Cat. No. CRL-1444; ATCC), HASMC, rat coronary artery smooth muscle cells (RCASMC), primary bovine aortic endothelial cells (BAEC, a gift from Paul E. DiCorleto, Department of Cellular and Molecular Medicine, LRI-CCF), primary human umbilical vein endothelial cells (HUVEC, a gift from Paul E. DiCorleto, Department of Cellular and Molecular Medicine, LRI-CCF), breast adenosarcoma epithelial cells (MCF-7; Cat. No. HTB-22; ATCC), human adrenal carcinoma epithelial cells (NC1-H295R; Cat. No. CRL-2128; ATCC), mouse myoblast cells (C2C12; Cat. No. CRL-1772; ATCC), rat myocardial myoblast cells (H9C2; Cat. No. CRL-1446; ATCC), mouse atrial cardiomyocyte cells (HL-1), HL1-AT_1R, pig kidney epithelial cells (LLCPK-1, obtained from the Department of Molecular Cardiology, LRI-CCF), rat kidney epithelial cells (NRK52E; Cat. No. CRL-1571; ATCC), rat liver epithelial cells (WB; obtained from Cell Culture Core, Lerner Research Institute, Cleveland Clinic). Majority of the cell types were cultured to approximately 70% confluency in Dulbecco's Modified Eagle Media (DMEM; Invitrogen, Grand Island, NY, USA) supplemented with 10% fetal bovine serum (FBS; Thermo Fisher Scientific, Waltham, MA, USA). HUVECs were cultured in VascuLife

Basal Medium (Cat. No. LM-0002; Lifeline Cell Technology, MD, USA) supplemented with Lifeline's EnGS LifeFactors Kit (Cat. No. LS-1019; containing L-Glutamine, FBS, rH EGF, Hydrocortisone hemisuccinate, Heparin, and EnGS).

HEK-293T-miR483 and the vector control HEK-293T cells were grown in 6-well plates to approximately 50-60% confluency and transiently transfected by Attractene Transfection Reagent (Cat. No. 1051561; QIAGEN) according to the manufacturer's instructions. Briefly, 2 μg of plasmid DNA, harboring the 3'-UTR of select genes was diluted to 100 μl with OPTI-MEM. To the DNA, 4.5 μl of Attractene was added, mixed by gentle pipetting and incubated for 15 min at room temperature. The mixture was then added drop-wise to the culture medium and incubated until processing. In experiments where an antagomir to miR-483-3p was utilized (Cat. No. MIN0002173; QIAGEN), 0.005uM of the antagomir was mixed with the plasmid DNA and diluted to 100 μl with OPTI-MEM. Attractene was then added and the mixture was incubated for 15 min at room temperature.

The HEK-293, HEK-293T, HEK-293T-miR483, HEK-AT_1R, HEK-AT_2R, RASMC, RASMC-AT_1R, RASMC-AT_2R, RASMC-miR483, AND HASMC were cultured in DMEM supplemented with 10% FBS (fetal bovine serum (FBS; Thermo Fisher Scientific, Waltham, MA, USA) and 100 IU penicillin/streptomycin (Sigma-Aldrich). HL1-AT_1R cells were cultured in Claycomb media supplemented with 10% FBS and 1% penicillin/streptomycin solution (Sigma-Aldrich). The HEK-293T-miR483 and RASMC-miR483 clonal cell lines stably expressing pre-miR-483 were established by

hygromycin selection (100 μg/ml and 300 μg/ml, respectively). All cell types were cultivated at 37°C in a humidified atmosphere containing 5% CO_2.

2.3 FACS Analysis

After 48 hours of incubation, HA-AT_1R and HA-AT_2R transfected cells were processed for a FACS Analysis. The cells were washed with PBS and treated with cell dissociation solution for approximately 3-5 min until the cells lifted from the plate. Three milliliters of PBS was added and the cell solution was centrifuged at 700 RPM for 5 minutes. The cells were resuspended in 500 μl 1X PBS supplemented with 3% FBS. Twenty microliters of HA-fluorescein (FITC), High Affinity antibody (Cat. No. 1988506; Roche Molecular Biochemicals, IN, USA) was added to an additional 500 μl of PBS supplemented with 3% FBS. The cell suspension and HA-FITC solution were combined and incubated in the dark with end-over-end rocking at 4°C for 30 min. The cells were centrifuged at 700 RPM for 5 min and washed with 2 mL 1X PBS supplemented with 3% FBS. The cells were again centrifuged at 700RPM for 5 min and washed an additional time. The cells were resuspended in 3 mL sorting solution (1X PBS, 25 mmol HEPES), which had been filter-sterilized, and sorted. Sorted cells, positive for HA-AT_1R or HA-AT_2R were collected in 100-mm culture dishes containing growth medium supplemented with 700 μg/ml of geneticin for selection. The transfection efficiency of these cells was low, which is why the sort was necessary. The final population of cells collected exhibited receptor expression.

Figure 2.6. FACS analysis of transfected RASMCs. A) HA-AT_1R cell sort data. **B)** HA-AT_2R cell sort data. Black outline around events represents the gate used for sorting. FSC, forward scattered light; SSC, side scatter detector.

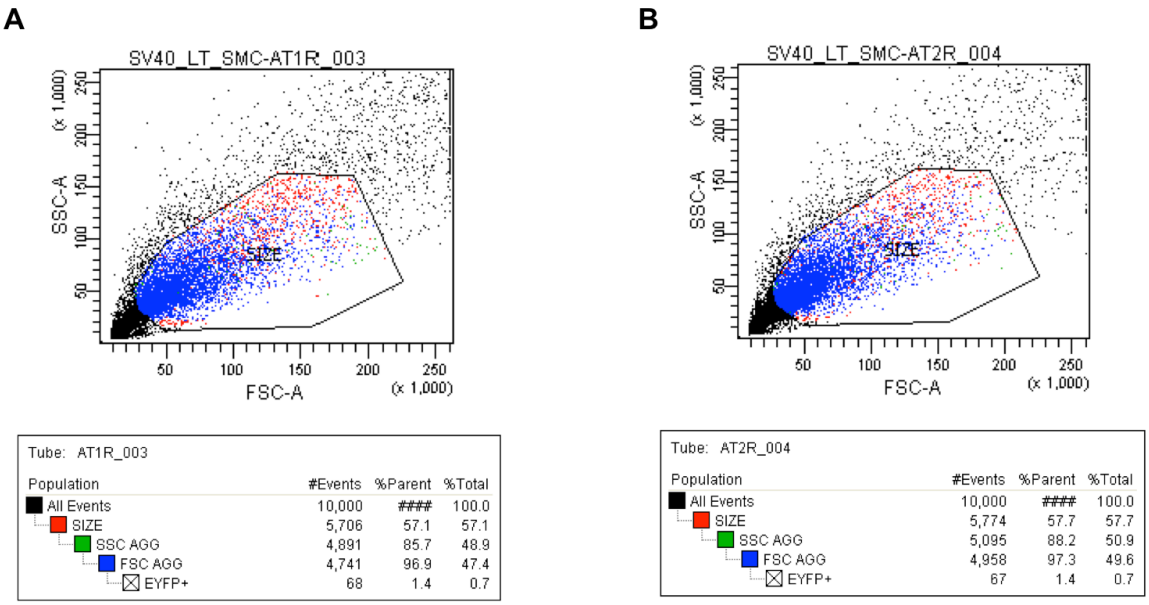

2.4 Immunocytochemistry

Following FACS analysis, RASMCs expressing HA-AT_1R or HA-AT_2R was plated onto fibronectin (Cat. No. 354008, BD Biosciences, CA, USA) coated coverslips and placed in 6-well culture dishes. Cells were cultured for 24 hours in DMEM supplemented with 10% FBS and switched to serum-free DMEM 18 hours before processing. Cells were washed twice with 1X PBS then fixed with 4% paraformaldehyde in 1X PBS for 15 min. Cells were washed 3 times with 1X PBS for 10 min each then permeabilized with 0.3% Triton X – 100 in 1X PBS for 20 min on ice. Cells were blocked with 5% nonfat dry milk in 1X PBS for 1 hour at room temperature then incubated overnight with mouse anti-HA monoclonal antibody (1:100) (Cat. No. 2362; Cell Signaling Technologies, MA, USA) in blocking buffer at 4°C. The following day, cells were washed and incubated with AlexaFluor 488 anti-mouse antibody (1:2000) (Cat. No. 2350; Cell Signaling Technologies) for 1 hour at room temperature in the dark. Cells were then washed and the coverslips were mounted onto glass slides with Vectashield with DAPI Nucleic Acid Stain (Cat. No. H1200; Vector Laboratories, CA, USA) for confocal microscopy.

Figure 2.7. Expression of HA-AT_1R and HA-AT_2R in RASMCs. A) Confocal image of HA-AT_1R RASMCs (magnification X60). **B)** Confocal image of HA-AT_2R RASMCs (magnification X60).

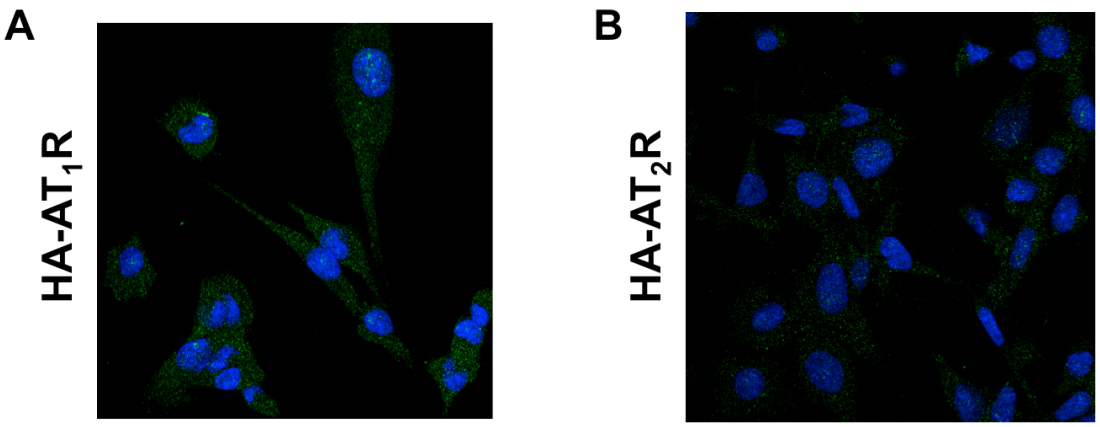

2.5 Ligand Treatment

When ≈70% confluent, cells were subjected to 4-hour starvation in serum-free DMEM. Then cells were treated with either 1μM [Sar^1]AngII or 1μM Losartan or Candesartan for a 24-hour time period. Untreated controls were kept in serum-free DMEM. After 24-hour treatment, cells were trypsinized and pelleted by centrifugation (800 x g). The cell pellets were washed with PBS, flash-frozen in liquid nitrogen and stored at -80°C until RNA was isolated.

2.6 Samples for miRNA Profiling

Characteristics and treatment conditions for twenty-three samples that were included in the miRNA profiling study are shown in Table II.II. The samples include a human embryonic kidney line expressing AT_1R or AT_2R, an immortalized rat aortic smooth muscle cell (RASMC) line expressing AT_1R or AT_2R and a mouse atrial cell line (HL-1) expressing AT_1R (White et al., 2004). Two independent human aortic smooth muscle cell (HASMC) samples were profiled to reduce potential bias that may result from the variability in primary cells (passage # 2-3). Hearts were obtained from age and gender matched transgenic (TG) mice over-expressing the human AT_1R under the mouse α-MHC promoter and corresponding littermate non-transgenic (NT) mouse lines in C3H and C57BL/6 genetic backgrounds (n = 3 each for TG and NT), which were previously obtained from Paradis *et al* (Paradis, 2000). The cardiac hypertrophy and HF phenotype were assessed by 1) measuring the heart weight to body weight ratio, 2) measuring ejection fraction and wall thickness by echocardiography (to monitor ejection fraction

and wall thickness), and 3) expression of BNP as an independent marker of heart failure as reported previously (Yue et al., 2010).

For primary comparison, correlations were made between the untreated and ligand treated cells or between NT and TG heart tissue samples. *Biological replicates control for biological diversity of a response, measure a quantity from different sources under the same condition and are often more powerful. Biological replicates in this study are defined as RNA isolated independently from multiple sources, each with a distinct genome under the same condition, AngII-activation of the AT_1R. Technical replicates are defined as RNA isolated from an AngII-responsive source with same genome under different treatment conditions.

Table II.II. Characteristics of biological and technical replicates* utilized in the microarray analysis.

Sample ID	Cell/Tissue Type	Experimental Condition	Measure of AT_1R Activation/Inhibition
SK-1	HEK-AT_1R	Untreated	Control
SK-2	HEK-AT_1R	AngII	ERK1/2, JAK, STAT3 phosphorylation
SK-3	HEK-AT_2R	Untreated	Control
SK-4	HEK-AT_2R	AngII	-
SK-5	HASMC	Untreated	Control
SK-6	HASMC	AngII	ERK1/2 phosphorylation
SK-7	HASMC	Losartan	ERK1/2 phosphorylation
SK-8	HASMC	Untreated	Control
SK-9	HASMC	AngII	ERK1/2 phosphorylation
SK-10	HASMC	Losartan	ERK1/2 phosphorylation
SK-11	HL1-AT_1R	Untreated	Control
SK-12	HL1-AT_1R	AngII	ERK1/2, JAK, STAT3 phosphorylation
SK-13	RASMC	Untreated	Control
SK-14	RASMC	AngII	ERK1/2 phosphorylation
SK-15	RASMC	Losartan	ERK1/2 phosphorylation
SK-16	RASMC-AT_1R	Untreated	Control
SK-17	RASMC-AT_1R	AngII	ERK1/2, STAT3 phosphorylation
SK-18	RASMC-AT_2R	Untreated	Control
SK-19	RASMC-AT_2R	AngII	-
SK-21	Whole heart (C3H NT)	Non-transgenic	Control
SK-22	Whole heart (C3H TG)	Cardiac-specific AT_1R transgene overexpression	ERK1/2, JAK, STAT3 phosphorylation, Cardiac Hypertrophy & HF Phenotype
SK-23	Whole heart (C57BL/6 NT)	Non-transgenic	Control
SK-24	Whole heart (C57BL/6 TG)	Cardiac-specific AT_1R transgene overexpression	ERK1/2, JAK, STAT3 phosphorylation, Cardiac Hypertrophy & HF Phenotype

2.7 Cardiac Tissue Harvest

The C3H and C57BL/6 transgenic mouse lines over-expressing the human AT_1R under the mouse α-MHC promoter were previously described by Paradis *et al* (Paradis, 2000). NT and TG mice were cared for in accordance with the *Guide for the Care and Use of Laboratory Animals* published by the US National Institute of Health (NIH publication No. 85-23, revised 1996) in the Biological Resources Unit of Lerner Research Institute. All experimental protocols described were reviewed and approved by the Animal Care and Use Committee at the Cleveland Clinic Foundation (CCF).

Parameters of cardiac structure and function in individual mice were determined by echocardiography and were correlated to expression of HF marker genes as previously reported (Yue et al., 2010). Briefly, echocardiography was performed on conscious mice without anesthetic. Doppler images were recorded using a 13 MHz linear transducer (Vivid 7; GE-Vingmed, Horten, Norway) placed at the left sternal border of the chest and analyzed by using Prosolv Cardiovascular Analyzer (v 3.5) software. Parameters obtained were left ventricular (LV) mass, ejection fraction (EF), a measure of left ventricular function; fractional shortening (FS), a measure of contractility, and wet heart weight/body weight (HW/BW) (Yue et al., 2010). Whole hearts from C57BL/6 and C3H mice with cardiac-specific AT_1R overexpression (TG) and non-transgenic (NTG) (Yue et al., 2010) mice were harvested. Upon removal, the heart was perfused in 0.1M KCL. Hearts were wrapped and flash-frozen in liquid nitrogen then maintained at -80°C until further analysis was performed.

2.8 RNA Isolation

Total RNA was isolated from heart tissue (n = 3 each for TG and NT), utilizing the RNeasy Fibrous Tissue Kit (Cat. No. 74704; QIAGEN) under RNase free conditions, according to manufacturer's protocol. Briefly, the heart was homogenized using a Mikro Dismembrator S (Sartorious Mechatronics Corp., Bohemia, NY, USA) in the RLT buffer with β-Mercaptoethanol added for 3 minutes at 1200 RPM. Proteinase K was added to the homogenate and incubated at 55°C for 20 minutes. The mixture was centrifuged at 20-25°C and 5000 x g for 5 minutes. The supernatant was transferred to a clean tube and 100% ethanol was added to each lysate. The sample was transferred to a midi spin column and centrifuged at 20-25°C and 5000 x g for 5 minutes, washed with the buffer provided then treated with a DNase I mixture at room temperature for 15 minutes. The column was washed and dried by centrifugation (at 20-25°C and 5000 x g) before the RNA was eluted with RNase free water.

Total RNA was isolated from cells using the miRNeasy Mini Kit (Cat. No. 217004; QIAGEN) under RNase free conditions, according to manufacturer's protocol. Briefly, the cell pellet was lysed in QIAzol Lysis Reagent at room temperature for 5 minutes. To the homogenate, chloroform was added and incubated for 3 minutes at room temperature. Following centrifugation for 15 minutes at 12,000 x g at 4°C, the upper aqueous phase was transferred to a new tube. To this 1.5 volumes of 100% ethanol was added and mixed and the mixture was pipetted into an RNeasy Mini spin column in a 2mL collection tube and centrifuged at ≥ 8000 x g for 15 seconds at room temperature. The sample was washed sequentially with buffers RWT and RPE and centrifuged for an

additional 15 seconds at ≥ 8000 x g each. The column was placed in a new collection tube and centrifuged at ≥14,000 x g for 1 minute. Finally, the column was transferred to a new 1.5mL collection tube and the RNA was eluted by centrifugation at 8000 x g in 50ul of RNase-free water.

A spectrophotometer reading was taken for each sample and a small aliquot was run on a 1% agarose gel to ensure RNA integrity (Figure 2.8). High-quality RNA preparations ($A_{260/280}$ ratio >1.8) were submitted to the Genomics Core Facility (http://www.lerner.ccf.org/services/gc/) for RNA processing.

Figure 2.8. Agarose gel fractionation of RNA samples for microarray. One microgram of total RNA was dissolved in H_2O in a total volume of 20 µl. Four microliters of 6X loading dye (Promega) was added. M, 2 µl of 1 Kb Plus DNA ladder (Life Technologies) mixed with 14 µl of TE buffer and 4 µl of 6X loading dye. Samples were run on a 1% agarose gel at 90 volts. Both 18S and 28S are visible on the gel for each RNA sample isolated (1-19).

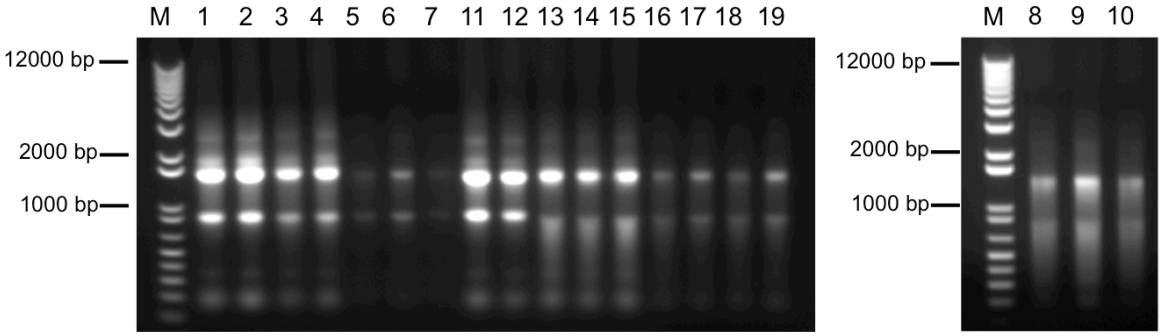

2.9 RNA Processing and Profiling

Two separate Mouse v2 MicroRNA Expression BeadChip arrays with UDG (Cat. No. MI-202–1124; Illumina, San Diego, CA, USA) were used for each sample, according to the manufacturers recommendations (Illumina MicroRNA Expression Profiling Assay Guide). This miRNA panel contained 656 assays to cover more than 96% of the miRNAs described in the miRBase release 12 database (http://www.mirbase.org).

The chemistry utilized by the miRNA BeadArray is available at http://www.illumina.com/downloads/MicroRNAAssayWorkFlow.pdf. Five hundred nanograms of total RNA was polyadenylated, and then converted into cDNA using a biotinylated oligo-dT primer with a universal primer-tag sequence at its 5' end. This was followed by annealing of a miRNA-specific oligonucleotide pool (MSO) which consists of three parts: a universal PCR priming site at the 5' end, an address sequence complementary to a capture sequence on the BeadArray, and a microRNA-specific sequence at the 3' end. Extension of MSO was facilitated by addition of a polymerase, but only if their 3' bases were complementary to the cognate sequence in the cDNA template. Common primers were used to amplify the cDNA templates; the primer complimentary to the BeadArray was fluorescently labeled. The single-stranded PCR product was hybridized to the Sentrix Array Matrix (SAM), where the labeled strand binds to the bead on the array containing the complementary address sequence. The SAMs were imaged using an Illumina iScan Reader, which measures the fluorescence intensity at each addressed bead location. Intensity files were analyzed using BeadStudio version 3.1.1.

Expression levels were depicted as an average signal value and was compared with untreated or NTG samples as baseline.

2.10 Statistical Analysis of miRNA Microarray Data

Raw data were read and preprocessed in BeadStudio and exported for further data processing and analysis in R (www.r-project.org). Initially, three datasets were generated for all of the samples: 1) the raw expression dataset exported directly from BeadStudio (containing 656 genes); 2) the normalized dataset, which was obtained based on the raw dataset after force-positive background correction, log2 transformation, and quantile normalization (containing 655 genes); 3) the quality control (QC) filtered dataset, which was obtained based on the normalized dataset by selecting present probes using the detection threshold of 0.05 (containing 610 genes).

In BeadStudio, we performed one sample to one sample comparisons using differential analysis with parameters set up as 'quantile normalization, subtract background'. All differential expression was compared with a reference group (*Ref Group*) with Illumina custom Error Model. *Raw p-values* were from the *Diff Pval* column of the Differential Expression Genes results. *Fdr p-values* were obtained by applying multiple testing corrections using Benjamini and Hochberg False Discovery Rate (a Fdr p-value of <0.05 was considered statistically significant).

Following quality control analysis, the expression and p-values were read in R for further graphical representation of the results (e.g., box plot, MA plot, volcano plots,

scatter plots). Hierarchical clustering was made on the three preprocessed datasets based on correlation distances in all cases. Comparisons were made for all the sample pairs (untreated versus treated) and plotted as volcano plots, showing the relationship between –log10 (p-value) and log2 (fold change) of all the genes in each comparison. Raw p-values and fold change were calculated. Genes were categorized as significantly expressed if their raw p-value was <0.001 and the fold change was $\geq$ threshold or $\leq$ 1/threshold. The threshold value of 1.2 – 1.3 cut-off for the threshold was adopted in our analyses, as recommended by Illumina (Chen et al., 2008).

2.11 RT-qPCR Analysis

The miScript PCR system (Cat. No. 218073, 218060; QIAGEN) was utilized according to the manufacturer's protocol for miRNA validation in independent VSMC samples treated with AngII and Candesartan (Figure 2.9 A). Two micrograms of template RNA was mixed with the 5x miScript RT buffer, RNase-free water, and the miScript reverse transcriptase mix. The reaction was incubated for 60 minutes at 37°C followed by heating the samples at 95°C for 5 minutes. For the qPCR, a reaction mix containing 2x QuantiTect SYBR Green PCR master mix, 10x miScript Universal Primer, 10x miRNA specific primer, and RNase-free water was prepared. MiRNA-specific primers were designed to amplify the mature miRNA (Table II.III.) The cDNA from the reverse transcription step was dispensed into the individual wells of a 96-well PCR plate and appropriate volumes of the reaction mix were added. The plate was briefly centrifuged at 1000 x g to collect the reaction at the bottom of each well and qPCR was started using the Applied Biosystems 7500 real-time cycler (Applied Biosystems, CA,

USA). The thermal cycling parameters used for the qPCR reaction were an initial denaturing step of 15 min at 95°C followed by 40 cycles of 94°C for 15 sec, 55°C for 30 sec, and 70°C for 30 sec. C_T values recorded were analyzed, following normalization to RNU6 (Cat. No. MS00033740), an endogenous control, and standardization to the untreated samples.

The miScript PCR system (QIAGEN) was also utilized for mRNA quantitation in VSMC-miR-483 and VSMC-vector control samples (Figure 2.9 B). Two micrograms of template RNA was used for cDNA synthesis as detailed above. For the qPCR, a reaction mix containing 2x QuantiTect SYBR Green PCR master mix, 10x QuantiTect Primer Assay, and RNase-free water was prepared. The QuantiTect Primer Assays (QIAGEN) utilized included forward and reverse primers targeting AGT (Cat. No. QT00177478), ACE-1 (Cat. No. QT00180439), ACE-2 (Cat. No. QT02480100), AGTR2 (Cat. No. QT01081864) (Table II.III.) The cDNA from the reverse transcription step was dispensed into the individual wells of a 96-well PCR plate and appropriate volumes of the reaction mix were added. The plate was briefly centrifuged at 1000 x g to collect the reaction at the bottom of each well and qPCR was started using the Applied Biosystems 7500 real-time cycler (Applied Biosystems). The thermal cycling parameters used for the qPCR reaction were identical to those used for miRNA quantitation. C_T values recorded were analyzed, following normalization to GAPDH (Cat. No. QT00199633), an endogenous control.

The comparative CT method ($\Delta\Delta C_T$) of analysis was utilized to calculate fold change in expression for all RT-qPCR data. This method involves comparing the C_T values of the samples of interest (i.e., ligand treated sample) with a control (i.e., untreated sample). The C_T values of both the control and the samples of interest are normalized to an appropriate endogenous housekeeping gene. $\Delta\Delta C_T = \Delta C_T$ sample $- \Delta C_T$ reference. Where, ΔC_T sample is the C_T value for any sample normalized to the endogenous housekeeping gene and ΔC_T reference is the C_T value for the control also normalized to the endogenous housekeeping gene. The fold change in gene expression is determined by calculating $2^{-\Delta\Delta C_T}$.

For quantitation of mRNA in RASMC-AT_1R, one microgram of total RNA was used for first-strand cDNA synthesis using the First Strand cDNA Synthesis Kit for RT-PCR (AMV+) (Cat. No. 11483188001; Roche Diagnostics, IN, USA). Real-time qPCR was performed on the Applied Biosystems 7500 real-time cycler (Applied Biosystems) using QuantiTect SYBR Green PCR kit (QIAGEN), with the primers described below (Table II.IV.). The thermal cycling parameters used for the qPCR reaction were an initial denaturing step of 10 min at 95°C followed by 40 cycles of 95°C for 15 sec, 60°C for 1 min. C_T values recorded were analyzed, following normalization to GAPDH gene expression.

Figure 2.9. miScript principle. A) MiRNAs are polyadenylated by poly (A) polymerase and subsequently converted into cDNA by reverse transcriptase with oligo-dT priming. The cDNA is then used for real-time quantification of mature miRNA (using a miRNA-specific primer and the miScript Universal Primer). **B)** MiRNAs are converted into cDNA by reverse transcriptase using both oligo-dT and random priming. The cDNA is used for real-time quantification of mRNA (using a QuantiTect Primer Assay). From the *miScript PCR System Handbook* (2nd Ed. 2009).

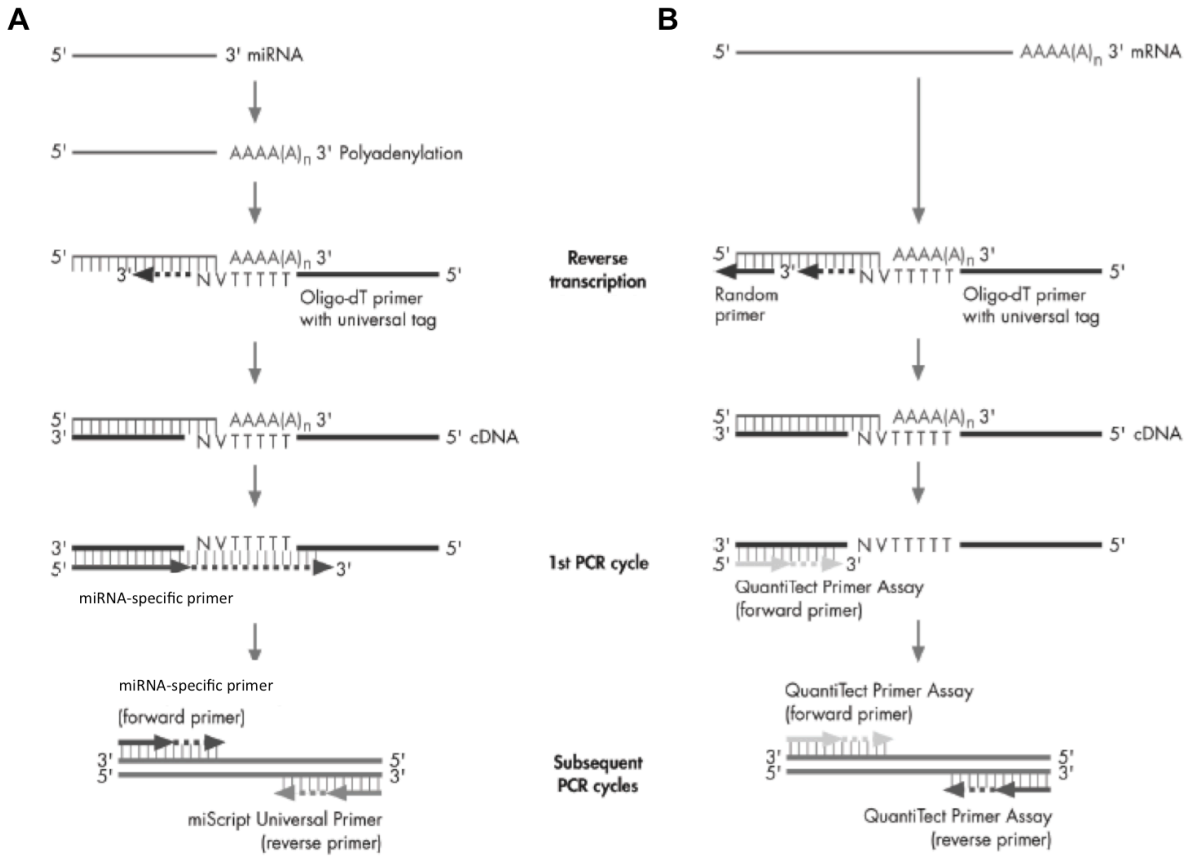

Table II.III. MiRNA-specific primers.

Primer	Sequence (5' → 3')	bp	%GC	TM
miR-675-5p	TGGTGCGGAAAGGGCCCA	18	66.67	70.47
miR-343	GTCTCCCTTCATGTGCCCA	19	57.90	62.10
miR-669C	GGGGATAGTTGTGTGTGGATGT	22	50.00	60.93
miR-467b*	GGGGATATACATACACACACCA	22	45.46	57.10
miR-218-1*	GGGAAACATGGTTCCGTCAAG	21	52.39	63.79
miR-32	GGGGGTATTGCACATTACTAAGT	23	43.48	58.42
miR-682	GGCTGCAGTCACAGTGAAGT	20	55.01	59.06
miR-1187	GGGGTATGTGTGTGTGTATGTG	22	50.00	58.56
miR-297b-3p	GGGGTATACATACACACATACC	22	45.46	53.43
miR-188-5p	GCATCCCTTGCATGGTGGA	19	57.90	65.41
miR-106a:9.1	GGGCAAAGTGCTAACAGTGCA	21	52.39	63.55
miR-466g	GGGATACAGACACATGCACAC	21	52.39	58.88
miR-325	GGGGTTTATTGAGCACCTCCTA	22	50.00	61.52
miR-467a*, -467d*	GGGGATATACATACACACACC	21	47.62	54.15
miR-1198	GTATGTGTTCCTGGCTGGC	19	57.90	59.11
miR-301b	GGGCAGTGCAATGGTATTGTC	21	52.39	62.60
miR-21*	CAACAGCAGTCGATGGGC	18	61.12	61.45
miR-483-3p	TCACTCCTCCCCTCCCGT	18	66.67	63.07
miR-297c	GGGGATGTATGTGTGCATGTAC	22	50.00	60.01
miR-669f	GGGGCATATACATACACACACA	22	45.46	58.18
miR-208a	GGGGATAAGACGAGCAAAAAGC	22	50.00	63.33
miR-33	GGGGGTGCATTGTAGTTGCATT	22	50.00	65.18

Table II.IV. Oligonucleotide primers for mRNA quantitation.

Primer	Sequence (5' → 3')	bp	% GC	TM
IGF2 Total sense	CGCTTCAGTTTGTCTGTTCG	20	50.00	60.00
IGF2 Total antisense	GCAGCACTCTTCCACGATG	19	58.00	61.00
IGF2 P1 sense	TTGCCACACAGTTTTCCCATTT	22	41.00	64.00
IGF2 P1 antisense	TCCCAAATCAGACCCTTGTC	20	50.00	60.00
IGF2 P2 sense	CAAGTGGATTAATTATACGCTTTCTG	26	35.00	60.00
IGF2 P2 antisense	AGAGGCGGGTAGGCTCAC	18	67.00	60.00
IGF2 P3'-UTR sense	GCGTCCCCAGGTTTGCAGCT	20	65.00	69.09
IGF2 P3'-UTR antisense	GCGGCAGGCACAGGTGACAT	20	65.00	69.19
GAPDH sense	AGCCAAAAGGGTCATCATCTCTG	23	47.83	63.86
GAPDH antisense	CATGAGTCCTTCCACGATACCAAA	24	45.84	64.38

2.12 RNA Solution Hybridization Assay

In addition to RT-qPCR, a RNA solution hybridization assay was used to detect and visualize miRNA expression. A DNA oligonucleotide template was designed to be specific for miR-483-3p and contain a T7 promoter sequence at the 3' end for the action of RNA polymerase (Figure 2.8 A). The experimental probe was generated using the miRvana Probe Construction kit (Cat. No. AM1550; Life Technologies) via *in vitro* transcription, which resulted in a 33-nucleotide RNA probe with a 25-nucleotide protected sequence. A positive control probe (for miR-16, provided by Life Technologies) was generated in parallel and produced a 36-nucleotide RNA probe with a 22-nucleotide protected sequence. According to the manufacturer's instructions, 2 µl of T7 promoter primer**,** 6 µl of DNA hybridization buffer, and 100 µM of the oligonucleotide template was mixed and heated to 70°C for 5 min. The mixture was then left at room temperature for 5 minutes to allow hybridization to occur. To the hybridized oligonucleotides, 2uL of 10X Klenow reaction buffer**,** 2uLof 10X dNTP mix**,** 4uL of nuclease-free water, and 2uL of Exo-Klenow was added. The solution was mixed by gentle pipetting and incubated at 37°C for 30 min. At room temperature, 1 µl each of the double-stranded DNA template, 10X transcription buffer, 10 mM ATP, 10 mM GTP, and 10 mM CTP were combined. To that mixture, 10 mM ^{32}P labeled UTP and 2 µl T7 RNA polymerase were added. The solution was mixed by gently pipetting and incubated at 37°C for 10 min. The template DNA was removed by digesting the transcription reaction with 1 µl DNase I at 37°C for 10 min.

Following transcription, an equal amount of Gel Loading Buffer II was added to the DNase-treated reaction and heated at 98°C for 3 min. The newly synthesized probe was then gel purified at 25 mAmp. A 12% polyacrylamide gel (13x15cm x0.75mm – 7.2 g Urea, 1.5 mL 10X Tris/Borate/EDTA, 4.5 mL 40% 19 acrylamide:1 bis acrylamide, 11 mL nuclease-free water, 75 µl 10% ammonium persulfate, 15 µl TEMED). After electrophoresis the gel fragment containing the full-length transcript was excised. One hundred microliters of probe elution buffer was added to the gel slice and incubated at 37°C for 30 minutes. The probe elution buffer, containing the eluted RNA was transferred to a clean microfuge tube and the elution step was repeated with an additional 100 µl of probe elution buffer. The elution fractions were pooled and the cpm/µl of the recovered RNA was determined by scintillation counting.

For hybridization of the miR-483-3p-specific probe in total RNA samples isolated from cells of interest, we utilized the miRvana miRNA Detection Kit (Cat. No. AM1552; Life Technologies) according to the manufacturer's instructions. A master mix containing, 10 µl of 2X hybridization buffer, 5 x 10^4 cpm of labeled RNA probe, 2 µg sample RNA, enough yeast RNA to make 5 µg total RNA, and nuclease-free water up to 20 µl was prepared. Two no-target controls were also prepared for each RNA probe. These consisted of 5 x 10^4 cpm labeled probe, 5 µg yeast RNA, 10 µl 2X hybridization buffer, and nuclease-free water up to 20 µl. The experimental and control tubes were heated at 98°C for 3 min and then incubated at 42°C overnight to allow hybridization to occur.

Excess probe and unhybridized temple RNA was digested with 150 µl RNase A/T1 (1:100 dilution in RNase digestion buffer) at 37°C for 45 min the following day. One control (for each RNA probe) was not RNase digested. The RNase was inactivated with RNase inactivation/PPT solution and the probe and hybridized target were precipitated with 100% ethanol at -20°C for 1 hour. The samples were centrifuged at 10, 000 x g for 15 min at 4°C and the supernatant was carefully removed. The protected fragments were air dried for 10 min at room temperature before suspending in gel loading buffer. For experimental samples and the RNase digested controls, the pellets were resuspended in 5 µl of buffer. For the undigested control, the pellet was resuspended in 10 µl of buffer and then diluted 1:4 in addition loading buffer. Each tube was vortexed for 15 sec then incubated at 98°C for 3 min. Each sample was loaded into a pre-run 15% denaturing polyacrylamide gel. The gel was exposed to an intensifying screen overnight at room temperature and imaged the following day using a Storm 860 Phosphorimager (GE Healthcare Life Sciences, PA, USA). Mean band intensity values were determined using the ImageQuant TL Software (v. 2003.03; GE Healthcare Life Sciences) for all samples.

Figure 2.10. Detection of short RNA molecules by solution hybridization. A) The DNA oligonucleotide template was designed to be specific to miR-483-3p (magenta) with an 8 base T7 promoter sequence at the 3' end (green). The stretch of T residues (blue) will generate an antisense RNA probe with a stretch of As, which can't be cleaved by RNase A/T. *In vitro* transcription generated a probe specific for miR-16 and a probe specific for miR-483-3p. **B)** Hybridization of the radiolabeled RNA probes was carried out in a step-wise fashion, which resulted in detection of miR-483-3p that could be visualized on a denaturing polyacrylamide gel.

A

5’ – TCACTCCTCTCCTCCCGTCTTTTTTCCTGTCTC – 3’

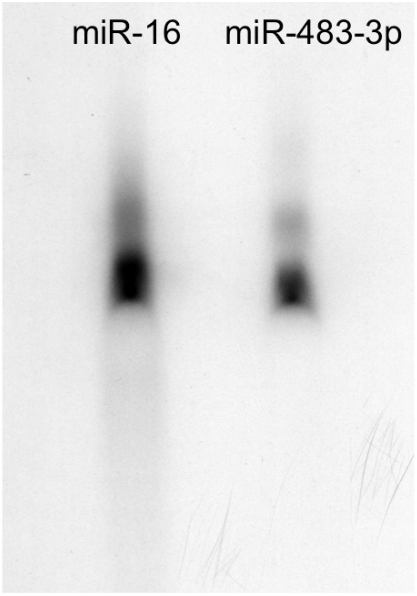

B

Target RNA + ^{32}P labeled antisense miR-483-3p

↓

Heat Denaturation (98°C)

↓

Hybridization (42°C)

↓

RNase A/T1 digestion (remove unhybridized RNA and excess probe)

↓

Hybridized probe and target are recovered
(RNase inactivation/nucleic acid precipitation)

↓

Analysis via denaturing polyacrylamide gel electrophoresis

2.13 Pharmacological Kinase Inhibition

RASMC-AT_1R cells subjected to serum starvation were treated with individual kinase inhibitors for a 1-hour period. Inhibitors to PKC (5μM – 1-O-Hexadecyl-2-O-methyk-rac-glycerol, Santa Cruz Biotechnology, Santa Cruz, CA, USA), MEK1 (10μM – PD98059, Cell Signaling Technology), JAK (5μM – JAK Inhibitor 1; EMD Chemicals, Darmstadt, Germany), JNK (1μM SP600125, A.G.Scientific, San Diego, CA, USA), and p38 (1μM – SB203580; Cell Signaling Technology) were reconstituted in DMSO. Following kinase inhibition, the cells were treated with 1μM [Sar^1]-AngII for 5 minutes and then harvested (see 3.3 for specific details). For RNA isolation, the cells were treated for 24-hour with 1μM [Sar^1]-AngII.

2.14 Protein Isolation

Cells were placed on ice and washed three times with PBS, scraped from the plate, and pelleted by centrifugation at 3900 RPM for 5 min at 4°C. Cells were lysed in 1mL 1X PBS, containing 50μl PopCulture Reagent (Cat. No. 71187; Novagen, Darmstadt, Germany), 100 U of Benzonase Nuclease (Cat. No. 70664; Novagen), 100X protease inhibitor cocktail (Cat. No. P8340; Sigma-Aldrich), and 100X phosphatase inhibitor cocktail (Cat. No. 78426; Thermo Scientific, Rockford, IL, USA). The lysates were incubated on ice for one hour then a standard Bradford Assay for protein estimation was performed using bovine serum albumin (BSA) as a concentration standard.

2.15 Analysis of ERK1/2 and STAT3 Phosphorylation

Fifty μg of total protein isolated from RASMC-AT_1R cells was used for the Western blotting assay. Fractions were boiled for 5 minutes and separated by SDS-PAGE (10%), and transferred onto a nitrocellulose membrane. After blocking in 150 mM of NaCl buffered with 10 mM of Tris and containing 0.1% Tween 20 and 5% milk powder, the membrane was incubated overnight in primary antibody specific for phospho-ERK $44/42^{MAPK}$ (Cat. No. 4370; Cell Signaling Technology) or phospho-STAT3 (Y705) (Cat. No. 9131; Cell Signaling Technology). The membrane was washed and then incubated in 1:5000 diluted IgG secondary antibody labeled with HRP for 1h. Using ECL Plus Western Blotting Reagent (GE Healthcare Life Sciences) specific bands were detected. The same blots were subsequently stripped and re-probed for total ERK $44/42^{MAPK}$ (Cat. No. 9102; Cell Signaling Technologies) and total STAT3 (Cat. No. 9139; Cell Signaling Technology). Densitometry analysis was performed for each experiment. Mean band intensity values (of phosphorylation activity) were determined using the Kodak® 1D Image Analysis Software (Version 3.6.5 K2 – 1B5331010; Eastman Kodak Company, Rochester, NY, USA). Phospho-ERK1/2 and phospho-STAT3 values were normalized to the total protein for each and compared to the untreated controls to determine the percent kinase inhibition.

2.16 MiRNA Target Prediction

MiRNAs represent an important class of small non-coding RNAs that regulate gene expression by targeting messenger RNAs. Various Internet-based databases exist, of which 4 were utilized for this study that allow for determining potential mRNA targets

of known miRNAs. TargetScan is based on conserved seed pairing of miRNAs to their targets in animals (Lewis et al., 2005). DIANA-microT 3.0 is an algorithm based on several parameters calculated individually for each microRNA and it combines conserved and non-conserved microRNA recognition elements into a final prediction score (Maragkakis et al., 2009). The PITA database incorporates the role of target-site accessibility, as determined by base-pairing interactions within the mRNA, in microRNA target recognition (Kertesz et al., 2007). Microcosm Targets uses the miRanda algorithm to identify potential binding sites for a given miRNA in genomic sequences. The current version uses dynamic programing alignment to identify highly complementary sites (Griffiths-Jones et al., 2006).

The 3'-UTR of Renin (ENSG00000143839), Renin Receptor (ENSG00000182220), AGT (ENSG00000135744), ACE-1 (ENSG00000159640), ACE-2 (ENSG00000130234), Chymase 1 (CMA1; ENSG00000092009), AGTR1 (ENSG00000144891), AGTR2 (ENSG00000180772), AT4 Receptor (ENSG00000113441), and $Ang^{(1-7)}$ Receptor (ENSG00000130368) was uploaded into each of the above described databases. The miRNAs that were predicted to bind as well as the region to which they would bind were recorded.

2.17 Luciferase Reporter Assay

Changes in luciferase gene expression were measured using the Dual-Glo Luciferase Assay System (Cat. No. E2920; Promega). The principle of luciferase gene expression is detailed in Figure 2.10. Cells were grown in 6-well culture dishes. Forty-

eights hours following transfection of the psiCHECK-2-3'-UTR DNA constructs, the cells were trypsinized, re-suspended in culture medium, and counted using the Cellometer. The cells were then seeded onto a poly-L-lysine coated 96-well, white, flat-bottom culture plate. Approximately 50,000 cells suspended in 50 µl of culture medium were plated per well and in triplicate. An additional 50 µl of medium was added to the wells and the cells were allowed to adhere overnight.

The following day, 75 µl of Dual-Glo Luciferase Assay Reagent was added to each well and incubated with gently rocking for 1 hour at room temperature. Relative luminescence units (RLUs) for Firefly were read using the FlexStation 3 Multi-Mode Microplate Reader (Molecular Devices, LLC, CA, USA) at 0.5 sec integration and from the bottom of the plate. Immediately following completion of the first luminescence reaction, 75 µl of Dual-Glo Stop and Glo reagent was added to each well. The plate was incubated with gentle rocking for 1 hour at room temperature. *Renilla* luminescence was then read. The ratio of Firefly to *Renilla* luminescence was calculated for each well. The ratio of the sample well(s) was normalized to the ratio of the control well(s).

Figure 2.11. Principle of luciferase gene expression. A) The psiCHECK-2 vector facilitates monitoring of changes in expression of a target gene fused to a reporter gene. *Renilla* luciferase is used as the primary reporter gene, and the 3'UTR is cloned into a multiple cloning region located downstream of the *Renilla* translational stop codon. Initiation of the RNAi process by synthetic miRNAs results in cleavage and subsequent degradation of the fused mRNA target. Measuring decreases in *Renilla* activity provides a convenient way of monitoring the RNAi effect. A second reporter gene, firefly luciferase allows normalization of *Renilla* luciferase expression**.** From Promega product resources. **B)** Biochemistry of firefly and *Renilla* luciferase expression. Converting the chemical energy of luciferin oxidation through an electron transition, forming the product molecule oxyluciferin, produces light. Firefly luciferase, a monomeric 61kDa protein, catalyzes luciferin oxidation using ATP-Mg2+ as a cosubstrate. Likewise, *Renilla* luciferase, a monomeric 36kDa protein, catalyzes coelenterazine oxidation by oxygen to produce light.

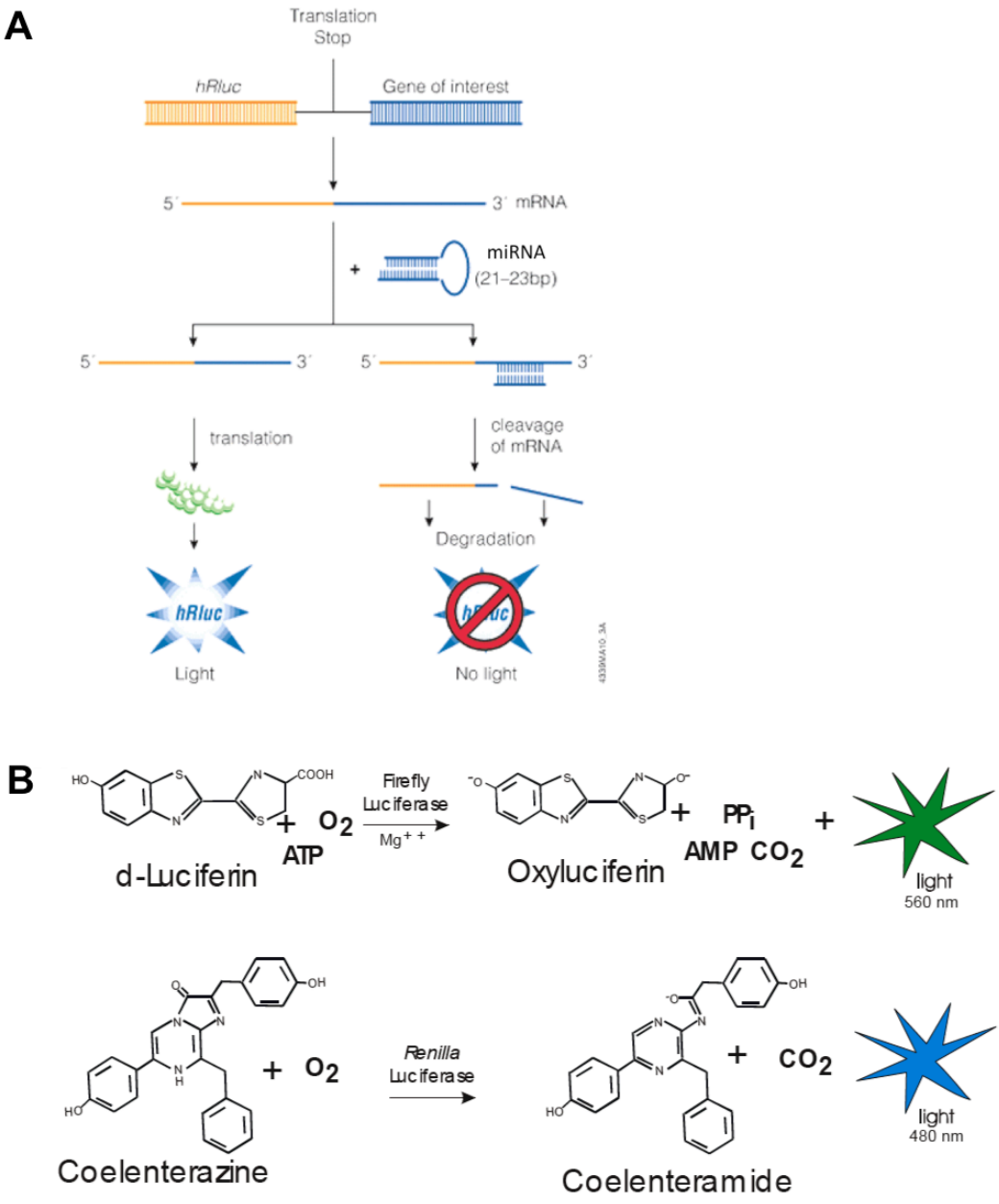
A
Translation
Stop
hRluc
Gene of interest
5´
3´ mRNA
miRNA
(21–23bp)
5´
3´
5´
3´
translation
cleavage
of mRNA
Degradation
hRluc
Light
No light
B
d-Luciferin
+ O2
ATP
Firefly
Luciferase
Mg++
Oxyluciferin
+ PPi
AMP CO2
+
light
560 nm
Coelenterazine
+ O2
Renilla
Luciferase
Coelenteramide
+ CO2
light
480 nm

2.18 Analysis of Endogenous RAS Components

Fifty μg of total protein isolated from RASMC-miR483 cells was used for the Western blotting assay. Fractions were boiled for 5 minutes and separated by SDS-PAGE (10%), and transferred onto a nitrocellulose membrane. After blocking in 150 mM of NaCl buffered with 10 mM of Tris and containing 0.1% Tween 20 and 5% milk powder, the membrane was incubated overnight in primary antibody specific for AGT (Cat. No. ab108334; Abcam, MA, USA), ACE-1 (Cat. No. ab134709; Abcam), ACE-2 (Cat. No.AF933 R & D Systems, MN, USA and Cat. No. ab108252; Abcam) or AGTR2 (Cat. No. AT21-A and AT22-A; Alpha Diagnostic International, TX, USA). The membrane was washed and then incubated in 1:5000 diluted IgG secondary antibody labeled with HRP for 1h. Using ECL Plus Western Blotting Reagent (Amersham Biosciences) specific bands were detected. The same blots were subsequently stripped and re-probed for actin (Cat. No. MAB1501; Millipore, MA, USA). Densitometry analysis was performed for each experiment. Mean band intensity values were determined using the Kodak® 1D Image Analysis Software (Eastman Kodak Company). Total protein values were normalized to actin and compared to the vector control samples.

2.19 Wound Healing Assay

The wound-healing assay was performed using Ibidi silicone culture inserts (Cat. No. 80241; Ibidi, LLC, WI, USA) according to the manufacturer's instructions. The silicone insert creates a 500 μm cell-free gap (Figure 2.12. A). Following coating with fibronectin, the wells of a 6-well plate were washed twice with 1X PBS and the insert was adhered. Cells were trypsinized, counted, and resuspended in growth medium.

Approximately 7 x 10^5 cells in 70 µl of medium were seeded into each well of the insert and allowed to attach overnight. The following day, the insert was removed with sterilized forceps and the cells were washed gently with 1X PBS three times. The cells were cultured in medium supplemented with 0.5% FBS and 1% penicillin/streptomycin, in addition to 1 µM [Sar^1]AngII and/or 1 µM Candesartan.

The progression of wound healing was monitored over a 24-hour period of time using a Leica DMI6000 inverted microscope (at 10X magnification) equipped with dual Hamamatsu cameras (ImageEM and Orca-R2) EM-CCD, an environmental chamber (heat/CO_2 incubator), and a motorized stage for capturing multiple time-lapse fields simultaneously. Images were collected in transmitted light mode every 15 minutes at five different locations along the wounded area. The area of the wound at time zero and 8 hours compared to the total area was quantified using ImagePro Plus 7.0 (Media Cybernetics, MD, USA) (Figure 2.12 B). Briefly, the images were processed using the large spectral filter and converted to grayscale. Additionally, each image was processed for morphological characteristics to fill the gaps and enlarge protrusions to connect objects that are close together. The cell-free area and the area containing cells were measured for each image. The percent wound area was normalized to the total area for each image.

Figure 2.12. Wound-healing principle and analysis. A) The Ibidi silicone insert creates a 500 µm defined cell-free gap that prevents leakage during cultivation and no material being left behind after the insert's removal. **B)** The area of the wound at time zero and 8 hours compared to the total area was quantified for each image (red).

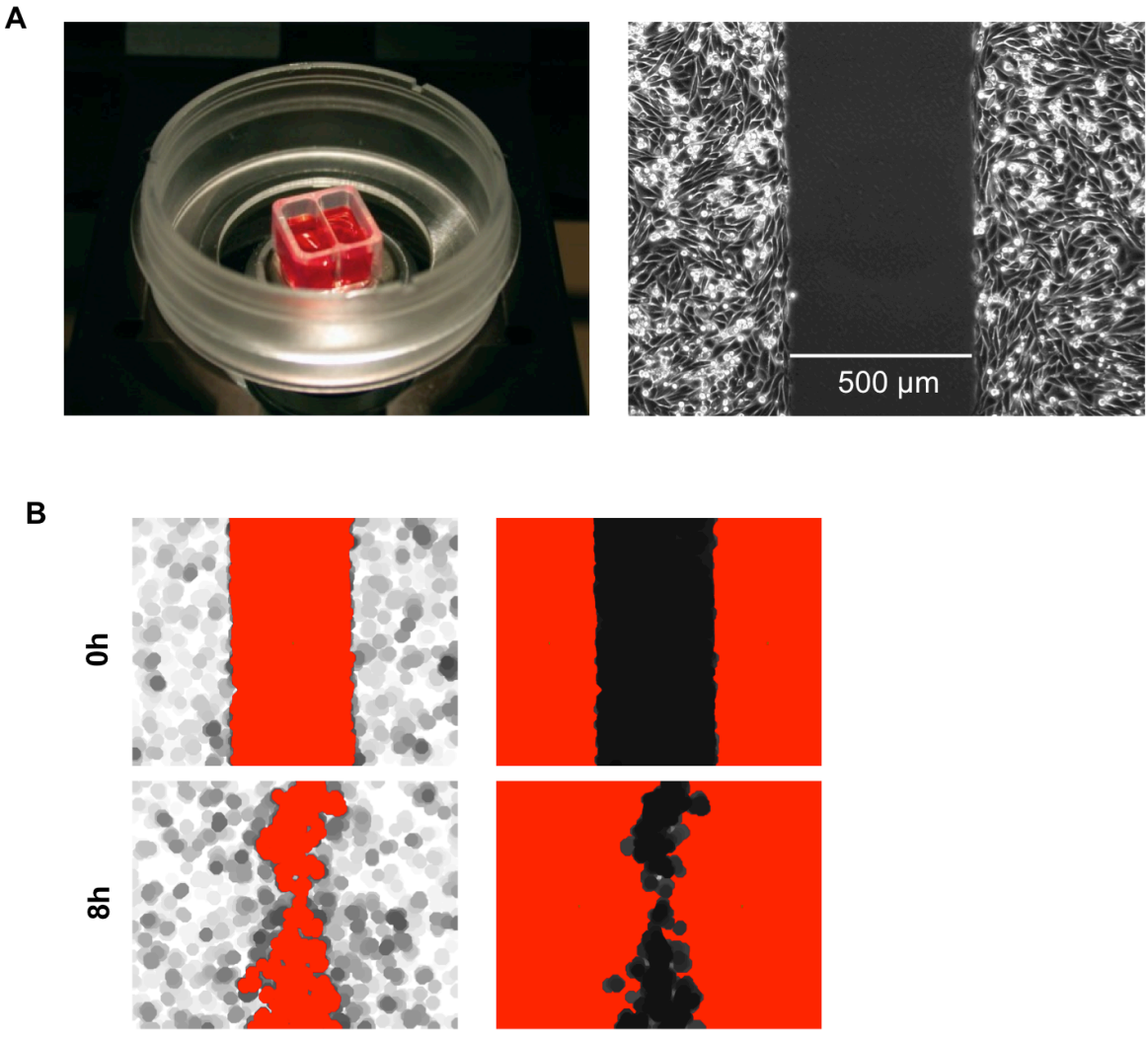

2.20 Statistical Analysis

All data are expressed as mean ± SEM (n = 3 experiments performed under identical conditions). Statistical analyses were performed using GraphPad Prism© with an unpaired Student t-test. A p-value <0.05 was considered statistically significant.

CHAPTER III

GLOBAL MIRNA EXPRESSION PROFILING

3.1 Introduction

In order to fully understand AT_1R-mediated gene expression, the expression profile of miRNAs in various tissues and disease states must be elucidated. Of significant importance is documenting the AngII-regulated miRNA profile for cardiovascular cells, as a means to enhance our knowledge of AngII biology. This study was designed for global miRNA expression profiling in biological replicates following chronic AngII activation.

It is estimated that a single miRNA orchestrates post-transcriptional regulation of ≈100-200 genes in a cell, either by inhibiting the translation or by promoting the degradation of specific target mRNAs. A comprehensive knowledge of AngII-regulated miRNAs is therefore exceedingly useful in the context of RAS physiology and pathology. The miRNA profiles presented here may bridge the gap in our knowledge concerning the molecular basis of pathogenesis during chronic RAS activation, which increases

angiotensinergic risk associated with morbidity and mortality from cardiovascular diseases. In many clinical settings, targeting RAS is an important therapeutic paradigm. Our study provides insights regarding how RAS-targeted therapies may affect miRNAs.

3.2 Distinct AngII-regulated miRNA Expression Profiles

We performed a genome-wide comparative analysis of miRNA expression in 23 small RNA libraries prepared from mice hearts (Yue et al., 2010) and cell types of human or rodent origins (Table II.II. for sample details). Selection of these samples resulted in adequate biological and technical replicates for making global comparisons. The comparisons of the cardiac HL-1 line and heart tissue, HL-1 and VSMCs, VSMCs from different species (i.e., human and rat), and cell lines from three species (i.e., human, rat and mouse) served as biological replicates. As indicated in Table II.II, in all of the biological replicates exposure to AngII led to activation of AT_1R-mediated signal transduction involving the JAK2/STAT3 and the ERK1/2 pathways (Figure 3.1). Samples not treated with AngII or treated with AT_1R-specific inhibitors (Losartan or Candesartan) and angiotensinergic stimulation through the AT_2R are technical replicates included in the analysis for validating the AT_1R-specific regulation of miRNAs. Each library was constructed from high-quality RNA preparations.

Figure 3.1. Measure of AT_1R activation and inhibition. A) The signal transduction pathway activation of the AT_1R by AngII. **B)** Activation of the receptor was confirmed by ERK1/2 phosphorylation (pERK1/2) and in some cases, JAK2-mediated STAT3 phosphorylation (pSTAT3), following treatment with 1 μM AngII. In addition, inhibition of AT_1R signaling was monitored in the presence of the AT_1R specific antagonist, losartan or the AT_1R specific inverse agonist, candesartan. Total ERK1/2 (tERK1/2) and total STAT3 (tSTAT3) are shown as loading controls.

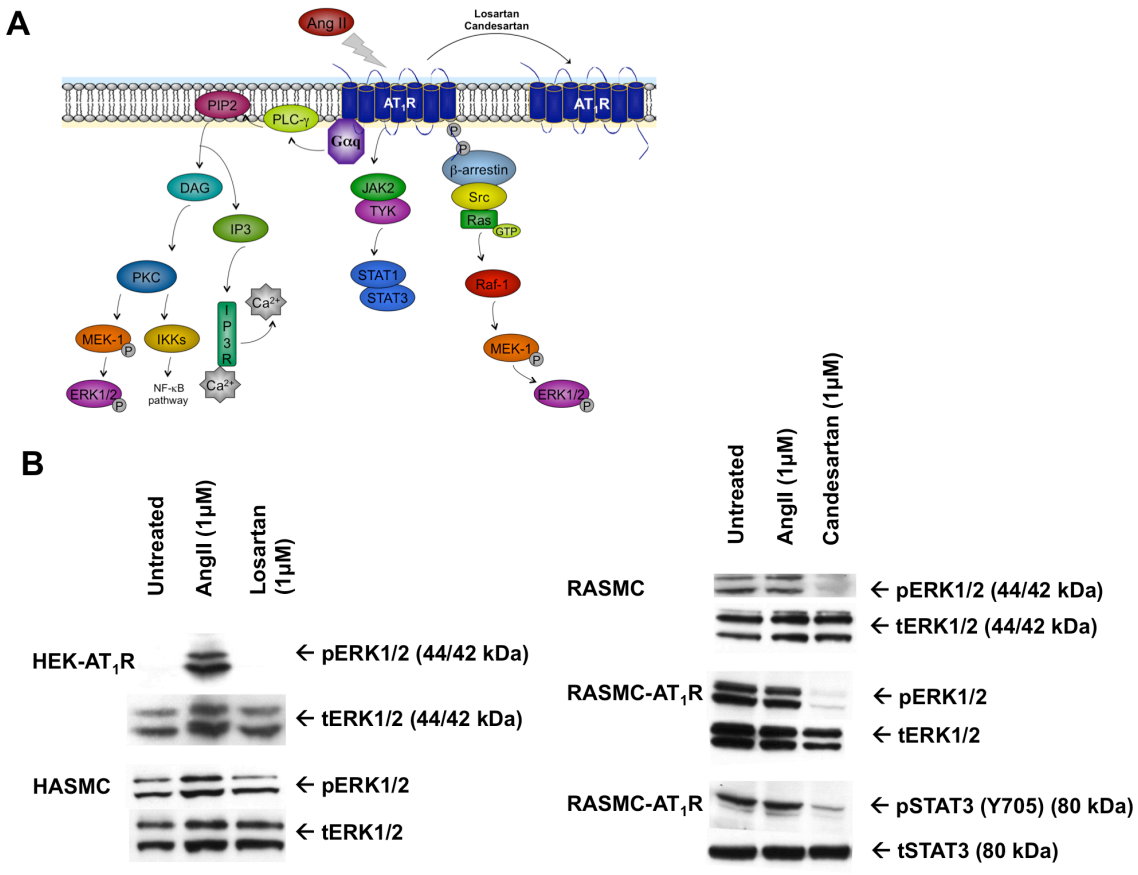

Under angiotensinergic stimulation, the miRNA expression profiling microarray data obtained from these samples was quantile normalized, background corrected, and $\log_2$ transformed (see methods). In addition, quality control measures were taken for selecting probes, using the detection threshold of $p < 0.05$. Altogether 655 miRNAs were detected in our array analysis, of which 610 miRNAs met quality control measures described in the methods. AngII regulated the expression of 468 miRNAs in all samples.

Most AngII-regulated miRNAs are evolutionarily conserved in related species and some even show conservation between invertebrates and vertebrates (Pasquinelli et al., 2000, Lagos-Quintana et al., 2001, Lau et al., 2001, Lee and Ambros, 2001). Our data provide evidence for AngII-regulated expression of 323 human, 334 mouse, and 109 rat miRNAs. When orthology relationships for these miRNAs are evaluated, 355 miRNA genes appear to be AngII-responsive in the mouse and rat genomes. Importantly, 237 of the AngII-regulated miRNA genes expressed in mouse and rat have human orthologs (as determined from miRBase 19). Of these, 168 human orthologs are clearly responsive to AngII in the two human cell types analyzed, demonstrating that genome-wide AngII-regulation of miRNA expression is robust.

Global trends evident in the miRNA expression array data are highlighted in Figure 3.2. The heat map shown, includes 468 miRNAs, which are significantly altered in at least one of the 13 experimental comparisons shown. A non-redundant set of 357 miRNAs appeared in two or more models listed in Table II.II and 111 miRNAs are unique to a cell type or a treatment condition. The comparison showed that 52% of the

microRNAs were downregulated, while 48% of the microRNAs were upregulated. The miRNA number observed as a differential response in transgenic mouse hearts [192 and 166], HASMCs [181], and HL-1-AT_1R cells [144] is comparable to the response detected in the engineered HEK- kidney cell line [233]. The number of AngII-responsive miRNAs in the immortalized RASMC line [60] is lower and is slightly increased [70] upon AT_1R overexpression (Tables III.I. – III.VII.).

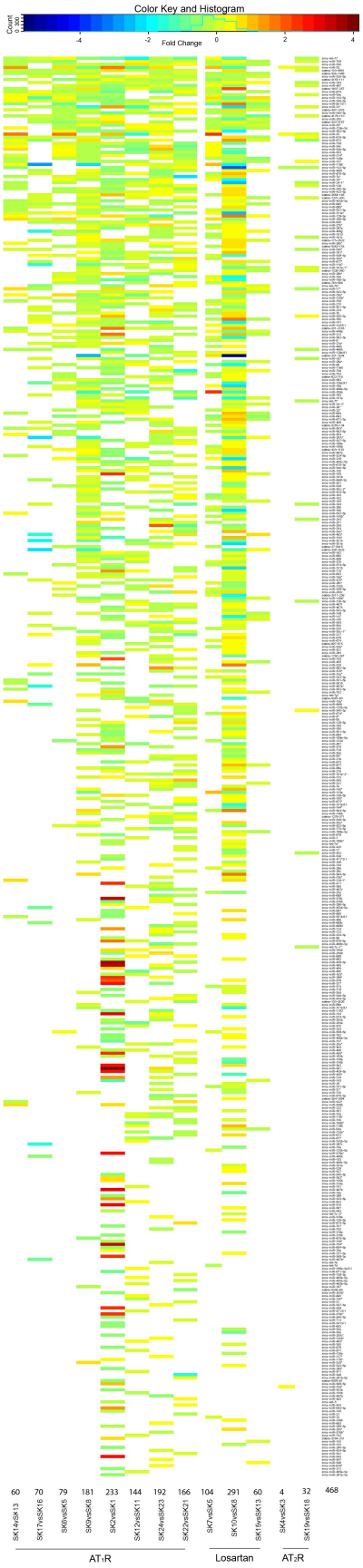

Figure 3.2. Heat map depicting miRNA expression across AngII activated samples. Fold change in miRNA gene expression between untreated and AngII/AT_1R samples (columns 1-8). In addition, comparisons for untreated and Losartan treated samples (columns 9-11) and untreated and AngII/AT_2R samples (columns 12 and 13) are shown as controls. A blue color indicates that the miRNA is downregulated in response to the treatment condition (see Table 1 for descriptions of treatments). A red color indicates that the miRNA is upregulated. The gradient scale above depicts all colors within the expression range, +4 to -4 fold change. The numbers at the bottom of each column indicates the number of miRNAs differentially regulated in a specific treatment condition.

Table III.I. AngII responsive miRNAs in transgenic mouse hearts (C57BL/6).

let-7b*	miR-1192	miR-130b	miR-146b	miR-181d
let-7c-1*	miR-1198	miR-130b*	miR-147	miR-185
let-7e	miR-122	miR-134	miR-153	miR-187
let-7g*	miR-124	miR-141	miR-154	miR-188-5p
let-7i*	miR-125a-3p	miR-142-3p	miR-155	miR-18b
miR-106a:9.1	miR-125b*	miR-142-5p	miR-15a*	miR-191*
miR-10a	miR-127*	miR-144	miR-15b*	miR-193b
miR-10b*	miR-128	miR-144:9.1	miR-16*	miR-194
miR-1186	miR-128a:9.1	miR-145*	miR-181a-2*	miR-196a
miR-1191	miR-129-3p	miR-146a	miR-181c	miR-200b
miR-200c	miR-222	miR-29b*	miR-326	miR-342-5p
miR-201	miR-224	miR-301a	miR-33	miR-343
miR-203	miR-24-1*	miR-30a*	miR-33*	miR-345-3p
miR-206	miR-25	miR-30b*	miR-330	miR-34b-3p
miR-208b	miR-26b*	miR-30c-1*	miR-331-3p	miR-34b-5p
miR-20a*	miR-27b*	miR-30e*	miR-335-3p	miR-34c
miR-21*	miR-28*	miR-31*	miR-335-5p	miR-34c*
miR-214*	miR-297a	miR-32	miR-337-3p	miR-362-3p
miR-218	miR-297c*, a*	miR-320	miR-337-5p	miR-362-5p
miR-221	miR-299*	miR-324-3p	miR-338-3p	miR-365
miR-375	miR-423-3p	miR-466d-3p	miR-467h	miR-505
miR-376a	miR-423-5p	miR-466f	miR-489	miR-542-3p
miR-376b	miR-425*	miR-466g	miR-494	miR-547
miR-376b*	miR-434-3p	miR-466h	miR-495	miR-574-3p
miR-376c	miR-434-5p	miR-466i	miR-497	miR-582-3p
miR-377	miR-450b-3p	miR-467a	miR-500	miR-582-5p
miR-378*	miR-455	miR-467a*, d*	miR-501-3p	miR-592
miR-381	miR-465c-5p	miR-467c	miR-501-5p	miR-615-3p
miR-409-5p	miR-466a-5p	miR-467e	miR-503	miR-669d
miR-411	miR-466c-5p	miR-467f	miR-504	miR-669f
miR-671-3p	miR-708	miR-874	solexa-1837-257	solexa-4179-110
miR-674	miR-709	miR-877*	solexa-200-2167	solexa-622-718
miR-675-3p	miR-744	miR-878-5p	solexa-201-2163	
miR-676	miR-744*	miR-9	solexa-2564-185	
miR-676*	miR-770-5p	miR-9*	solexa-27-9416	
miR-677	miR-7a	miR-93*	solexa-284-1594	
miR-683	miR-7a*	solexa-103-3961	solexa-3062-153	
miR-685	miR-7b	solexa-1278-371	solexa-308-1456	
miR-689	miR-801:9.1	solexa-1328-360	solexa-3253-144	
miR-700	miR-872	solexa-1780-267	solexa-4153-111	

Table III.II. AngII responsive miRNAs in transgenic mouse hearts (C3H).

let-7b*	miR-107	miR-137	miR-181a-2*	miR-193*
let-7i*	miR-10b	miR-138	miR-181b	miR-196a
miR-1	miR-1187	miR-139-3p	miR-181d	miR-199a-3p
miR-101a	miR-1198	miR-140	miR-182	miR-199a-5p
miR-101a*	miR-122	miR-142-3p	miR-183	miR-199b, b,*
miR-101a:9.1	miR-125b-3p	miR-146a	miR-184	miR-19a
miR-101b	miR-128	miR-146b	miR-18a*	miR-200c
miR-106a	miR-128a:9.1	miR-154	miR-190	miR-201
miR-106b	miR-129-5p	miR-17	miR-191*	miR-204
miR-106b*	miR-133a*	miR-181a-1*	miR-193	miR-206
miR-208a	miR-222	miR-30c-1*	miR-338-3p	miR-34c
miR-20b	miR-224	miR-30c-2*	miR-338-5p	miR-34c*
miR-21	miR-26b*	miR-31	miR-340-3p	miR-351
miR-210	miR-291b-5p	miR-322*	miR-342-3p	miR-362-5p
miR-212	miR-296-5p	miR-324-5p	miR-343	miR-409-3p
miR-214*	miR-297a	miR-330	miR-345-3p	miR-411*:9.1
miR-215	miR-29a*	miR-330*	miR-346	miR-421
miR-217	miR-29c	miR-335-3p	miR-34a	miR-423-5p
miR-218	miR-301a	miR-335-5p	miR-34b-3p	miR-425
miR-221	miR-30b*	miR-337-5p	miR-34b-5p	miR-433
miR-434-3p	miR-490	miR-669f	miR-7a*	solexa-1328-360
miR-450a-5p	miR-497	miR-672	miR-801:9.1	solexa-1837-257
miR-450b-3p	miR-501-5p	miR-673-5p	miR-872*	solexa-231-1844
miR-451	miR-503	miR-674*	miR-874	solexa-308-1456
miR-455*	miR-503*	miR-675-3p	miR-877	solexa-4153-111
miR-466d-3p	miR-504	miR-689	miR-877*	solexa-447-1003
miR-466f	miR-505	miR-699	miR-92b	solexa-5306-86
miR-467a*, d*	miR-541	miR-703	miR-93	solexa-783-586
miR-467c	miR-582-3p	miR-708	miR-93*	
miR-467h	miR-582-5p	miR-709	miR-99b*	
miR-470	miR-615-3p	miR-712	solexa-03-3961	
miR-483	miR-668	miR-715	solexa-1201-400	
miR-483*	miR-669c	miR-770-5p	solexa-1278-371	
miR-485*	miR-669d	miR-7a	solexa-130-3526	

Table III.III. AngII responsive miRNAs in primary HASMC culture.

let-7f*	miR-10a*	miR-130b	miR-146b*	miR-185
let-7g*	miR-10b*	miR-132	miR-149	miR-186
let-7i*	miR-1186	miR-133a	miR-150	miR-187
miR-101a	miR-1187	miR-138	miR-16*	miR-188-3p
miR-101a*	miR-1198	miR-141	miR-181a-1*	miR-188-5p
miR-101b	miR-1224	miR-142-5p	miR-181b	miR-18a*
miR-101b:9.1	miR-125a-3p	miR-144:9.1	miR-181c	miR-18b
miR-106a:9.1	miR-125b*	miR-145*	miR-181d	miR-191*
miR-106b*	miR-126-3p	miR-146a	miR-182	miR-192
miR-107	miR-129-3p	miR-146b	miR-183	miR-193
miR-193*	miR-204	miR-224	miR-29b	miR-32
miR-194	miR-206	miR-24-1*	miR-29b*	miR-320
miR-195	miR-208a	miR-24-2*	miR-29c*	miR-324-5p
miR-196a	miR-20b	miR-26b*	miR-301b	miR-325
miR-196b	miR-21*	miR-27a*	miR-30a	miR-325*
miR-197	miR-210	miR-27b*	miR-30a*	miR-326
miR-19a	miR-212	miR-28*	miR-30b*	miR-33
miR-19a*	miR-214*	miR-293	miR-30c-1*	miR-33*
miR-19b	miR-219	miR-297a	miR-30c-2*	miR-330
miR-201	miR-22*	miR-297c*, a*, b-	miR-30d	miR-331-3p
miR-331-5p	miR-34a	miR-423-3p	miR-466i	miR-503*
miR-335-5p	miR-34b-3p	miR-423-5p	miR-467a	miR-532-5p
miR-337-5p	miR-34b-5p	miR-449a	miR-483*	miR-504
miR-339-3p	miR-34c	miR-450b-3p	miR-484	miR-542-5p
miR-339-5p	miR-34c*	miR-451	miR-489	miR-509-5p
miR-340-3p	miR-362-3p	miR-465c-5p	miR-491	miR-574-5p
miR-340-5p	miR-362-5p	miR-466a-5p	miR-497	miR-582-5p
miR-342-5p	miR-378	miR-466f	miR-499	miR-592
miR-345-3p	miR-384-3p	miR-466f-3p	miR-501-5p	miR-598
miR-345-5p	miR-384-5p	miR-466g	miR-503	miR-615-5p
miR-652	miR-709	miR-9	solexa-1780-267	solexa-403-1161
miR-674	miR-718	miR-92b	solexa-1837-257	solexa-4153-111
miR-675-5p	miR-720	miR-93	solexa-200-2167	solexa-4179-110
miR-676	miR-760	miR-96	solexa-2011-236	solexa-447-1003
miR-679	miR-7a*	miR-99a	solexa-231-1844	solexa-622-718
miR-682	miR-7b	miR-99b	solexa-239-1823	solexa-783-586
miR-685	miR-801:9.1	miR-99b*	solexa-2564-185	solexa-897-515
miR-690	miR-872	solexa-103-3961	solexa-27-9416	
miR-694	miR-874	solexa-1201-400	solexa-3062-153	
miR-703	miR-877*	solexa-1328-360	solexa-308-1456	
miR-706	miR-878-5p	solexa-173-2522	solexa-3253-144	

Table III.IV. AngII responsive miRNAs in HL-1-AT_1R cell line.

let-7f*	miR-1198	miR-138	mmu-miR-181c	miR-199a-3p:9.1
let-7i*	miR-125a-3p	miR-139-5p	mmu-miR-183*	miR-199b*
miR-1	miR-125b*	miR-140*	mmu-miR-188-3p	miR-19a
miR-101a	miR-125b-3p	miR-141	mmu-miR-188-5p	miR-19a*
miR-101a:9.1	miR-126-3p	miR-150	mmu-miR-190b	miR-19b
miR-107	miR-128	miR-15a*	mmu-miR-191*	miR-200a
miR-10a	miR-129-3p	miR-16*	mmu-miR-192	miR-208a
miR-1187	miR-130b	miR-181a-1*	mmu-miR-194	miR-20a*
miR-1191	miR-133a*	miR-181a-2*	mmu-miR-196a	miR-21*
miR-1196	miR-133b	miR-181b	mmu-miR-196b	miR-210
miR-219	miR-301a	miR-339-5p	miR-378	miR-465c-5p
miR-22*	miR-301b	miR-340-5p	miR-421	miR-466f-3p
miR-24-1*	miR-30b*	miR-342-5p	miR-423-3p	miR-467f
miR-24-2*	miR-32	miR-343	miR-423-5p	miR-470
miR-27a*	miR-33	miR-345-3p	miR-425*	miR-471
miR-27b*	miR-33*	miR-345-5p	miR-450b-5p	miR-471:9.1
miR-28*	miR-330	miR-34b-5p	miR-463*	miR-486
miR-29a*	miR-331-3p	miR-34c	miR-465a-3p family	miR-490
miR-29b	miR-335-5p	miR-362-5p	miR-465a-5p	miR-491
miR-29b*	miR-339-3p	miR-365	miR-465b-5p	miR-497
miR-499	miR-709	miR-873	solexa-1201-400	solexa-5067-90
miR-500	miR-715	miR-878-3p	solexa-1278-371	solexa-622-718
miR-503	miR-741	miR-878-5p	solexa-130-3526	solexa-783-586
miR-505	miR-742	miR-880	solexa-173-2522	solexa-897-515
miR-542-3p	miR-743b-3p	miR-9	solexa-1837-257	
miR-671-3p	miR-770-5p	miR-9*	solexa-201-2163	
miR-677	miR-801:9.1	miR-92b	solexa-231-1844	
miR-684	miR-802	miR-96	solexa-2564-185	
miR-690	miR-871	miR-99b*	solexa-4153-111	
miR-699	miR-872	solexa-103-3961	solexa-447-1003	

Table III.V. AngII responsive miRNAs in HEK-AT_1R kidney cell line.

let-7b*	miR-10b*	miR-129-3p	miR-141	miR-154
let-7d*	miR-1186	miR-129-5p	miR-142-3p	miR-154*
let-7f*	miR-1187	miR-132	miR-142-5p	miR-155
let-7g*	miR-1192	miR-134	miR-143	miR-16*
let-7i	miR-1197	miR-135b	miR-144	miR-17*
let-7i*	miR-1224	miR-137	miR-144:9.1	miR-183*
miR-101b	miR-124	miR-138	miR-145	miR-184
miR-106a:9.1	miR-125b*	miR-138*	miR-146b*	miR-187
miR-107	miR-128	miR-139-5p	miR-147	miR-188-3p
miR-10a*	miR-128a:9.1	miR-140	miR-150	miR-18a*
miR-190	miR-19a*	miR-210	miR-24-1*	miR-296-3p
miR-190b	miR-200a	miR-211	miR-24-2*	miR-296-5p
miR-191*	miR-200b	miR-212	miR-26b*	miR-297a
miR-192	miR-200b*	miR-214*	miR-27a*	miR-299
miR-193	miR-200c*	miR-215	miR-27b*	miR-299*
miR-193b	miR-203	miR-216b	miR-28*	miR-29a
miR-194	miR-204	miR-217	miR-290-3p	miR-29a*
miR-195	miR-208b	miR-22*	miR-291a-3p	miR-29b*
miR-196a*	miR-20b	miR-223	miR-293	miR-29c*
miR-199a-5p	miR-21*	miR-23a	miR-295*	miR-302b
miR-30a	miR-330	miR-342-5p	miR-369-5p	miR-382*
miR-30b*	miR-330*	miR-345-3p	miR-375	miR-409-3p
miR-30c-1*	miR-331-3p	miR-345-5p	miR-376a*	miR-409-5p
miR-30c-2*	miR-335-3p	miR-34a	miR-376b	miR-410
miR-32	miR-335-5p	miR-34b-3p	miR-376c	miR-411
miR-323-3p	miR-337-5p	miR-34c	miR-376c*	miR-411*:9.1
miR-324-5p	miR-338-3p	miR-362-3p	miR-377	miR-423-5p
miR-328	miR-338-5p	miR-362-5p	miR-379	miR-449b
miR-33	miR-339-3p	miR-363	miR-381	miR-450b-3p
miR-33*	miR-341:9.1	miR-369-3p	miR-382	miR-451
miR-465c-5p	miR-540-3p	miR-668	miR-760	solexa-1837-257
miR-466a	miR-540-5p	miR-671-5p	miR-762	solexa-200-2167
miR-466f	miR-542-3p	miR-676	miR-7b	solexa-2011-236
miR-466h	miR-542-5p	miR-679	miR-801:9.1	solexa-201-2163
miR-467a	miR-543	miR-684	miR-872*	solexa-2054-231
miR-467h	miR-551b	miR-690	miR-873	solexa-2564-185
miR-485*	miR-551b:9.1	miR-692	miR-874	solexa-3062-153
miR-486	miR-574-5p	miR-694	miR-878-3p	solexa-403-1161
miR-487b	miR-582-3p	miR-702	miR-878-5p	solexa-4153-111
miR-494	miR-592	miR-703	miR-879	solexa-4179-110
miR-495	miR-615-3p	miR-706	miR-92b	solexa-5067-90
miR-497	miR-615-5p	miR-707	miR-96	solexa-5593.81
miR-499	miR-652	miR-708	miR-98	
miR-501-5p	miR-653	miR-715	miR-99a	
miR-503	miR-654-3p	miR-718	miR-99b*	
miR-532-3p	miR-654-5p	miR-719	solexa-103-3961	
miR-539	miR-667	miR-744*	solexa-173-2522	

Table III.VI. AngII responsive miRNAs in immortalized RASM cell line.

let-7i*	miR-19a*	miR-331-5p	miR-532-3p	miR-872
miR-101a*	miR-214*	miR-345-5p	miR-542-5p	miR-874
miR-107	miR-218-1*	miR-34a	miR-551b	miR-99b*
miR-1198	miR-24-1*	miR-34b-3p	miR-551b:9.1	solexa-103-3961
miR-125a-3p	miR-26b*	miR-34b-5p	miR-615-5p	solexa-1837-257
miR-128	miR-32	miR-34c	miR-652	solexa-201-2163
miR-129-3p	miR-322*	miR-449a	miR-684	solexa-308-1456
miR-138	miR-324-5p	miR-449b	miR-685	solexa-4153-111
miR-142-3p	miR-33	miR-450b-3p	miR-706	solexa-4179-110
miR-146a	miR-330	miR-466h	miR-709	solexa-447-1003
miR-17*	miR-330*	miR-503*	miR-7a*	
miR-188-5p	miR-331-3p	miR-504	miR-801:9.1	

Table III.VII. AngII responsive miRNAs in RASMC-AT_1R cell line.

let-7b*	miR-188-5p	miR-21*	miR-467a*, d*	miR-92b
met-7i*	miR-193	miR-212	miR-467b*	miR-99b*
miR-101a*	miR-194	miR-335-3p	miR-483*	solexa-103-3961
miR-106a:9.1	miR-196b	miR-335-5p	miR-489	solexa-1201-400
miR-10a*	miR-20b	miR-339-3p	miR-500	solexa-173-2522
miR-1186	miR-142-5p	miR-345-5p	miR-501-5p	solexa-200-2167
miR-1187	miR-149	miR-34a	miR-503*	solexa-239-1823
miR-1198	miR-21*	miR-425*	miR-615-5p	solexa-2564-185
miR-125b*	miR-212	miR-450b-3p	miR-669c	solexa-308-1456
miR-141	miR-217	miR-450b-5p	miR-669f	solexa-4179-110
let-7b*	miR-224	miR-466f	miR-685	
let-7i*	miR-27a*	miR-466f-3p	miR-709	
miR-142-5p	miR-297c	miR-335-3p	miR-760	
miR-149	miR-297c*, a*, b-3p	miR-335-5p	miR-872	
miR-17*	miR-301b	miR-466g	miR-874	
miR-184	miR-325	miR-466h	miR-877*	
miR-187	miR-330*	miR-466k	miR-878-5p	

We further observed that AT_1R stimulation with AngII affects multiple human miRNA clusters, defined as regions of the genome harboring two or more miRNAs that are transcribed from adjacent genes within 10 kb of each other. We observed that 24 known miRNA clusters in the human genome (Zhang et al., 2012, Yu et al., 2006), located on 14 different chromosomes respond to AT_1R stimulation as shown by only one or a few specific miRNAs expressed from each cluster (Table III.VII.).

In addition to determination of AngII-regulated miRNAs previously determined, we identified 30 new miRNAs that have only been predicted in the Solexa sequencing database (www.switchtoi.com) with unclear functional annotation (Table III.VIII.). Only the mature sequence is known for each miRNA species reported, which was annotated from the illumina-sequencing chip.

Table III.VIII. Human miRNA clusters differentially regulated upon AngII treatment.

Cluster #	miRNA Cluster	Chromosome	miRNAs Differentially Regulated in Untreated v. AngII models
1	miR-29b-2 ~ 29c	1	miR-29c
2	miR-200	1	miR-200b, miR-200a
3	miR-181b-1-181a-1	1	miR-181b-1
4	miR-466-467-669	2	miR-466f-1, miR-669d, miR-467b*, miR-466c-1, miR-467e, miR-466a, miR-466d, miR-297a
5	miR-15b ~ 16-2	3	miR-15b, miR-16-2
6	miR-106b-93-25	5	miR-106a, miR-93, miR-25
7	miR-29b-1 ~ 29a	6	miR-29a
8	miR-290 ~ 293 ~ 295	7	miR-290, miR-291a, miR-291b, miR-293
9	miR-25 ~ 93 ~ 106	7	miR-25, miR-93, miR-106b
10	miR-23a ~ 27a ~ 24-2	8	miR-23a, miR-27a*, miR-24-2*
11	let-7a-1 ~ 7f ~7d	9	let-7f*
12	miR-8 ~ 141 ~ 200	12	miR-200c, miR-141
13	miR-379 ~ 411 ~ 758	12	miR-379, miR-329, miR-667, miR-668, miR-154, miR-410
14	miR-23b-27b-24-1	22	miR-27b*, miR-24-1
15	miR-16-1 ~ 15a	13	miR-15a
16	miR-17-19a-92a-1	13	miR-17*, miR-18a, miR-19a, miR-20a,
17	miR-106a-92a-2	14	miR-92a-1*, miR-106a, miR-18b, miR-20b, miR-19b-2*, miR-92a-2*, miR-363
18	miR-222 ~ 221	X	miR-222, miR-221
19	miR-98 ~ let-7f-2	X	miR-98
20	miR-181c-181d	X	miR-181c, miR-181d
21	miR-99b ~ 125 ~ let-7e	19	miR-99b, miR-125, let-7e
22	miR-23a ~ 27a ~ 24-2	19	miR-24-2, miR-23a, miR-27a
23	miR-99a ~ let-7c	19	miR-99a, let-7c
24	let-7a-3 ~ 7b ~ miR-4763	21	let-7b

Table III.IX. Novel miRNAs regulated in response to AT_1R activation by AngII.

	miRNA	Mature Sequence
1	Solexa-103-3961	TCCTCGTTAGTATAGTGG
2	Solexa-1201-400	GGTCAAGAGGCGCCTGGGAAC
3	Solexa-1278-371	GTAAAGGCTGGGCTTAGACGTGG
4	Solexa-130-3526	CAAGAAGTAGTTTAATTAGA
5	Solexa-1328-360	ACGCCCTTCCCCCCCTTCTTCA
6	Solexa-173-2522	ACCGTGGCTTTCGATTGTTACT
7	Solexa-1780-267	GAACATCACAGCAAGTCTGTGCT
8	Solexa-1837-257	TATGGAGGTCTCTGTCTGACTT
9	Solexa-200-2167	GTCAGGATGGCCGAGCGGTCTAAG
10	Solexa-201-2163	ACCTTGGCTCTAGACTGCTTACT
11	Solexa-2011-236	AATCAGCAAGTATACTGCCCTA
12	Solexa-2054-231	AGCGAGGTTGCCCTTTGTATATT
13	Solexa-231-1844	ATCTCCATAGTGACCA
14	Solexa-239-1823	CTAGCCCTAGCCCTACA
15	Solexa-2564-185	ACCTGGCATACAATGTAGATTTCTGT
16	Solexa-27-9416	TCCCTGGTGGTCTAGTGGTTAGGATTCGGC
17	Solexa-284-1594	GGCTCGTTGGTCTAGGGGTATGATTC
18	Solexa-3062-153	TGGATATGATGACTGATTACCTGAGA
19	Solexa-308-1456	GCCCGGCTAGCTCAGTCGGTAGA
20	Solexa-3253-144	GGGCTGGAGAGATGGCTCAGCCGTT
21	Solexa-403-1161	GTCTACGGCCATACCACCCTGA
22	Solexa-4153-111	GACCTCGTGGCGCAATGG
23	Solexa-4179-110	CTCACTGAACAATGAATGCAA
24	Solexa-447-1003	GTCAGGATGGCCGAGTGGTCTAAGG
25	Solexa-5067-90	GAAGTTCTGTTATACACTCAGG
26	Solexa-5306-86	ACCCGTCCCGTTCGTCCCCGGA
27	Solexa-5593-81	GCTGGGAAGGCAAAGGGACGT
28	Solexa-622-718	GGGGATGTAGCTCAGTGGTAGA
29	Solexa-783-586	GTGCAGTGCTGCATCTC
30	Solexa-897-515	TTGGAGTTCATGCAAGTTCT

3.3 AT_1R Specificity of miRNA Expression

AngII activation of the AT_2R in the human kidney cell line affected only four miRNAs, out of which the regulation of three miRNAs was antagonistic to regulation by AT_1R (Figure 3.3 A). In contrast, 32 miRNAs were affected by AngII activation of the AT_2R in RASMC. The expression pattern of 18 miRNAs common to AT_1R and AT_2R data (Figure 3.3 B) was mostly indicative of the well known antagonistic signaling by these AngII receptors (de Gasparo et al., 2000). In addition, treatment with the AT_1R blocker, Losartan, altered 90% of the VSMC miRNAs in a manner opposite from that of AngII treatment. Thus, the AT_1R specificity of regulation of miRNAs in our analysis is clear.

The results discussed in this chapter demonstrate global miRNA expression profiling in biological replicates following chronic AngII activation. The miRNA changes in individual comparisons showed a range between 60 and 234 miRNA genes per sample. This finding is consistent with the miRNA expression profiles characterized in complex tissues, sorted cells and individual cell lines, which demonstrated that on average ≈70-150 miRNA genes were expressed per sample (Landgraf et al., 2007, Chiang et al., 2010). The inclusion of RNA derived from tissue, primary cells and established cell lines in our analysis demonstrates that this miRNA fingerprint is not derived from complex heterotypic cell-cell interactions nor influenced by a multitude of endocrine, paracrine or autocrine and neuronal influences, a common confounding problem in many analyses.

Figure 3.3. Venn diagrams of miRNAs altered in response to AngII treatment. A) AngII activation of the AT_2R in the human kidney cell line affected only four miRNAs, out of which the regulation of three miRNAs was antagonistic in HEK-AT_2R compared to regulation in HEK-AT_1R. **B)** AngII activation of the AT_2R in the immortalized RASMCs affected 32 miRNAs. Eighteen of those miRNAs are common to the expression fingerprint observed in the AT_1R RASMCs, albeit the manner of expression is antagonistic. Arrows pointing up (🡅) are indicative of an increase in expression while those pointing down (🡇) indicate a decrease in expression. A solid line denotes no change.

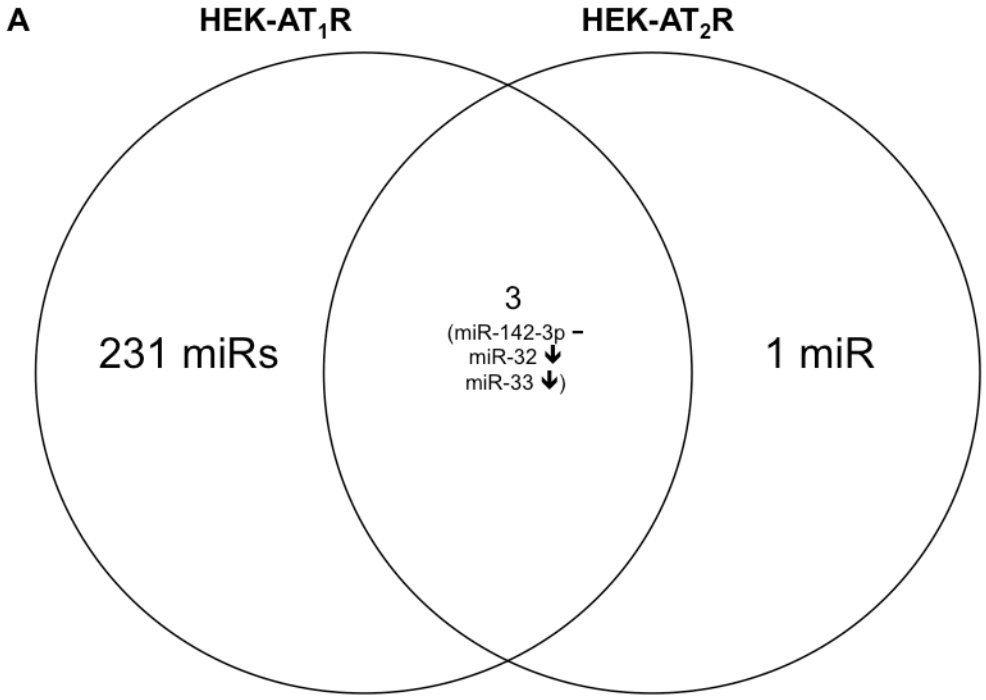
A
HEK-AT1R
HEK-AT2R
231 miRs
3
(miR-142-3p –
miR-32 ↓
miR-33 ↓)
1 miR

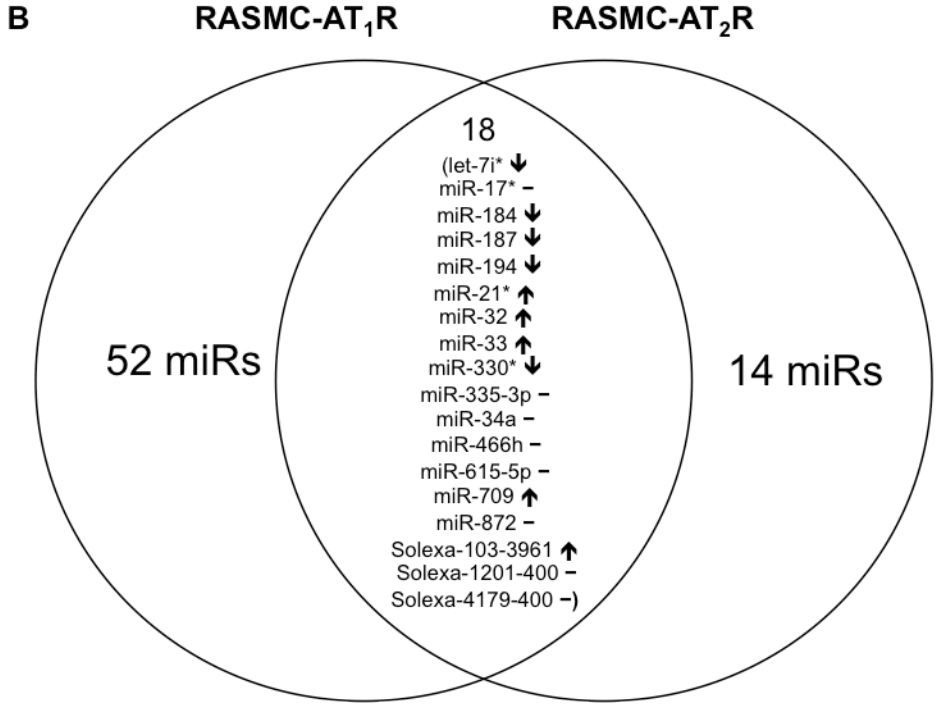
B
RASMC-AT1R
RASMC-AT2R
52 miRs
18
(let-7i* ↓
miR-17* –
miR-184 ↓
miR-187 ↓
miR-194 ↓
miR-21* ↑
miR-32 ↑
miR-33 ↑
miR-330* ↓
miR-335-3p –
miR-34a –
miR-466h –
miR-615-5p –
miR-709 ↑
miR-872 –
Solexa-103-3961 ↑
Solexa-1201-400 –
Solexa-4179-400 –)
14 miRs

Demonstrating miRNA specificity is important in elucidating the regulation of these small RNAs, which is our reasoning for determining the miRNA expression pattern in response to the AT_2R and following treatment of the AT_1R with losartan. In both instances, we showed that expression of miRNAs was antagonized following AT_2R activation by AngII and Losartan blockade of AT_1R in both VSMCs and HEK-AT_1R cells, thus displaying that the miRNA profiles generated across each model system with AngII treatment are AT_1R specific.

In addition, several miRNAs mapped to multicopy miRNA genes. Expression of a specific miRNA or a select few from the cluster suggests stimulus-specificity of processing of individual miRNAs from polycistronic pri-miRNA transcripts, as previously observed in human studies (Baskerville and Bartel, 2005). With the global miRNA profile known, we sought to identify a common set of miRNAs expressed in all cell types in response to AngII activation of the AT_1R.

CHAPTER IV

ANGII-REGULATED MIRNAS

4.1 Introduction

The tissue and cell-type specific regulation of miRNAs points to the vast role of these small regulatory RNAs in physiology and in various diseases. As an important RAS hormone, AngII must play a wider role in regulating the relative abundance and specificity of expression of miRNAs in order to regulate a variety of physiological and adaptive tissue remodeling processes. Thus, the miRNA regulation is a critical aspect of effectiveness of hormones such as AngII in various cells.

Regulation of miRNAs in VSMCs by a local increase in AngII can adversely affect vessel functions due to the high density of the AT_1R on VSMCs. Distinct VSMC phenotypes accumulate within arteries of individuals with disorders such as systemic and pulmonary hypertension, atherosclerosis, and asthma. During insult, VSMCs switch to a proliferative phenotype of poor contractility/excitability, exhibit changes in lipid

metabolism, and have high extracellular matrix production leading to vessel remodeling. In contrast, the phenotype of healthy adult VSMCs is restricted cellular plasticity, in which the cells are geared for contraction with a unique repertoire of contractile proteins, agonist-specific receptors, ion channels, and signaling molecules. Thus VSMCs are an interesting model system for studying miRNA-modulated mechanisms of cell maintenance, differentiation, and phenotypic modulation (Rensen et al., 2007, Daugherty and Cassis, 2004). Regulation of specific miRNAs as contributors to vascular disease (e.g., miR-155, -143, -145, -21, -126) has been studied (Urbich et al., 2008), but a comprehensive analysis targeting AngII-regulation of miRNAs in VSMCs and its associated diseases is lacking.

4.2 MiRNAs Regulated Universally by AngII

Understanding the miRNA expression fingerprint in various cell and tissue types is an important step in elucidating miRNA function. Two miRNAs, let-7i* and solexa-103-3961 were AngII-responsive in all AT_1R activated models consisting of six cell lines and two TG hearts. The AngII-responsive miRNA number increased to six when we relaxed the cut-off to 7 out of 8 AT_1R activated samples. Since regulation of miRNA expression in a tissue, such as the heart is complex, we evaluated instances of the same miRNA appearing specifically in the cellular models.

Eighteen miRNAs were differentially altered in 5 out of 6 AT_1R activated cell lines, which represent three mammalian genomes in the context of three different cell types (Table IV.I). Thirty-two miRNAs are differentially expressed in at least 6 AT_1R activated models including both cell lines and heart tissue from TG mice. These 32 miRNAs are AT_1R-specific because all of these were not expressed upon AngII activation of the AT_2R in HEK-293 cells and in VSMCs. In addition, AngII-regulated pattern of expression of these miRNAs was antagonized by blockade of the AT_1R by Losartan. We designated these 32 miRNAs as a common set of novel endogenous molecules that regulate *in vivo* responses to AngII activation of the AT_1R, and may also modulate the effectiveness of AT_1R blockade used to treat various pathologies.

Table IV.I. AngII-responsive miRNAs across AT_1R overexpressing model systems.

miRNA	Manner of Expression	Heart	VSMCs	HEK
let-7i*	Δ‡*◊	+	+	+
miR-330	Δ‡*◊	+	+	+
Solexa-103-3961	Δ‡*◊	+	+	+
Solexa-4153-111	Δ‡*◊	+	+	+
Solexa-1837-257	Δ‡*◊	+	+	+
miR-874	Δ‡*◊	+ (tissue only)	+	+
miR-34a	Δ*◊	+ (tissue only)	+	+
miR-142-5p	Δ*	+ (tissue only)	+	+
miR-345-5p	Δ*	+	+	+
miR-21*	Δ*	+	+	+
miR-138	Δ*	+	+	+
miR-34c	Δ*	+	+	+
miR-99b*	Δ*	+ (tissue only)	+	+
miR-92b	Δ*	+	+	+
miR-19a*	Δ*	+	+	+
miR-709	Δ	+	+	
miR-33	Δ	+	+	+
Solexa-308-1456	Δ	+ (tissue only)	+	
miR-335-5p	Δ	+	+	+
miR-497	Δ	+	+ (human only)	+
miR-801:9.1	Δ	+	+	+
miR-345-3p	Δ	+	+ (human only)	+
miR-34b-5p	Δ	+	+	
miR-503	Δ	+	+ (human only)	+
miR-214*	Δ	+ (tissue only)	+	+
miR-1198	Δ	+	+	
miR-34b-3p	Δ	+	+	+
miR-423-5p	Δ	+	+	+
Solexa-2564-185	Δ	+	+	+
miR-450b-3p	Δ	+	+	+
miR-615-5p	*		+	+
miR-27a*	*	+ (cell line only)	+	+

4.3 MiRNA Signature in Human and Rat VSMCs

Relationships between the expression patterns of miRNAs in the biological replicates in our analysis are shown by pairwise sample comparisons shown in Figure 4.1. The profile of each AngII treated compared to the respective untreated control showed a strong correlation (>0.95). Comparison of profiles between unrelated replicates (e.g., SK-1 and SK-24) produced a scatter plot with weak correlation (<0.7). Interestingly, the miRNA expression in the human and rodent VSMC model systems (purple box) yielded correlation coefficients >0.95, indicating a unique pattern of expression. This pattern arises from data consisting of >30 upregulated and >30 downregulated miRNAs in all sixteen possible comparisons, demonstrating a robust AngII responsive miRNA signature in VSMCs.

Comparison of miRNA expression in the VSMCs to all other samples examined in this study indicates that 26 miRNAs are highly specific for smooth muscle cells. The volcano plot de-convoluted the miRNA signature as $\log_2$ fold change in expression of miRNA whose abundance is significantly ($p > 0.0001$) altered in response to AngII. Twenty-one miRNAs were significantly down regulated and 5 were significantly upregulated, following AT_1R activation by AngII (Figure 4.2 A). The chromosomal locations of the 22 VSMC-specific miRNAs are shown. Many of these miRNAs are encoded within intronic regions in the mouse genome, in which the parent gene is also known and annotated (Figure 4.2 B).

Figure 4.1. Pairwise plot of sample comparisons. Differential miRNA expression in all AngII activated AT_1R model systems compared. Each blue bar graph represents the overall miRNA profile for a given sample (starting with SK-1 in the upper left hand corner). The corresponding scatter plot shows the general trend of miRNAs altered when comparing the untreated sample to the AngII treated sample. The unique miRNA expression pattern in the human and rodent VSMC model systems, indicated in purple box. The correlation coefficient is listed for each comparison. In addition, the numbers of miRNAs that are upregulated (>2) are shown in red and the numbers of miRNAs that are downregulated (>2) are shown in blue for the VSMC model systems (lower purple box).

Pairwise Plot with Sample Comparison

Figure 4.2. Characteristics of VSMC-specific miRNAs. Profiles of miRNAs pooled from all VSMCs either treated for 24 hours with 1μM AngII or left untreated. **A)** The volcano plot shows the $\log_2$ fold change in expression of miRNA whose abundance is significantly altered in response to AngII. Twenty-one miRNAs were significantly downregulated (highlighted in blue) and 5 were significantly upregulated (highlighted in red), following AngII receptor activation. **B)** The mouse chromosomal locations of the twenty-two VSMC-specific miRNAs. Many of the miRNAs are encoded within intronic regions in the mouse genome, in which the parent gene is also known and annotated in the corresponding figure legend.

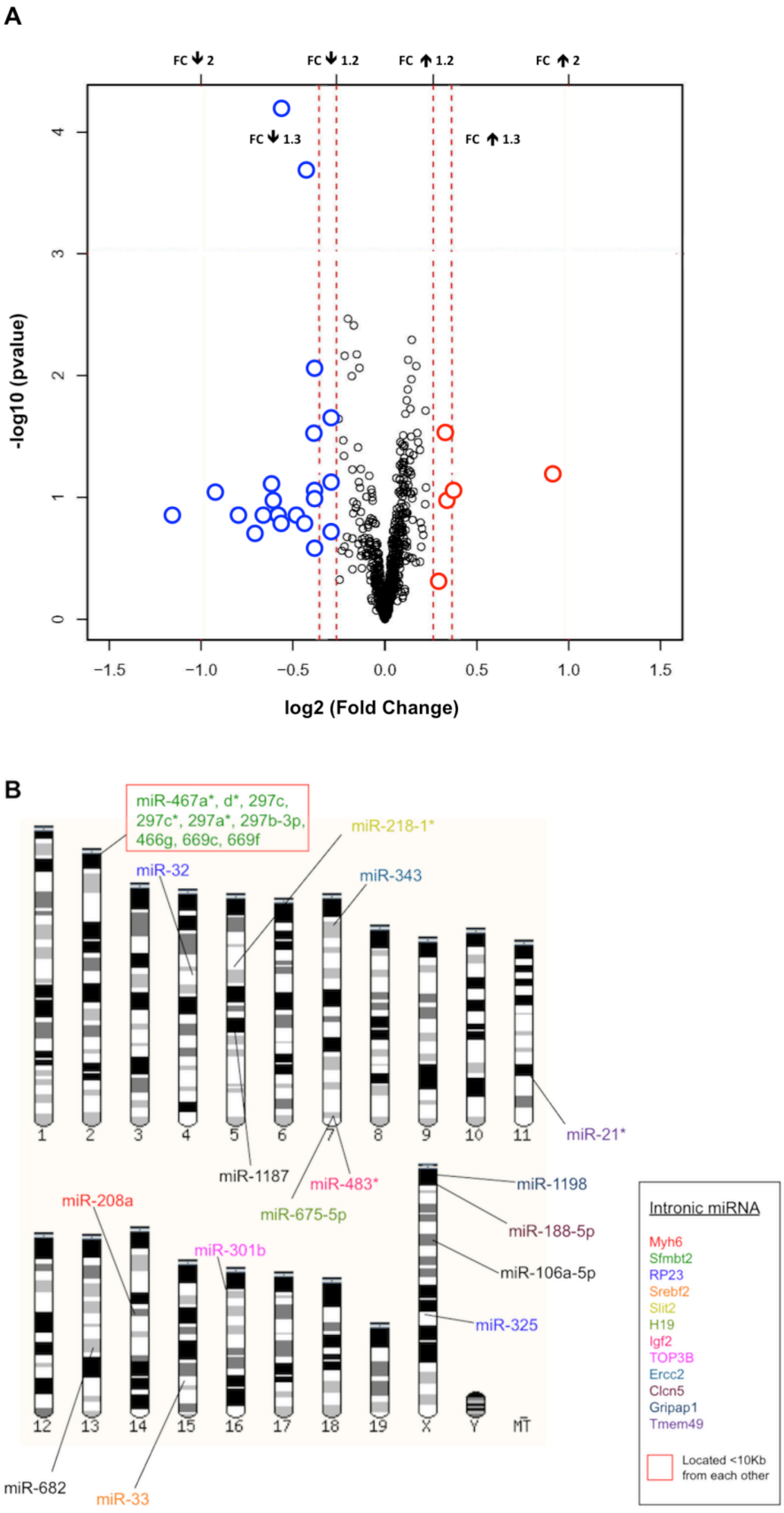
A
FC ↓ 2
FC ↓ 1.2
FC ↑ 1.2
FC ↑ 2
FC ↓ 1.3
FC ↑ 1.3
-log10 (pvalue)
log2 (Fold Change)
B
miR-467a*, d*, 297c, 297c*, 297a*, 297b-3p, 466g, 669c, 669f
miR-218-1*
miR-32
miR-343
miR-21*
miR-1187
miR-483*
miR-675-5p
miR-1198
miR-208a
miR-188-5p
miR-301b
miR-106a-5p
miR-325
miR-682
miR-33
Intronic miRNA
Myh6
Sfmbt2
RP23
Srebf2
Slit2
H19
Igf2
TOP3B
Ercc2
Clcn5
Gripap1
Tmem49
Located <10Kb from each other

Conserved expression of several miRNAs observed in three species in our study was previously unknown (Table IV.I.). The mouse genome is known to contain the VSMC-specific miRNAs listed; however, the gene assignment for the human equivalent for 11 of the miRNAs is not yet available by genome BLAST analysis (shown with a hyphen). However, the expression of miRs-682, -1187, -297c*, -466g, and -1198 were experimentally detected in the HASMC samples although the genes are not annotated for these miRNAs. Interestingly, 7 miRNAs are clustered to a single region of the genome, the miR-466-467-669 cluster (Table III.I).

The results discussed in this chapter importantly demonstrate that thirty-two miRNAs were AngII regulated in most human and rodent samples, which we deemed as universally responsive to AngII activation of the AT_1R. Expression of these miRNAs were antagonized following AT_2R activation by AngII and Losartan blockade of AT_1R in both VSMCs and HEK-AT_1R cells, suggesting that expression of these miRNAs is a hallmark of AngII action through the AT_1R, which is targeted in most clinical settings.

Table IV.II. Genomic characteristics of VSMC-specific miRNAs.

miRNA	Mature Sequence	Fold Change (VSMCs)	Fold Change (HEKs)	Chromosome # for Human Homologue
miR-675-5p	UGGUGCGGAAAGGGCCCACAGU	-1.47	0.93	11
miR-343	UCUCCCUUCAUGUGCCCAGA	-1.33	0.66	-
miR-669c	AUAGUUGUGUGUGGAUGUGUGU	-1.22	0.82	-
miR-467b*	AUAUACAUACACACACCAACAC	-1.29	0.15	-
miR-218-1*	AAACAUGGUUCCGUCAAGCACC	1.24	0.04	4
miR-32	UAUUGCACAUUACUAAGUUGCA	1.86	0.45	9
miR-682	CUGCAGUCACAGUGAAGUCUG	-1.22	0.99	-
miR-1187	UAUGUGUGUGUGUAUGUGUGUAA	-1.55	0	-
miR-297c*, 297a*, 297b-3p	UAUACAUACACACAUACCCAUA	-1.92	0.81	-
miR-188-5p	CAUCCCUUGCAUGGUGGAGGG	1.30	0.58	X
miR-106a:9.1	CAAAGUGCUAACAGUGCAGGUA	-1.29	0	X
miR-466g	AUACAGACACAUGCACACACA	-1.52	0.19	-
miR-325	UUUAUUGAGCACCUCCUAUCAA	1.28	0.99	X
miR-467a*, 467d*	AUAUACAUACACACACCUACAC	-1.51	1	-
miR-1198	UAUGUGUUCCUGGCUGGCUUGG	-2.23	0.06	-
miR-301b	CAGUGCAAUGGUAUUGUCAAAGC	-1.51	0.12	22
miR-21*	CAACAGCAGUCGAUGGGCUGUC	-1.40	0.35	17
miR-483-3p	UCACUCCUCCCCUCCCGUCUU	-1.48	0.93	11
miR-297c	AUGUAUGUGUGCAUGUACAUGU	-1.37	0.99	-
miR-669f	CAUAUACAUACACACACACGUAU	-1.23	0.99	-
miR-208a	AUAAGACGAGCAAAAAGCUUGU	-1.29	0.99	14
miR-33	GUGCAUUGUAGUUGCAUUGCA	1.23	0.31	22

Our analysis of AngII-regulated miRNAs in rat and human VSMC cell lines (Table IV.III.) indicated for the first time a unique fingerprint consisting of novel miRNAs and miRNAs with known functions. As shown, a significant number of the AngII-regulated miRNAs have been implicated in pathogenesis of other organs and tissues, implying that a systematic study of their role in vasculature is important. Many of the miRNAs have been previously implicated in various forms of cancer (e.g., miRs-218-1, -32, -297b-3p, -106a, -483-3p), while some have been shown to play in a role in cardiac and vascular disturbances (e.g., miRs-218-1, -188-5p, -208a, -483-3p). Using this AngII-induced VSMC miRNA profile will allow for enhancement of our understanding of RAS-mediated vascular abnormalities.

Table IV.III. Involvement of VSMC-specific miRNAs in various tissues and disease states.

miRNA	Expression Context (Manner of Alteration)
miR-675	NA
miR-343	NA
miR-669c	NA
miR-467b*	Hepatic steatosis in non-alcoholic fatty liver disease (downregulated)
miR-218-1	Vascular patterning (upregulation), gastric cancer, oral squamous cell carcinoma (downregulated)
miR-32	Androgen-regulated prostate cancer (upregulated), antiviral defense, human myeloid leukemia (upregulated)
miR-682	Muscle regeneration (upregulated)
miR-1187	TNFα-mediate hepatic apoptosis (upregulated)
miR-297b-3p	Lymphoma/carcinogenesis (upregulated)
miR-188-5p	Homocysteine-induced cardiac remodeling (upregulated)
miR-106a	Malignant bronchial epithelial, human T-cell leukemia, gastric cancer (upregulation), colon cancer (downregulation)
miR-1198	NA
miR-325	Stress-induced suppression of luteinizing hormone secretion (upregulated)
miR-301b	Stimulates induced pluripotent stem cells (upregulated)
miR-467a	Growth regulation of mouse embryonic stem cells (upregulated)
miR-669f	NA
miR-208a	Cardiac hypertrophy/diastolic dysfunction, electrical conductance, acute myocardial infarction (upregulated)
miR-483-3p	Wilms' tumors, hepatocellular carcinoma, colorectal cancer, adrenocortical tumours, pancreatic cancer, proliferation in wounded epithelial cells (upregulated), myocardium of obesity-prone rats, melatonin synthesis in pineal gland (downregulated)
miR-33	Cholesterol homeostasis in macrophages, atherosclerosis (upregulated)

CHAPTER V

REGULATION OF MIRNAS BY ANGII

5.1 Introduction

Validation of expression patterns is an important aspect of miRNA biology that must always be considered. Recapitulating the manner of expression observed by microarray (i.e., upregulated or downregulated) in independent samples sets is crucial for teasing out the functional roles of individual miRNAs. In the current study, we have demonstrated a robust miRNA response following chronic AngII treatment and activation of the AT1R. Confirming expression of the VSMC-specific miRNAs determined in the profiling experiment will be useful to determine the important players for regulation of cellular activities and RAS pathologies where VMSC gene expression is altered.

5.2 Validation of VSMC miRNAs by RT-qPCR

To validate the microarray data and confirm the VSMC-specific miRNA signature, the stemloop primer-based real-time RT-qPCR analysis was performed on

independent RNA samples. The levels of miR-483-3p, miR-32, miR-669f and miR-1198 compared in untreated samples revealed that basal levels of these miRNAs changed in RASMC-AT_1R compared to RASMC (Figure 5.1. A). The change in the level of these four miRNAs in AngII treated samples followed similar pattern in RASMC-AT_1R compared to RASMC, suggesting that the AngII dependent effects are not altered due to AT_1R over expression in the RASMC-AT_1R.

Figure 5.1 B shows ligand-dependent changes in the levels of 20 VSMC-specific miRNAs, following treatment with either AngII or Candesartan for 24 hours (n = 3). Since basal levels of miRNAs were altered in the RASMC-AT_1R cells due to mere overexpression of the AT_1R, the inverse agonist, Candesartan was used to inhibit the basal AT_1R-specific effect. The result was then compared to the AngII-induced effect in each case. Of the VSMC candidate miRNAs that were identified from the microarray, 17 showed the same trend in expression (i.e., upregulated or downregulated) in the independent samples in response to AngII. In addition, Candesartan treatment produced distinct response for these miRNAs. Either the miRNA expression was reversed or miRNA expression was less diminished compared to treatment with AngII (Figure 5.1 B). Both types of responses suggest that these miRNAs do respond to AngII activation of the AT_1R, however, the variability in the type of response may point to additional regulatory events downstream of the receptor. Taken together, our data demonstrate that AngII activation of AT_1R in VSMCs produces a specific miRNA signature that is validated independently.

Figure 5.1. RT-qPCR validation of VSMC miRNAs. A) Relationship of AT_1R cellular levels and miRNA expression analyzed by the stem-loop primer-based real-time RT-qPCR. Expression of 4 representative miRNAs was monitored in RASMCs and RASMC-AT_1R cells (n = 3). Data are presented as fold over U6 RNA internal control following normalization. **B)** MiRNA expression modulated by AT_1R-specific ligands. Change of expression of 20 miRNA in the AT_1R RASMCs following 1uM AngII or Candesartan treatment for 24 hours (n = 3). Data are presented following normalization to U6 RNA, the cellular levels of which did not vary under different experimental conditions and standardization to an untreated control.

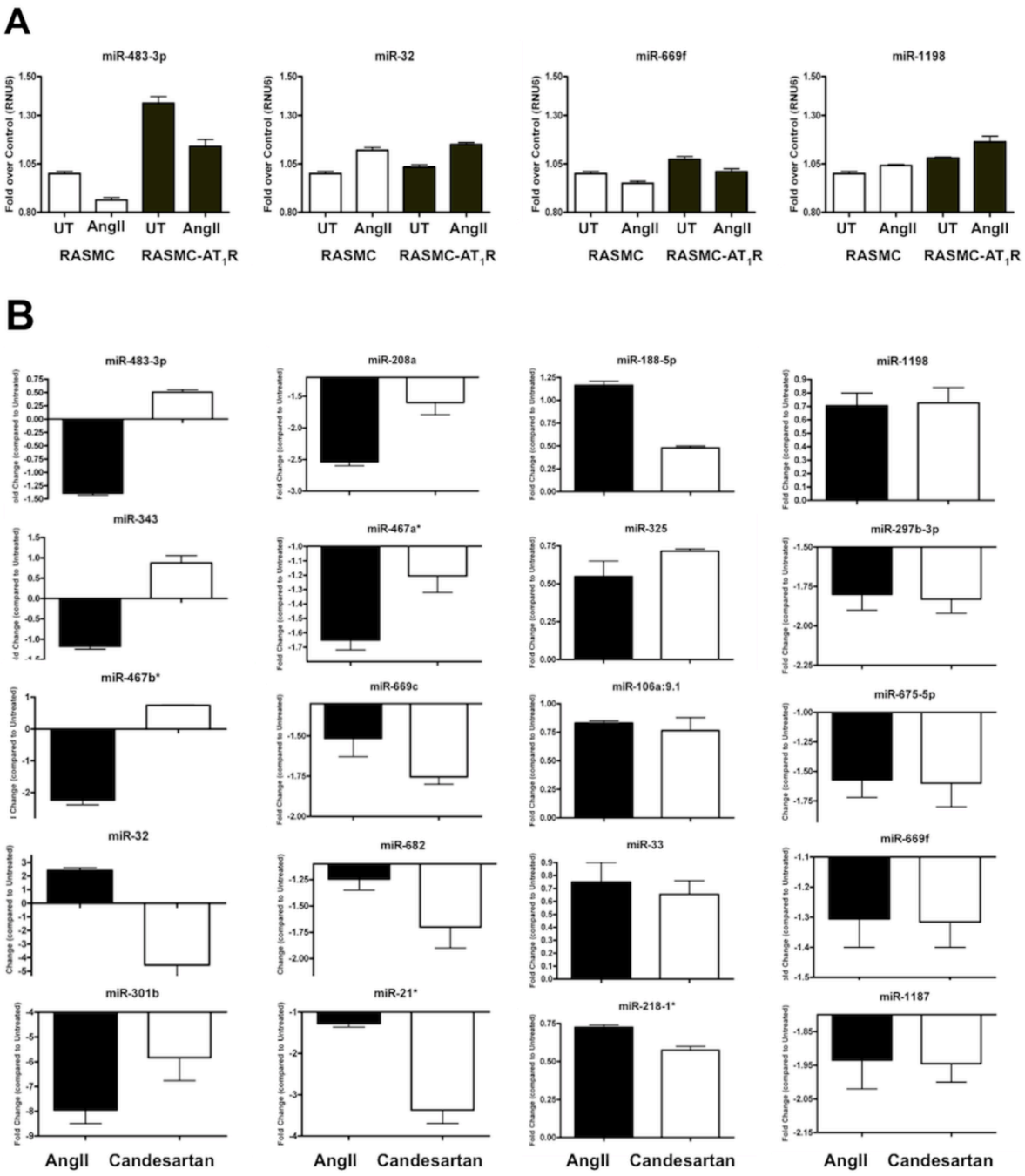
A
miR-483-3p
miR-32
miR-669f
miR-1198
Fold over Control (RNU6)
UT
AngII
RASMC
RASMC-AT1R
B
miR-483-3p
miR-208a
miR-188-5p
miR-1198
miR-343
miR-467a*
miR-325
miR-297b-3p
miR-467b*
miR-669c
miR-106a:9.1
miR-675-5p
miR-32
miR-682
miR-33
miR-669f
miR-301b
miR-21*
miR-218-1*
miR-1187
Fold Change (compared to Untreated)
AngII
Candesartan

5.3 Modulation of the AngII-regulated VMSC miRNA Pool

Transcriptional regulation of miRNA genes and posttranscriptional processing of pri-miRNA could be affected by AT_1R-regulated kinases. Therefore, we blocked PKCζ, MEK1, JAK2, JNK, and p38 cascades during AngII activation of the AT_1R and measured the effects on cellular miRNA levels. Inhibitors of PKCζ, JNK, and p38 did not interfere with AngII-mediated miRNA regulation, but inhibitors of JAK2 and MEK1 had a significant effect.

To examine whether the AT_1R-activated MEK1 and JAK2 pathways regulate the miRNA pool globally or if miRNAs are regulated individually, the RASMC-AT_1R cells were pretreated with inhibitors of MEK1 or JAK2 and were then treated with AngII and processed. As shown in Figure 5.2 A and B, the effect of MEK1 inhibition (iMEK1) was monitored by a decrease in ERK1/2 phosphorylation and the effect of JAK2 inhibition (iJAK) was monitored by a decrease in phosphorylation of STAT3. Under conditions of inhibition, both blockers had an effect that was of equal strength or exceeded the inhibition of the AT_1R caused by Candesartan. We observed no significant change in the expression of the endogenous U6 control RNA under the same experimental conditions.

Figure 5.2. Inhibition of AngII-mediated ERK1/2 and STAT3 phosphorylation. A) Activation of phospho-ERK1/2 and phospho-STAT3 (Y705) in AT_1R RASMCs samples untreated (lane 1), treated with 1μM AngII (lane 2), 1μM Candesartan +0.1μM AngII (lane 3), 30μM MEK1 inhibitor +1μM AngII (lane 4), and 5μM JAK inhibitor +1μM AngII (lane 5) was visualized. **B)** Densitometry quantification of iMEK1 and iJAK effects on phosphorylation of ERK1/2 and STAT3. The MEK1 inhibitor (iMEK1) completely inhibited ERK1/2 phosphorylation and the JAK inhibitor (iJAK) inhibited approximately 98% of STAT3 phosphorylation ($n = 3$, $p < 0.01$).

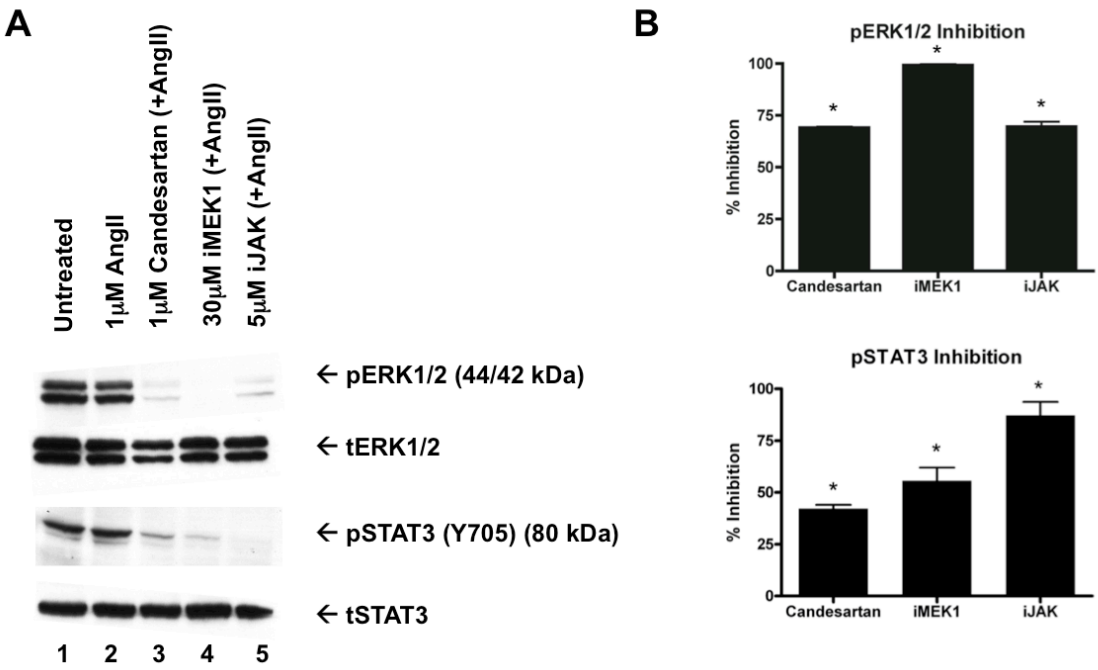

The RT-PCR data in Figure 5.3 shows that levels of miR-483-3p, miR-33 and miR-301b increased, but the levels of miR-188-5p and miR-208a were not significantly altered by MEK1 blockade. In contrast, inhibition of JAK2 had the opposite effect. When JAK2 was blocked, the levels of miR-188-5p and miR-208a increased while the levels of miR-483-3p, miR-33, and miR-301b did not significantly change.

Combined iMEK1 and iJAK2 impacted all five miRNAs, demonstrating that MEK1 and JAK2 are essential for the AngII-mediated modulation of distinct miRNAs. Furthermore, loss of any individual protein kinase function is not compensated by the remaining cellular kinases, which suggests a parallel, non-overlapping effect of different signaling circuits on miRNA regulation. Our data identifies non-redundant roles played by MEK1 and JAK2, emphasizing non-canonical pathways.

Figure 5.3. Effect of kinase inhibition, iMEK1 and iJAK2, on miRNA levels. Levels of miRNA in AT_1R RASMCs monitored by qRT-PCR after inhibition of the AngII-specific kinases, MEK1 and JAK. The 5 candidate miRNAs tested exhibited a distinct changes, for instance changes in miR-483-3p ($p < 0.0001$), miR-188-5p ($p = 0.0005$), and miR-301b ($p < 0.0001$) expression observed under iMEK1 and changes in miR-33 ($p = 0.0002$) and miR-208a ($p = 0.004$) expression observed under iJAK2 condition ($n = 3$).

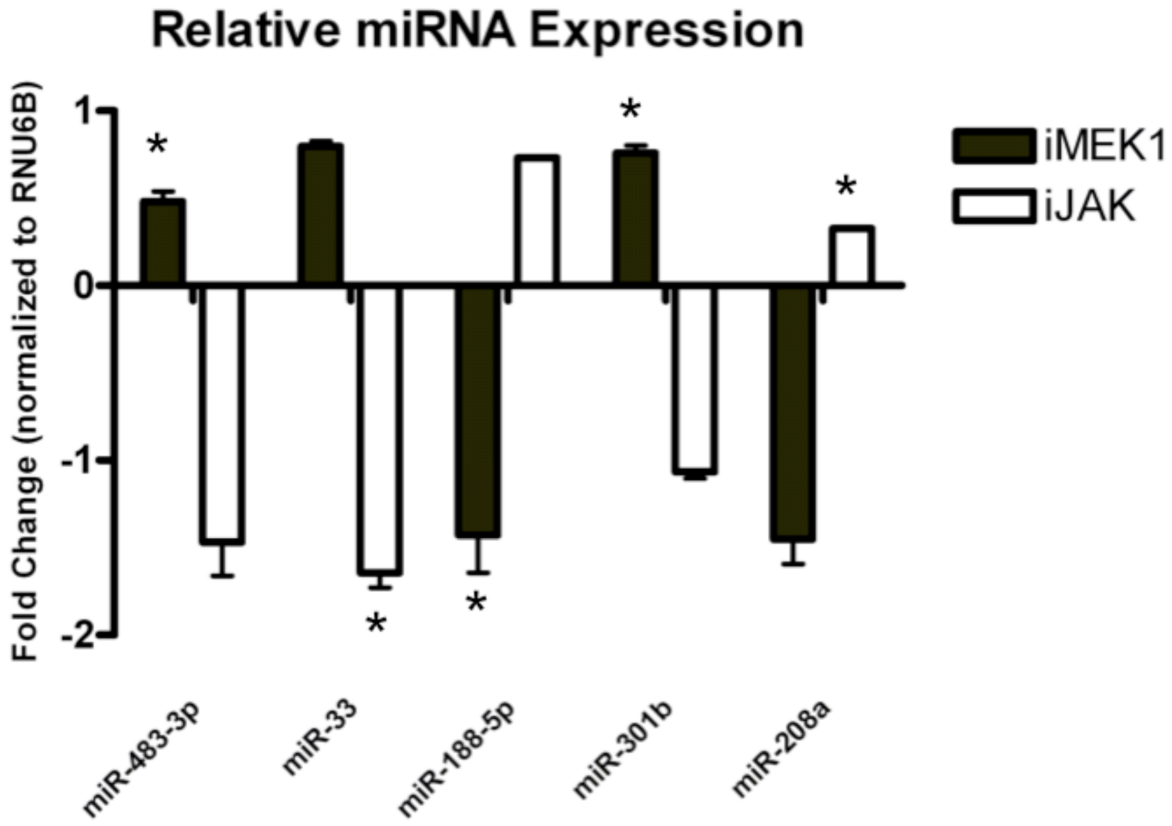

Kim *et al* showed that the proteins involved in miRNA biogenesis (e.g., Drosha, TRBP, Dicer, Ago 2) could be phosphorylated by protein kinases. Accordingly, AngII-activated kinases may potentially target Drosha, TRBP, Dicer, or Ago 2 to regulate biogenesis or degradation of miRNAs (Kim et al., 2010) (Figure 5.4 A). As a means to understand the mechanism of AngII-induced miRNA regulation, we looked at AngII-mediated signaling molecules that could alter expression of miRNA biogenesis proteins and thereby alter the expression of the miRNAs. In RASMC-AT_1R samples, we analyzed total protein levels of Drosha, TRBP, and Ago2 by western immunoblotting to determine if these miRNA maturation proteins were affected by inhibition of MEK1 and JAK2. We observed that upon inhibition of these kinases, there was no change in total protein levels of Drosha, TRBP, or Ago2 when compared to AngII treated samples (Figure 5.4 B). This suggests that post-translational modification of these biogenesis proteins is the driving force behind altering the miRNA pool or that other components all together are participating in altering the AngII/AT_1R induced expression of miRNAs.

Figure 5.4. Mechanism of AngII-induced miRNA regulation. A) Pri-miRNAs are processed by a number of proteins within the nucleus and cytoplasm to yield the mature miRNA. A recent review reported that protein factors, which are involved in the miRNA biogenesis pathway, can be subjected to various posttranslational modifications (Kim et al., 2010). **B)** Total protein levels for Drosha, TRBP, and Ago2 in RASMC-AT_1R samples untreated (lane 1), treated with 1μM AngII (lane 2), 1μM Candesartan +0.1μM AngII (lane 3), 30μM MEK1 inhibitor +1μM AngII (lane 4), and 5μM JAK inhibitor +1μM AngII (lane 5) was visualized. The corresponding plots show densitometry values for each protein normalized to actin. There is no change in total levels of these three proteins (n = 1).

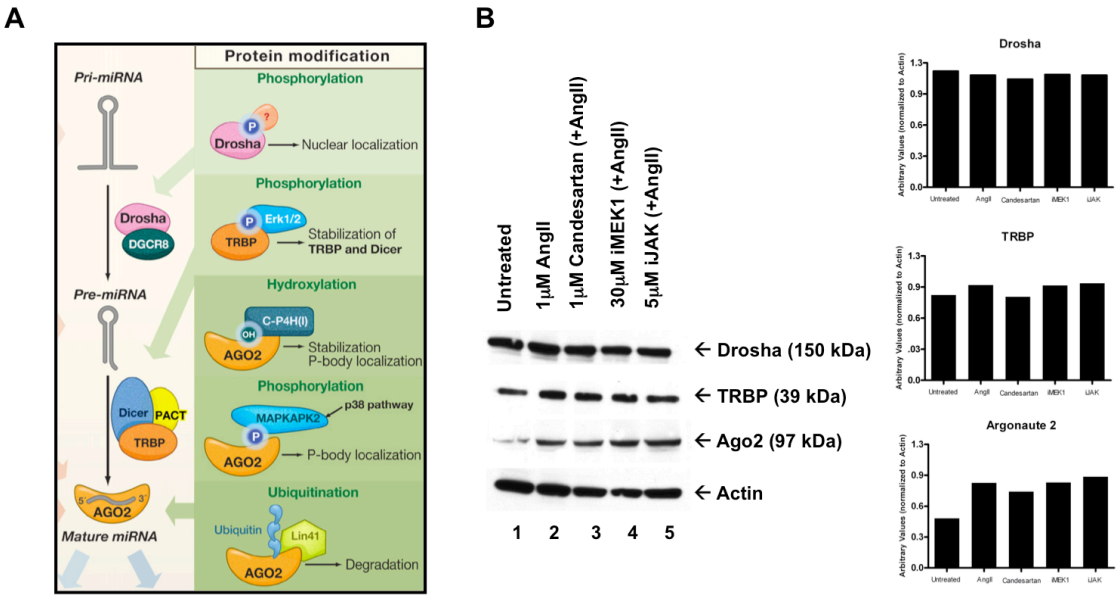

The results presented in this chapter display evidence of unconventional regulation of miRNA levels in VSMCs through AT_1R signaling. Our data indicate that AT_1R signaling through JAK2 and MEK1 regulate two completely independent miRNA pools. Both MEK1 and JAK2 inhibitors inhibited ERK1/2 activation, but these inhibitors affected distinct miRNAs, suggesting that the AngII-activated JAK2 and MEK1 signaling alters non-canonical and perhaps miRNA-specific regulatory steps.

CHAPTER VI

MIR-483-3P: A NOVEL ANGII-REGULATED MIRNA

6.1 Introduction

The genome-wide miRNA expression profiling provided us with a subset of AngII-responsive miRNAs across various model systems. For this study, we focused our efforts on a single VSMC-specific miRNA, miR-483-3p, which until now had an unknown functional role in SMC biology.

The role of miR-483-3p in SMC physiology and pathology is unknown. Since 2010 several groups have reported a functional role for miR-483-3p in various *in vitro* and *in vivo* systems, which gives us confidence that this miRNA could also possess an important function in our model system. Veronese and colleagues observed that miR-483-3p was overexpressed in 100% of Wilms' tumors and highly expressed in 30% of the cases of colon, breast, and liver cancers (Veronese et al., 2010). Coregulation with IGF2 mRNA was detected in some, but not all tumors, suggesting that the miRNA can act

concomitantly or autonomously as an oncogene. MiR-483-3p was observed to regulate the proapoptotic protein PUMA, acting as an antiapoptotic oncogene. The same group reported that miR-483 expression could be induced independently of IGF2 by the oncogene beta-catenin. They also show that beta-catenin is a target of miR-483-3p, triggering a negative feedback loop that becomes ineffective in cells harboring a beta-catenin mutation (Veronese et al., 2011). It has been reported that miR-483-3p is strongly enhanced in pancreatic cancer and that Smad4 is a direct target of miR-483-3p, promoting cell proliferation and colony formation in vitro (Hao et al., 2011). In a non-cancerous disease state, miR-483-3p was implicated in regulating melatonin synthesis and expression in adipose tissue of diabetics (Ferland-McCollough et al., 2012). Most recently, miR-483-3p was observed to target CDC25A and contribute to cell-cycle arrest (Bertero et al., 2013).

Important for our purposes, researchers demonstrated that miR-483-3p is upregulated in 2 distinct epithelial models of wound healing (scratch and wounded skin). They show that 483-3p expression peaks at the final stage of wound closure (Bertero et al., 2011). In addition, the study determined that miR-483-3p inhibits keratinocyte migration and proliferation and use of an antagomir rescues this observation. Kinase MK2, proliferation marker MK167, and transcription factor YAP1 were confirmed to be direct targets of miR-483-3p in this study. Finally, it has been observed that Igf2 derived miR-483 can induce proliferation in hepatocellular carcinoma cells (Ma et al., 2012). The group showed that suppressor of cytokine signaling 3 (Socs3) is a target of miR-483.

What has yet to be determined regarding miR-483-3p is its role as an AngII responsive miRNA in VSMC behavior. In this chapter we describe the logic behind choosing miR-483-3p for in-depth analysis and the importance that this miRNA could have in terms of AngII biology.

6.2 Selection of miR-483-3p for Analysis

We performed extensive bioinformatic analyses on each of the 26 VSMC-specific miRNA that we obtained from our genome-wide miRNA expression profiling experiment. We completed miRNA target prediction analyses using Target Scan, DIANA, PITA, and MicroCosm databases. Additionally, we utilized Ingenuity Pathway Analysis (IPA) to construct functional networks of the miRNAs with their predicted targets. We eliminated miRNA candidates that had already been extensively studied and focused on those VSMC-specific miRNAs that would have some role in SMC physiology. Of the 21 downregulated miRNAs and 5 upregulated miRNAs, we chose miR-483-3p, which is significantly downregulated in response to chronic AngII treatment (Figure 6.1).

Figure 6.1. Volcano plot of VSMC-specific miRNAs. The volcano plot shows the $\log_2$ fold change in expression of miRNAs whose abundance is significantly altered in response to AngII. MiR-483-3p was observed to be significantly downregulating in response to AngII receptor activation (depicted with a solid arrow).

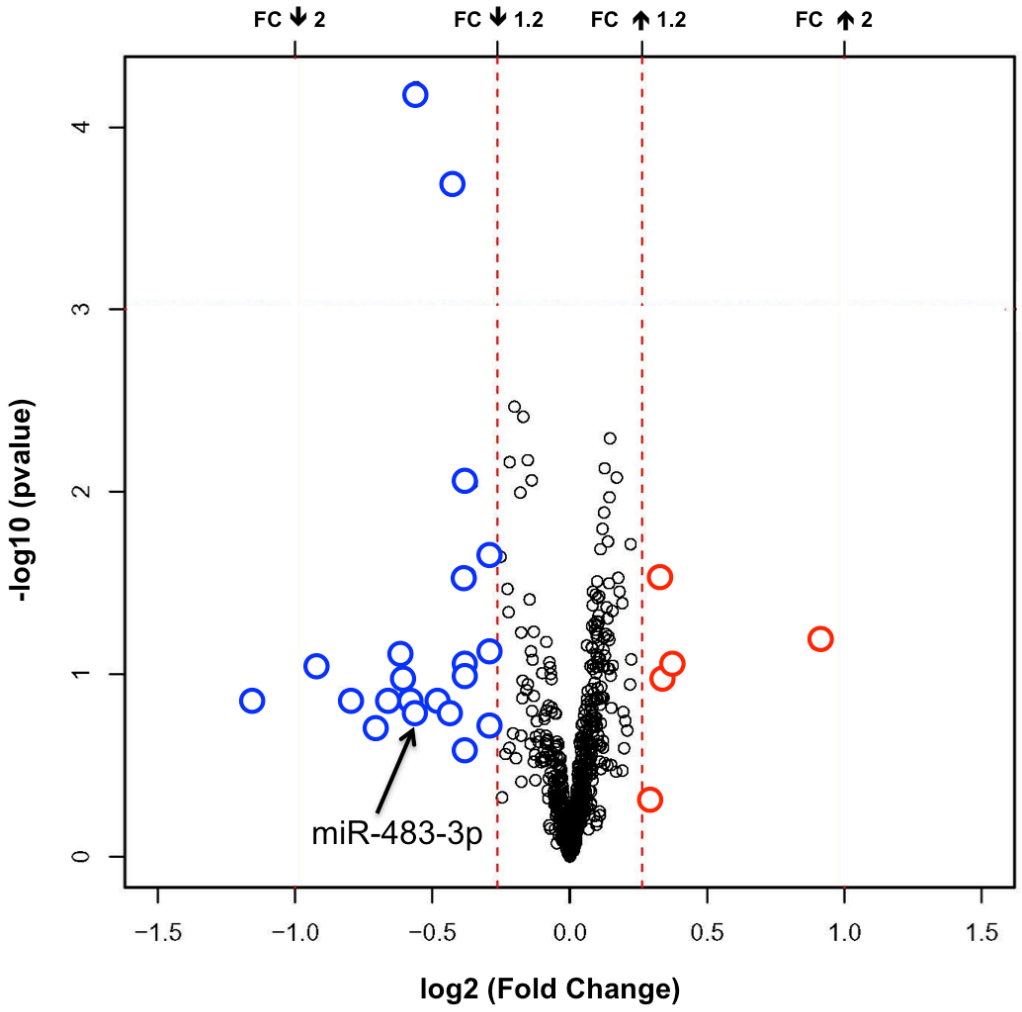

Tissue RAS activation is known to be a major cause of SMC disease. Therefore, we sought to explore the involvement of miRNAs in potentially targeting components of RAS. We examined the 3'-UTRs of each RAS component (e.g., Renin, Renin Receptor, AGT, ACE-1, ACE-2, AGTR1, AGTR2, AT_4 receptor, $Ang^{(1-7)}$ Receptor) to see which of the VSMC-specific miRNAs could potentially target these genes. We observed that miR-33 could potentially target the AT_1R. MiR-33, an intronic miRNA located within the gene encoding sterol-regulatory element-binding factor-2 (SREBF-2), has been extensively studied and has been shown to be a regulator of cholesterol metabolism. The miRNA targets the adenosine triphosphate-binding cassette transporter, thereby attenuating cholesterol efflux to apolipoprotein A1. In mouse macrophages, miR-33 also targets ABCG1, reducing cholesterol efflux to nascent high-density lipoprotein (Rayner et al., 2010). In addition, we observed that miR-188-5p could potentially target ACE-2. This miRNA was previously implicated in homocysteine-induced cardiac remodeling during heart failure, wherein the miRNA is downregulated, which upregulates MMP-2, -9 and TIMP-1, and -3 (Mishra et al., 2009).

MiR-483-3p is one of the 26 VSMC-specific miRNAs that was predicted to potentially target 4 key components of the RAS; thereby, regulating the whole pathway. The seed sequence of miR-483-3p is complementary to regions within the 3'-UTR of AGT, ACE-1, ACE-2, and AGTR2 (Figure 6.1). In addition, complementary regions for miR-483-3p exist within the coding regions of AGT and ACE-1, suggesting that this miRNA could act most potently *in vivo* on these genes.

Figure 6.1. MiR-483-3p target prediction. Using multiple target prediction databases, miR-483-3p was predicted to target the 3'-UTR of AGT, ACE-1, ACE-2, and AGTR2 with near complete complementarity. The regions of potential miRNA (red) binding to the 3'-UTR (black) of each gene is shown below.

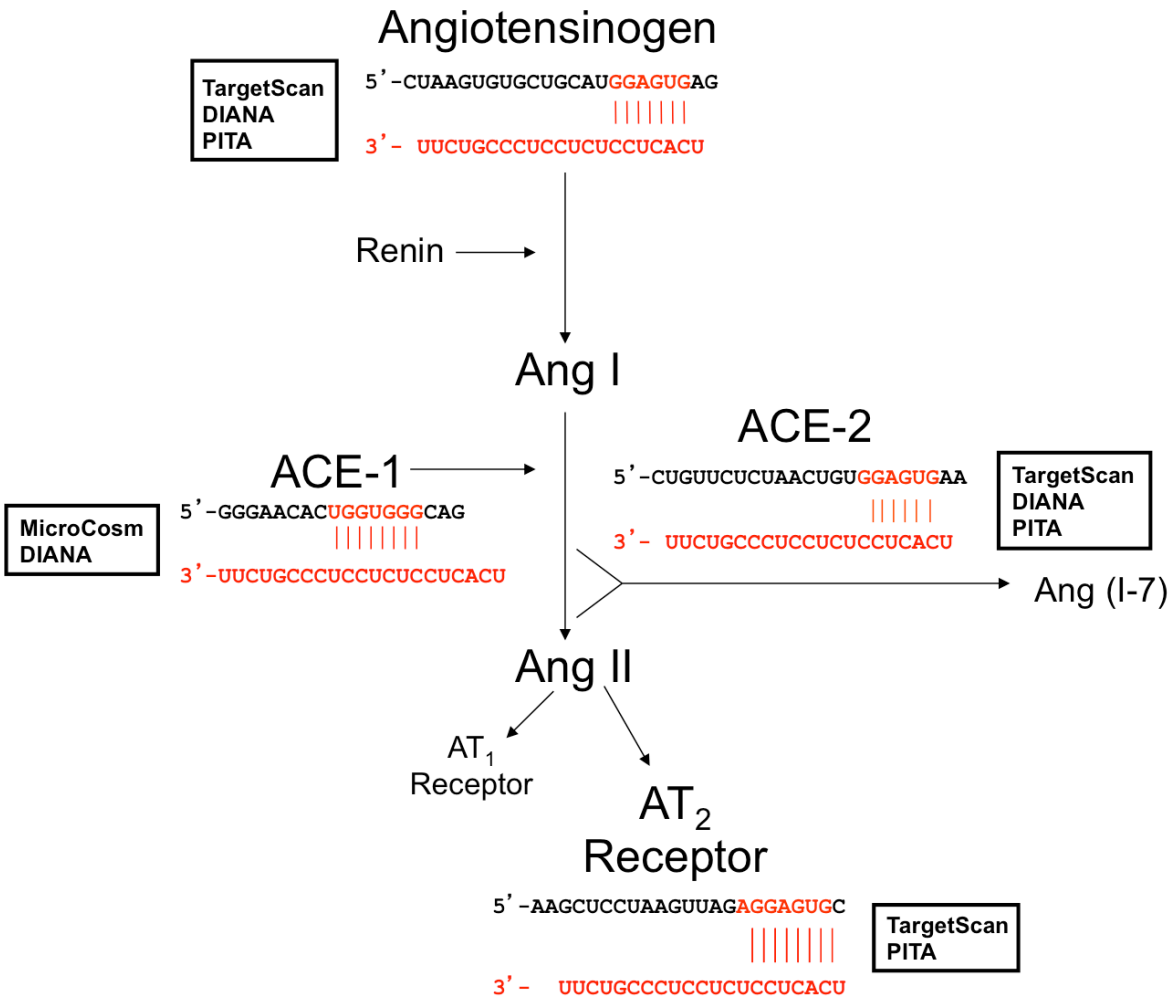

During our bioinformatic analysis, we also determined that miR-483-3p does not target any of the components of the ANF system, which is a counter-regulatory system to RAS with similar complexity. Taken together, this suggests that miR-483-3p could be a selective mechanism for regulating tissue RAS.

In addition to miR-483-3p being predicted to target multiple components of tissue RAS, it is also known that the gene for miR-483 is encoded within intron 2 of Insulin-like growth factor 2 (IGF2). IGF2 is an imprinted gene with expression resulting favorably from the paternally inherited allele. It has growth-regulating, insulin-like and mitogenic activities. IGF2 is believed to be a major growth factor during gestation, as it promotes development of fetal pancreatic islet cells (Bergman et al., 2012). Perhaps most importantly, IGF2 is a signaling molecule that is known to interact with AngII signaling. Studies have shown that an increase in Igf2 expression in the left ventricle corresponds to blood pressure increase (Kadlecova et al., 2008) and that AngII-induced IGF2 gene expression has been positively correlated with cardiomyoblast apoptosis in animals with hypertension (Lee et al., 2006). In addition, targeted expression of Igf2 transgene in SMCs shortens life span, leading to bradycardia and hypotension (Zaina et al., 2003). We have observed that in response to chronic AngII treatment, the transcript levels of IGF2 are enhanced in RASMC-AT_1R cells (Figure 6.2).

Figure 6.2. IGF2 abundance in VSMCs after AngII treatment. Transcript levels of IGF2 were quantitated by RT-qPCR, following treatment of RASMC-AT_1R cells with 1 μM AngII for 24 hours (n = 3). Data are presented following normalization to GAPDH, the cellular levels of which did not vary under different experimental conditions and standardization to an untreated control. IGF2 is synergistically enhanced, following treatment with AngII.

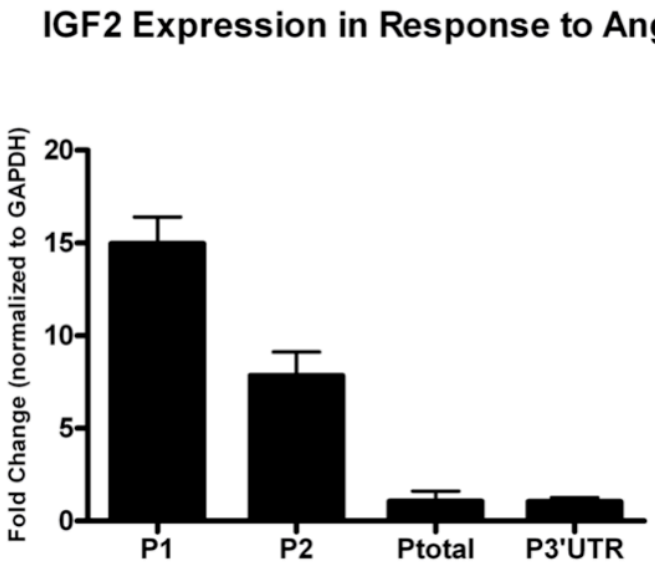

Upon transcription of IGF2 in the 3' direction, 11 transcripts are produced, all of which contain intron 2 and the coding region for miR-483 (Figure 6.3). The pri-miRNA is independently produced from intron 2 and is processed in the nucleus to yield a precursor-miRNA stem-loop structure. This pre-miR is exported into the cytoplasm where it is cleaved to form a double-stranded miRNA duplex of miR-483-5p and miR-483-3p. The guide strand of this duplex, which is miR-483-3p (or the antisense strand) in our case, is loaded into RISC and carries out its function by binding to target mRNAs, resulting in translational repression.

Additional observations were made during our bioinformatic analyses of miR-483-3p, which suggested that this miRNA is favored over its hairpin counterpart, miR-483-5p. First and foremost, the AngII stimulated miRNA profile showed only miR-483-3p as being significantly altered in the VSMC model systems. RNA sequencing databases also consistently show that miR-483-3p is the most frequently expressed and conserved miRNA across a range of species (Figure 6.4). Finally, by looking at the sequence of the miRNA itself, we see that miR-483-3p is very AU-rich, which makes it a perfect candidate for seed recognition by Ago2 and loading into RISC for translational silencing.

The results described in this chapter provide the logic and reasoning for selection of the novel AngII-regulated miR-483-3p from the 26 VSMC-specific miRNAs. Due to the ability of this miRNA to potentially target and regulate multiple components of the

RAS and its location within the genome, miR-483-3p is a prime candidate for understanding the functional role of AngII-responsive miRNAs in SMC biology.

Figure 6.3. MiR-483 encoded in intron 2 of IGF2. Pri-miR-483 is encoded in and produced from intron 2 of IGF2. Following processing by canonical miRNA biogenesis proteins, pre-miR-483 is exported into the cytoplasm where it is further processed to yield the mature miR-483-3p, which has a functional role.

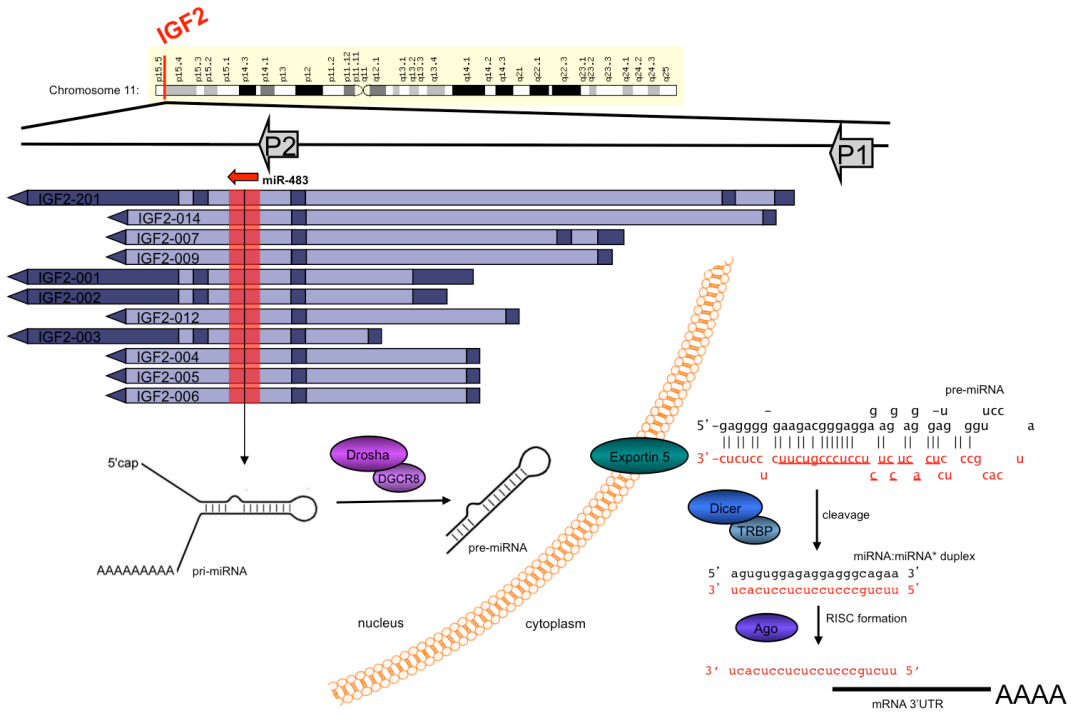

Figure 6.4. MiR-483-3p expression is favored over miR-483-5p expression. Deep sequencing efforts by miRBase have shown IGF2 encoded miR-483-3p to be expressed by all species, but miR-483-5p has only been shown to be experimentally expressed in human and mouse.

	miR-483-5p	miR-483-3p
Homo sapiens, **IGF2**	aagacgggaggaaagaagggag	ucacuccucuccucccgucuu
Mus musculus, **Igf2**	aagacgggagaagagaagggag	ucacuccucccccucccgucuu
Rattus norvegicus, **Igf2**	-not yet reported-	ucacuccucccccucccgucuugu
Bos Taurus, **Igf2**	-not yet reported-	ucacuccucuccucccgucuu
Canis familiaris, **Igf2**	-not yet reported-	ucacuccucccccucccgucuu

CHAPTER VII

EXPRESSION AND FUNCTIONAL ROLE OF MIR-483-3P

7.1 Introduction

Characterization of individual miRNAs is important in order to fully understand the biological role that these small, non-coding RNAs possess. Therefore, it is imperative to examine both the expression pattern of the miRNA of interest and also to determine its functionality, in terms of ability to translationally suppress predicted target genes. In this chapter we describe both of these aspects for miR-483-3p as a means to understand its role in regulating tissue RAS.

7.2 Validation of miR-483-3p

Using two independent assays, we were able to validate miR-483-3p expression in RASMC-AT_1R samples treated with AngII. In the RNA solution hybridization assay, we detected and visualized miR-483-3p expression using a ^{32}P labeled antisense probe specific for miR-483-3p. Following time-course treatment with AngII, total RNA was

isolated and hybridized to the miR-483-3p probe. Recovered hybrids were analyzed on a denaturing polyacrylamide gel (Figure 7.1. A). The densitometry for miR-483-3p and miR-16 (control) for a single experiment (upper panel) and the calculated fold change in expression of miR-483-3p compared to miR-16 is shown in triplicate (lower panel) in Figure 7.1 B.

We have also detected this miRNA by RT-qPCR using a miR-483-3p specific primer. Following treatment with either AngII or Candesartan, levels of miR-483-3p were quantified in RASMC-AT_1R cells (Figure 7.2). We observed a decrease in miR-483-3p expression upon treatment with AngII and an increase in expression upon treatment with Candesartan.

In both assays, miR-483-3p showed the same trend in expression (i.e., downregulated) in the independent samples in response to AngII as we observed in the profiling experiment. In addition, Candesartan treatment produced a distinct response, in which miR-483-3p expression was reversed. Validation of this miRNA in independent VSMC samples gives us confidence that miR-483-3p is robustly regulated by AngII receptor activation.

Figure 7.1. Detection of miR-483-3p by solution hybridization. A) Following treatment with 1μM AngII at various time points, total RNA from RASMC-AT_1R cells was hybridized to a miR-483-3p radiolabeled probe and analyzed by denaturing polyacrylamide gel electrophoresis (lanes 6-10, red box). The miR-16 probe was utilized as a control and detected in mouse kidney RNA (lane 3). Each probe was loaded without (lanes 1 and 4) and with (lanes 2 and 5) RNase digestion. **B)** The corresponding plots show the densitometry analysis of miR-483-3p (closed bar) and miR-16 (open bar) for a single experiment (upper panel) and the calculated fold change for miR-483-3p normalized to miR-16 (n = 3; ** p = 0.0005, *** p = 0.0001) (lower panel).

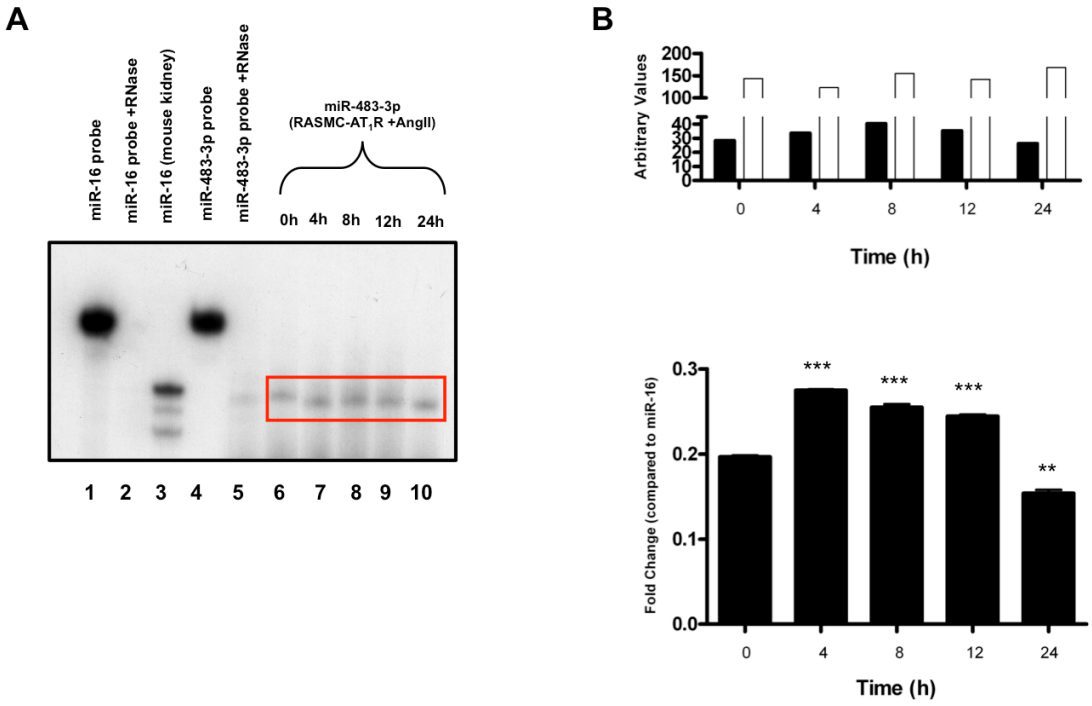

Figure 7.2. Quantitation of miR-483-3p by RT-qPCR. MiRNA expression modulated by AT_1R-specific ligands. Change of expression of miR-483-3p in the AT_1R RASMCs following 1uM AngII or Candesartan treatment for 24 hours (n = 3). Data are presented following normalization to U6 RNA, the cellular levels of which did not vary under different experimental conditions and standardization to an untreated control.

7.3 Muscle Cell Lineage Expression of miR-483-3p

We demonstrated that miR-483-3p is selectively expressed in various human and rodent VSMCs and validated its expression by two distinct methods. As a means to determine its expression across a broad range of cell types, we utilized the solution hybridization technique to detect miR-483-3p. Interestingly, we have found miR-483-3p to be present at basal levels in cardiac (HL-1, H9C2), kidney (NRK52E), and carcinoma cell lines (MCF-7, NC1-H295R) (Figure 7.3). Each of the cell types in which miR-483-3p is present at basal levels are important in tissue RAS, suggesting that miR-483-3p may be an important regulator of the RAS in these cell types.

Importantly, we do not detect miR-483-3p in HEK 293 or HEK-AT_1R cells after treatment with AngII via solution hybridization (Figure 7.4). This observation, along with selective expression of miR-483-3p in VSMCs and cardiomyocytes (HL-1) allows us to be further confident in classifying this miRNA as a muscle cell lineage specific miRNA.

Figure 7.3. Basal miR-483-3p expression across various cell lines. A) Solution hybridization of total RNA from multiple cell lines shown below to a radiolabeled probe specific to miR-483-3p was performed. **B)** Densitometry analysis in provided in the corresponding plot for each sample. Expression in the RASMC line was considered basal expression for our purposes. Anything at or above that level was important.

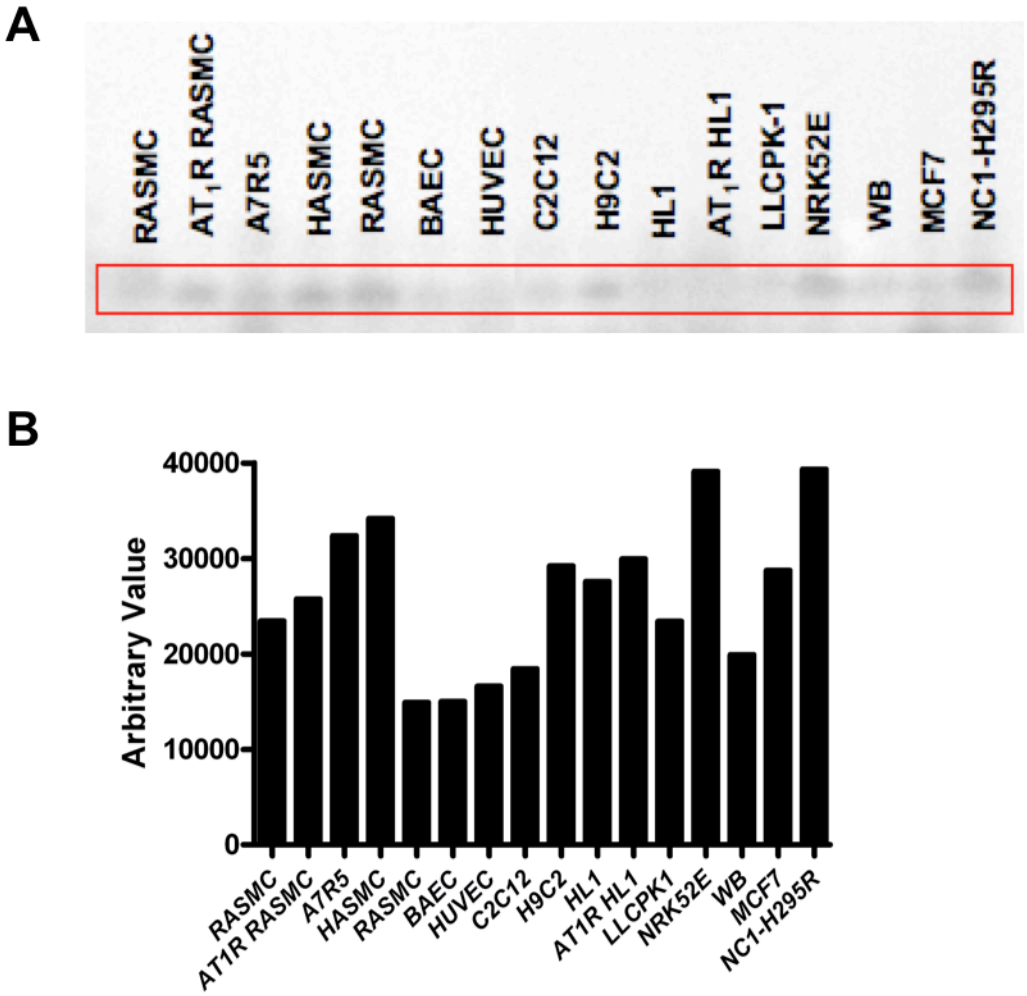

Figure 7.4. MiR-483-3p is undetectable in HEK-AT$_1$R cells. Using RASMC-AT$_1$R cells for comparison, we performed solution hybridization of total RNA from HEK-AT$_1$R cells to miR-483-3p specific probe, following treatment with 1 μM AngII at various time points (lanes 6-15). miR-16 probe was used as a control and detected in mouse kidney RNA (lane 3). Each probe was loaded without (lanes 1 and 4) and with (lanes 2 and 5) RNase digestion. miR-483-3p was undetectable in the HEK cell line.

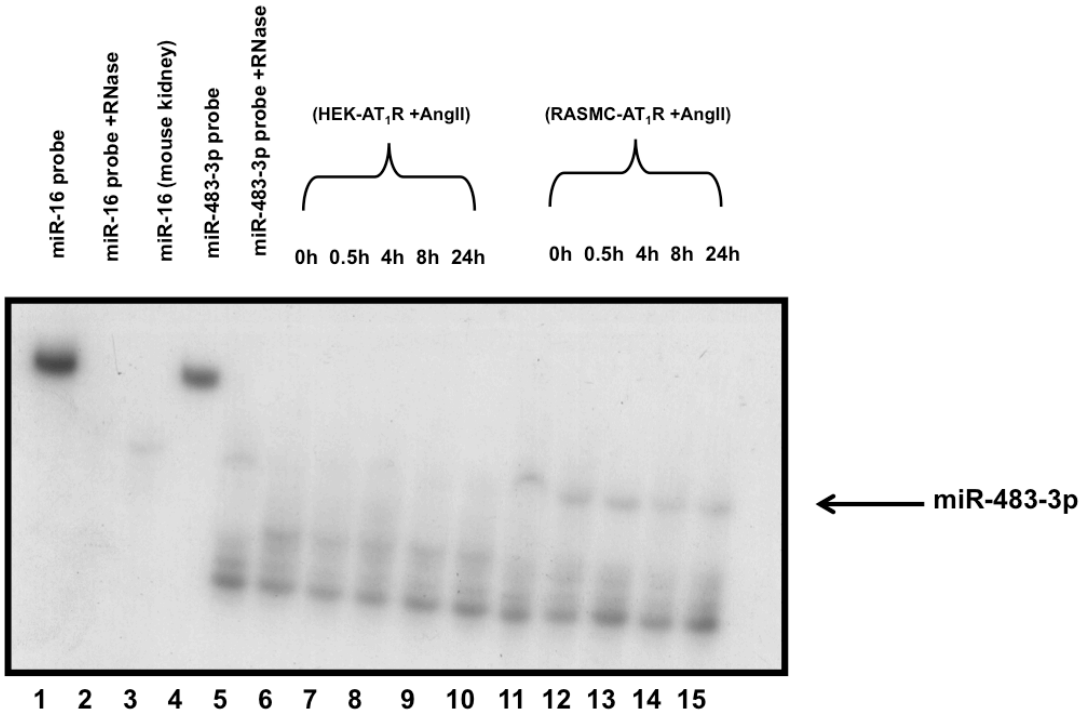

7.4 Functionality of miR-483-3p

To determine the functionality of miR-483-3p *in vitro* we constructed 3 independent cell lines using the miR-483 expression cassette. HEK-293T, RASMC, and RASMC-AT_1R cells were nucleofected with pRNA U6.1-miR483. Cells were cultured in selection medium containing hygromycin and clones were screened for miR-483-3p expression by solution hybridization. We chose clones with the highest detectable level of miR-483-3p for use in our functional assay. Clone #5 in HEK-293T cells (Figure 7.5), clone #3 in RASMC, and clone #10 in RASMC AT_1R cells (Figure 7.6) was chosen as the highest expressing clone and used for further analyses. Control cell lines were also constructed with the pRNA U6.1 empty expression vector and exposed to hygromycin selection.

The HEK-293T-miR483 cells were primarily used for analysis of miR-483-3p targets in a functional luciferase assay. We cloned the 3'UTRs of AGT, ACE-1, ACE-2, and AGTR2 into a dual luciferase expression vector. Following transfection of the HEK-293T-miR483 cells with the 3'-UTR constructs, the cells were subjected to a luciferase substrate and firefly luciferase activity was measured. The cell lysates were then subjected to a second luciferase substrate and *Renilla* luciferase activity was measured. The *Renilla* luciferase expression was then normalized to firefly luciferase activity.

Figure 7.5. Stably expressing miR-483-3p in HEK-293T cells. Of the 10 clones that were picked for HEK-293T cells, we chose clone #5 as having the highest level of miR-483-3p expression, which was determined by solution hybridization. Phase-contrast images (15X) of live cells in culture are shown for both the vector control and miR-483 lines.

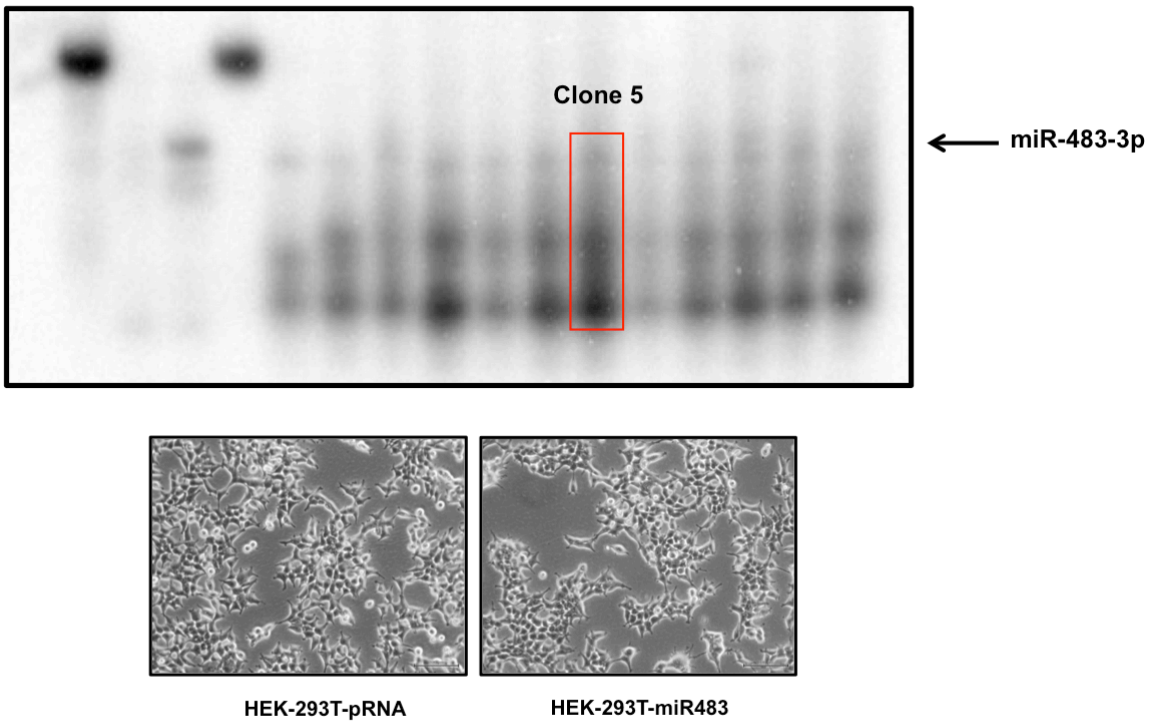

Figure 7.6. Stably expressing miR-483-3p in RASMC and RASMC-AT$_1$R cells. Of the 10 clones that were picked for both RASMC and RASMC-AT$_1$R cells, we chose clone #3 and clone #10, respectively as having the highest level of miR-483-3p expression as determined by solution hybridization. Phase-contrast images (15X) of live cells in culture are shown for both the vector control and miR-483 lines.

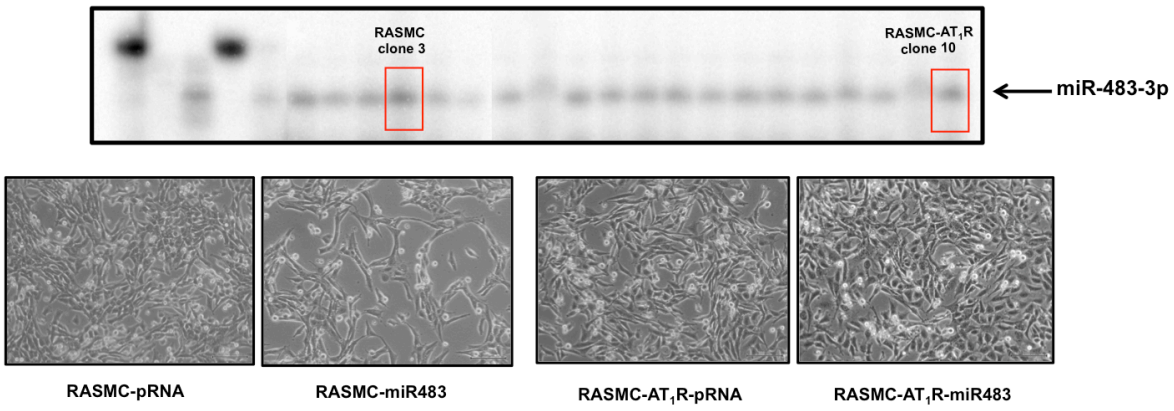

In our vector system, *Renilla* luciferase expression is stabilized by the presence of the 3'UTR, and activity decreases in each case in the presence of miR-483-3p. In addition, in the presence of an antagomiR specific to miR-483-3p, we are able to rescue the luciferase expression in each 3'-UTR example (Figure 7.7). Thus, miR-483-3p can effectively initiate the RNAi process on the target 3'-UTR, suggesting that this miRNA could be a global regulator of tissue RAS.

In addition to the functional readout for the luciferase assay, we also monitored levels of endogenous AGT and ACE-1 by western immunoblotting in the RASMC-AT_1R cells stably expressing miR-483-3p. We demonstrated that in the presence of the miRNA protein levels of AGT and ACE-1 decreased, which can be rescued with the antagomir for miR-483-3p (Figure 7.8). The suppression of ACE-1 levels was not as dramatic as the effect of miR-483-3p on AGT, suggesting that miR-483-3p more strongly regulates AGT endogenously. Unfortunately the AGTR2 and ACE-2 primary antibodies utilized were not functional. We also looked at mRNA levels of the 4 targets and observed no change in AGT, ACE-1, ACE-2, or AGTR2 transcripts in the presence of miR-483-3p. Thereby suggesting that miR-483-3p is acting post-transcriptionally on these target genes.

Figure 7.7. MiR-483-3p targets components of tissue RAS. HEK-293T-miR483 cells were transfected with a 3'-UTR construct and both firefly and *Renilla* activity were measured. In each 3'-UTR target assay, *Renilla* luciferase activity decreased in the presence of miR-483-3p. When a miR-483-3p specific antagomir was introduced into the system, the dampened luciferase activity was rescued to basal levels.

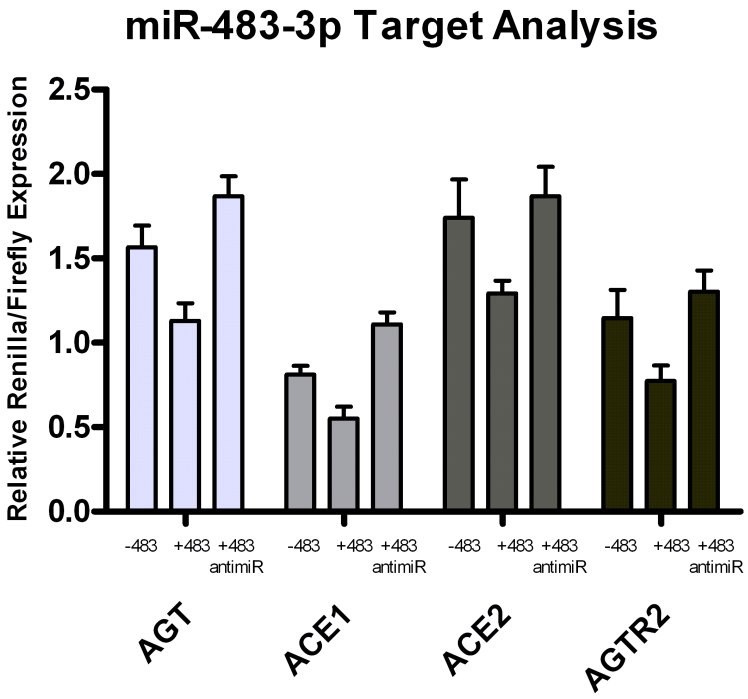

Figure 7.8. MiR-483-3p alters expression of endogenous AGT and ACE-1. A) Western immunoblotting for endogenous AGT and ACE-1 in RASMC-pRNA (lane 1), RASMC-miR483 (lane 2), and RASMC-miR483 + antagomir (lane 3) was visualized. **B)** Densitometry quantification of AGT and ACE-1 levels. Transfection of an antagomir specific for miR-483-3p significantly reduced the levels of AGT, but had a lesser effect on ACE-1 levels (n = 3; *p < 0.05).

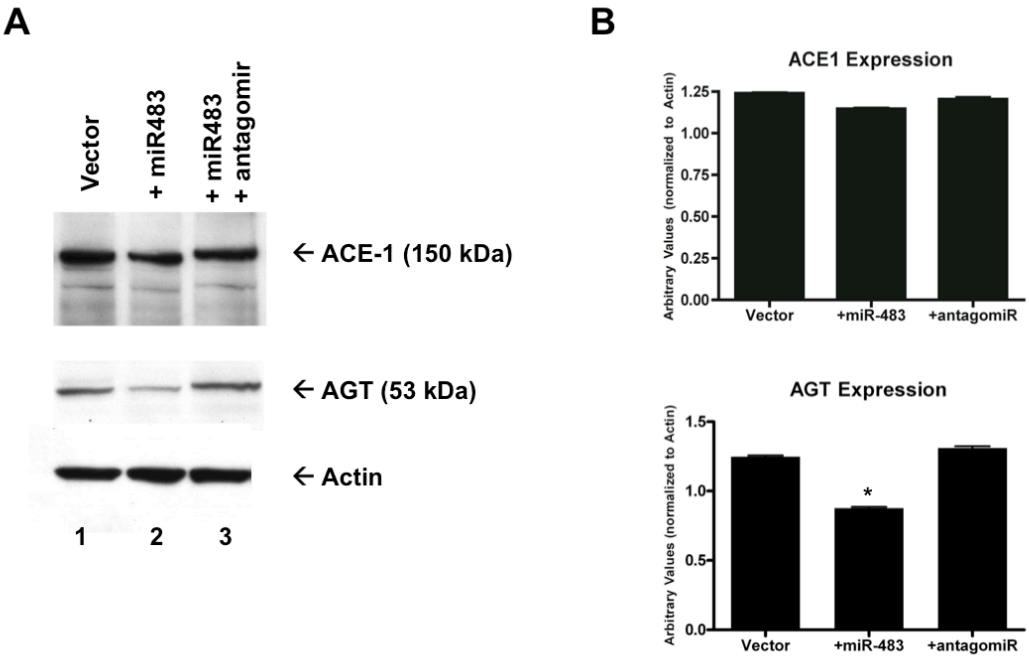

We have demonstrated that upon stimulation with AngII, the AT_1R is activated, leading to a decrease in miR-483-3p expression, which would ultimately result in an increase in the RAS targets of this miRNA. In our initial efforts of understanding the mechanism by which the VSMC-specific miRNAs are regulated by AngII, we utilized MEK1 and JAK2 inhibitors and monitored miRNA expression. We observed that upon inhibition of MEK1 only, miR-483-3p expression increased. An increase in miR-483-3p expression would lead to a decrease in RAS target expression (Figure 7.9 A). Following inhibition with MEK1 and JAK2, we monitored levels of AGT and ACE-1 by western immunoblotting. We determined that MEK1 inhibition causes a decrease in endogenous AGT, but we don't see the effect with ACE-1 (Figure 7.9 B). This result further solidifies the idea that miR-483-3p acts most potently on AGT.

The results presented in this chapter provide significant insight into the expression pattern and functional role of miR-483-3p in targeting and regulating tissue RAS. We have demonstrated expression of this miRNA in multiple cell types of muscle cell lineage, which is important for cardiovascular biology and for fully understanding the effects that AngII has on those tissues. Additionally, we have shown that miR-483-3p, which is in part regulated by the AngII-mediated kinase MEK1, functions biologically to inhibit multiple components of the RAS. From our studies, endogenous AGT appears to be most altered in response to miR-483-3p expression. Demonstrating that this VSMC-specific miRNA has a functional role prompted us to determine whether miR-483-3p could affect VSMC behavior and phenotype.

Figure 7.9. Effect of MEK1 inhibition on endogenous AGT and ACE-1. A) AngII stimulation of the AT_1R causes activation of the AngII-mediated kinase MEK1, which leads to a decrease in miR-483-3p expression and a subsequent increase in RAS target genes. Conversely, inhibition of MEK1 leads to an increase in miR-483-3p, which should lead to a decrease in RAS target genes. **B)** Following kinase inhibition of RASMC-AT_1R-miR483 cells, we detected a decrease in AGT, but not ACE-1 by western immunoblotting (lane 4, n = 1).

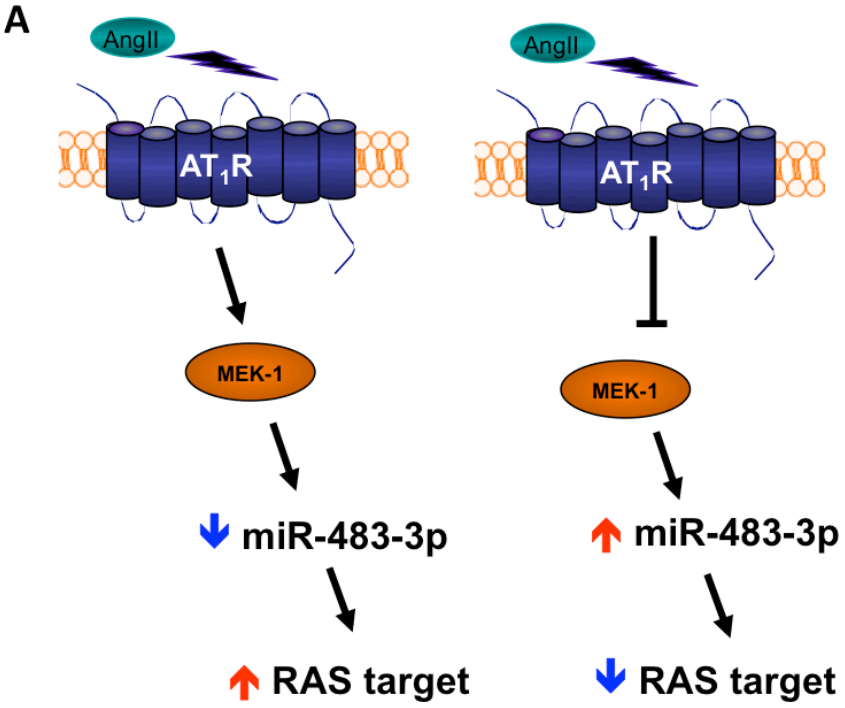
A
AngII
AT1R
MEK-1
miR-483-3p
RAS target
AngII
AT1R
MEK-1
miR-483-3p
RAS target

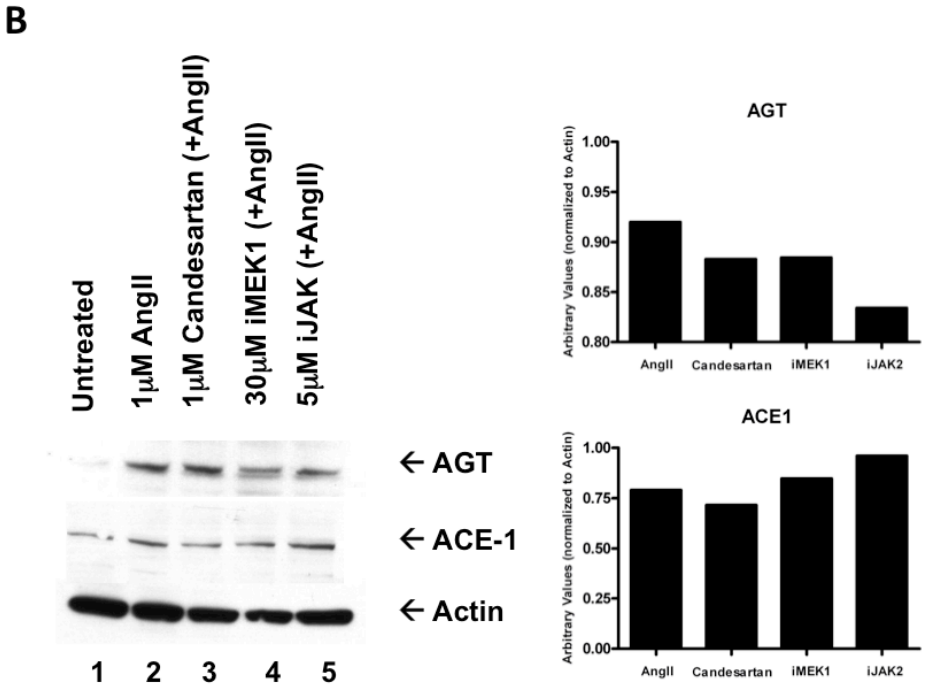
B
Untreated
1μM AngII
1μM Candesartan (+AngII)
30μM iMEK1 (+AngII)
5μM iJAK (+AngII)
← AGT
← ACE-1
← Actin
1 2 3 4 5
AGT
Arbitrary Values (normalized to Actin)
1.00
0.95
0.90
0.85
0.80
AngII
Candesartan
iMEK1
iJAK2
ACE1
Arbitrary Values (normalized to Actin)
1.00
0.75
0.50
0.25
0.00
AngII
Candesartan
iMEK1
iJAK2

CHAPTER VIII

MODULATING VSMC PHENOTYPE

8.1 Introduction

To further characterize the function of miR-483-3p, we have observed its effects on VSMC phenotype. It is well known that various stimuli, including AngII, can cause VSMCs to switch between contractile and proliferative states due to global gene expression changes, which play a central role in cell motility and diverse vascular diseases. Understanding the extent to which miR-483-3p plays a role in this phenomenon will reveal if this miRNA acts as a critical regulator of cellular phenotype as a potential player in various vascular pathologies (Figure 8.1).

Figure 8.1. Effect of miR-483-3p on VSMC phenotypic switching. Due to the high density of AT_1 receptors on VSMCs, AngII is able to induce VSMCs to switch from a contractile to the synthetic state, which can ultimately lead to increased cell motility and vascular abnormalities.

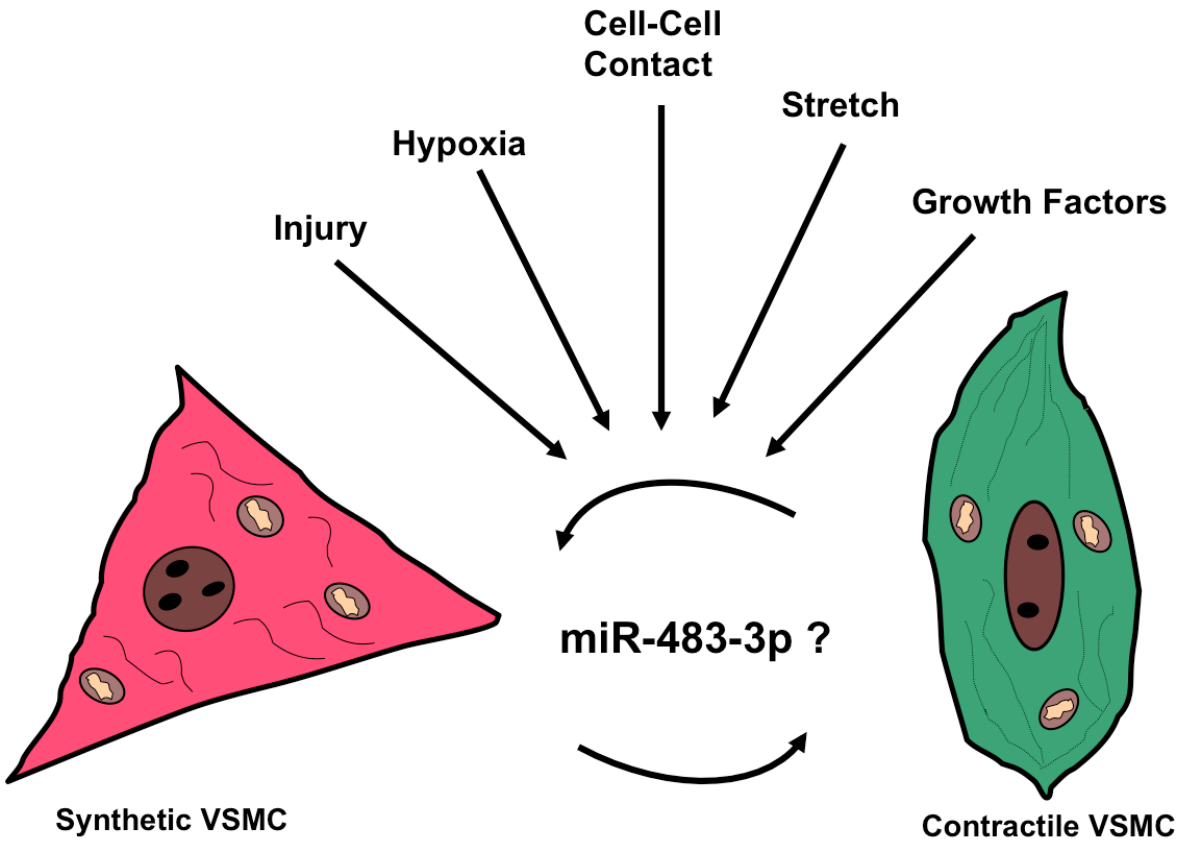

8.2 Effects of miR-483-3p on VSMC Migration

To determine the involvement of miR-483-3p in VSMC *in vitro* migration we utilized the RASMC-AT_1R cells, stably expressing miR-483-3p. Using a standard wound-healing assay, we monitored cell movement into a wounded or cleared area for a period of 24 hours. We performed this experiment in the presence of 1 μM AngII and Candesartan to understand the effects that AT_1R-specific ligands would have on this phenomenon.

In cells that were left untreated, there was no significant difference in the wounded area when comparing presence and absence of miR-483-3p. We observed that by 8 hours, miR-483-3p action significantly decreased AngII-mediated VSMC migration when compared to conditions where the miRNA was absent (Figure 8.2 A). This same effect was observed under treatment with Candesartan. The area of the wound was determined, in relation to the total area, for each well and the percent wound area was calculated (Figure 8.2 B).

The results discussed in this chapter examine a novel role of miR--483-3p in mediating VSMC phenotype. In response to AngII, VSMCs enter into the synthetic and migratory phenotype, giving rise to vascular pathologies. MiR-483-3p functions to slow the rate of AngII-mediated VSMC migration in culture, thereby suggesting that when this miRNA is downregulated in response to AngII molecules involved in cellular movement would be independently and adversely increased. This effect could ultimately give rise to vascular abnormalities *in vivo*.

Figure 8.2. MiR-483-3p decreases AngII-mediated cell migration. A) Wound healing was observed in RASMC-miR483 and RASMC-pRNA untreated (panel 1), treated with 1 μM AngII (panel 2), or 1 μM Candesartan (panel 3) for a period of 24 hours. By 8 hours, RAMSC-miR483 cells exhibited a decrease in AngII-mediated migration (red box). In addition, in cells containing miR-483-3p and treated with Candesartan, the cell migration was decreased. **B)** The corresponding plot shows the quantitation of the results using ImagePro Plus software. The area of the wound and the total area at time 0h and 8h were determined for 2 different positions in each well (n = 3; ns, not significant, *** p = 0.0003, ** p = 0.0045).

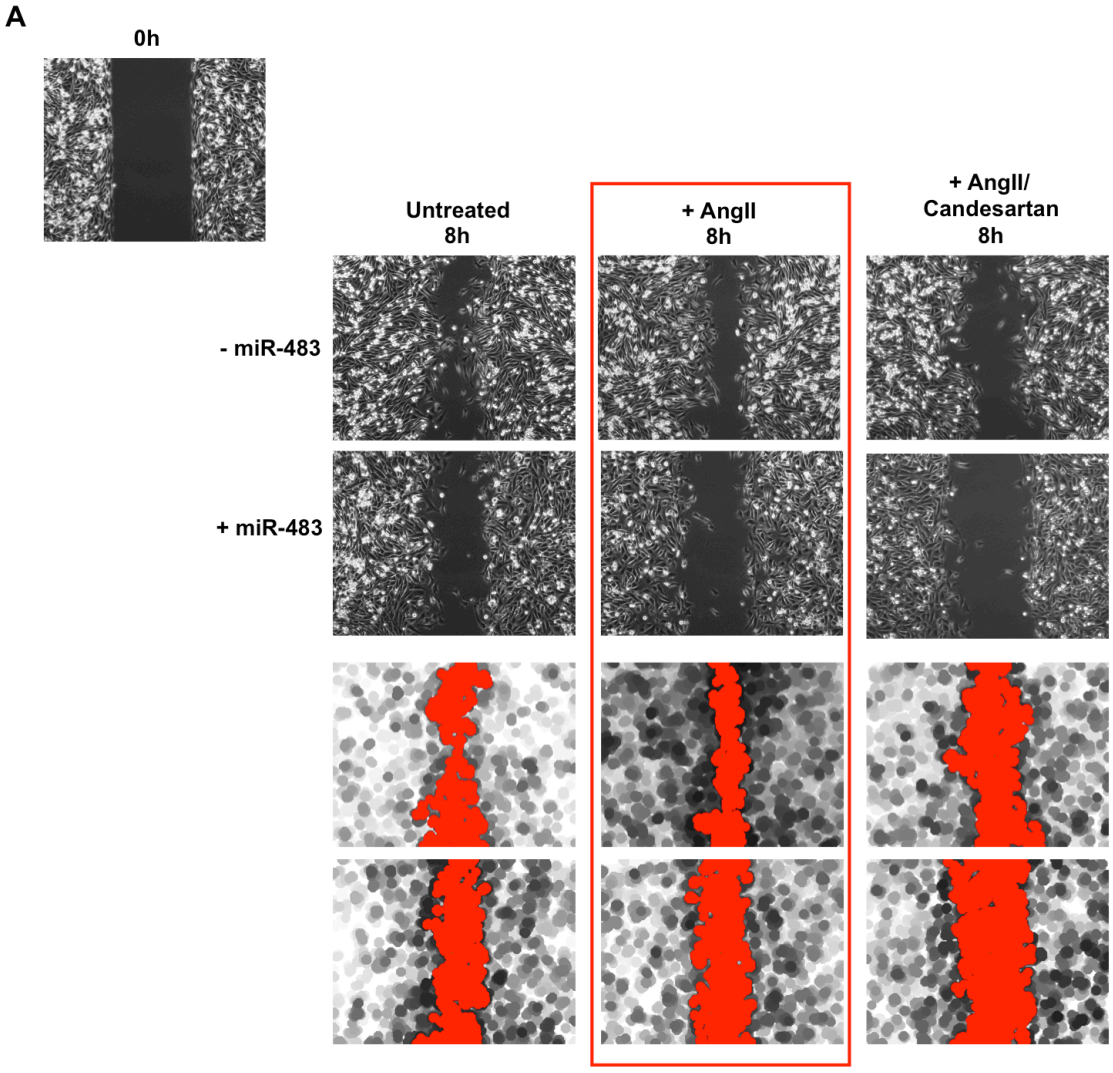
A
0h
Untreated
8h
+ AngII
8h
+ AngII/
Candesartan
8h
- miR-483
+ miR-483
B
% Wound Area (Normalized to Total Area)
35
30
25
20
15
10
5
0
ns
***
**
Vector
miR-483-3p
UT
AngII
Candesartan
Treatment Condition

CHAPTER IX

FUTURE DIRECTIONS

9.1 Comprehensive Description of miR-483-3p

As a means to fully characterize the function of miR-483-3p, we will turn to monitoring the effects of miR-483-3p on additional phenotypic phenomena, including adhesion and proliferation via thymidine (DNA) or leucine (protein) incorporation. Additionally, we aim to determine the ability of this miRNA to regulate the cell cycle. We have performed one cell cycle analysis and observed that miR-483-3p has the ability to alter the number of cells in the G2 phase; however, additional experiments need to be performed in order to wholly demonstrate the effect of miR-483-3p on cell cycle control. A critical aspect of our study is to understand the mechanism by which miR-483-3p effects AngII-mediated VSMC migration. In so doing, we will determine changes in contractile proteins (e.g., α-actin, myosin) and possible secretion of SMC-specific ECM components (e.g., collagen, fibronectin, laminin, tenascin) that would be important in regulating phenotypic alterations. Further, we will determine if miR-483-3p affects the

secretion of AngII-specific cytokines (e.g., MCP-1, IL-1, IL-6, TNF-α) and chemokines (e.g., RANTES, IP-10, CyPB) and accumulation of reactive oxygen species, all of which have been previously shown to play a role in VSMC physiology and pathology. Taken together, these future studies will allow us to determine the full capacity of the AngII-regulated miR-483-3p on vascular biology.

Ultimately, our goal is to see if the effect miR-483-3p has in the cellular system (i.e., inhibition of RAS components and ability to decrease VSMC migration) is also a phenomenon that can bee seen *in vivo*. We would expect that expression of the miRNA would protect the vessels against activation of tissue RAS, creating an overall beneficial effect. Thereby, preventing VSMCs from entering into the synthetic migratory phenotype. Using a lentiviral system, we will first recapitulate the effect of miR-483-3p in VSMCs infected with the lentivirus produced from a viral vector (Figure 9.1). The BLOCK-IT™ technology from Life Technologies is designed to express artificial miRNAs. Using this system, a double-stranded DNA oligonucleotide encoding miR-483 would be cloned into one of the BLOCK-iT™ entry expression vectors and the miRNA cassette would be transferred into the lentiviral destination vector by Gateway® recombination. The vectors would be transfected into the viral producer cells to produce viral stocks, which can be used immediately or stored at –80°C. The viral supernatants would be harvested and the viral titer determined. Finally, the lentiviral stocks could be transduced to any cell type, specifically VSMCs.

We will then monitor the effect of miR-483-3p in a hypertensive mouse model by injecting the virus into the tail vein (Figure 9.2). One mouse model utilized in hypertensive research consists of crossbreeding a transgenic mouse containing the human renin gene (hRN 8-12; 10 copies of a 15 kbp human DNA fragment containing the renin gene) with a transgenic mouse for human angiotensinogen (hAG 2-5; 100 copies of a 14 kbp human DNA fragment containing the angiotensinogen gene). This results in a mouse with high blood pressure.

By monitoring the phenotype of these animals, through either determining that this miRNA could prevent or reduce development of hypertension (by measuring blood pressure) and vascular changes (by examining vessel wall thinning), we would be able to determine if tmiR-483-3p has the capability of regulating a physiological phenomenon *in vivo*, such as the RAS.

Overall, observing the full effect of miR-483-3p *in vitro* and *in vivo* will allow us to understand its capacity as a regulatory molecule. Most importantly, we will be able to discern its involvement in RAS pathologies within the cardiovascular system.

Figure 9.1. Lentiviral expression system. Viral delivery of RNAi vectors is a powerful alternative to transfection for primary cell types as well as for in vivo applications. The procedure for creating a lentiviral expression system consists of cloning the double-stranded DNA oligonucleotide encoding a miR RNAi into one of the BLOCK-iT™ entry expression vectors. The RNAi cassette is transferred into the lentiviral destination vector by Gateway® recombination and transfected into the viral producer cells to produce viral stocks, Viral supernatants are harvested and titers are determined. Finally, the lentiviral stocks can be transduced into any cell type of used *in vivo* (From Life Technologies).

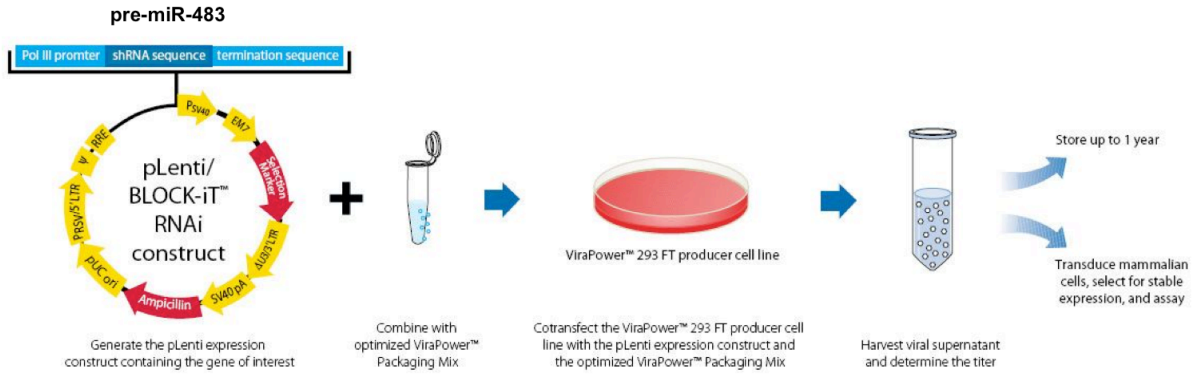

Figure 9.2. Genetic murine models constructed to exhibit increased blood pressure. Through manipulation by overexpression (yellow) or knockout (orange) of various components of the RAS, hypertensive mouse models exist and are useful for understanding biological functions *in vivo* From (Lerman et al., 2005).

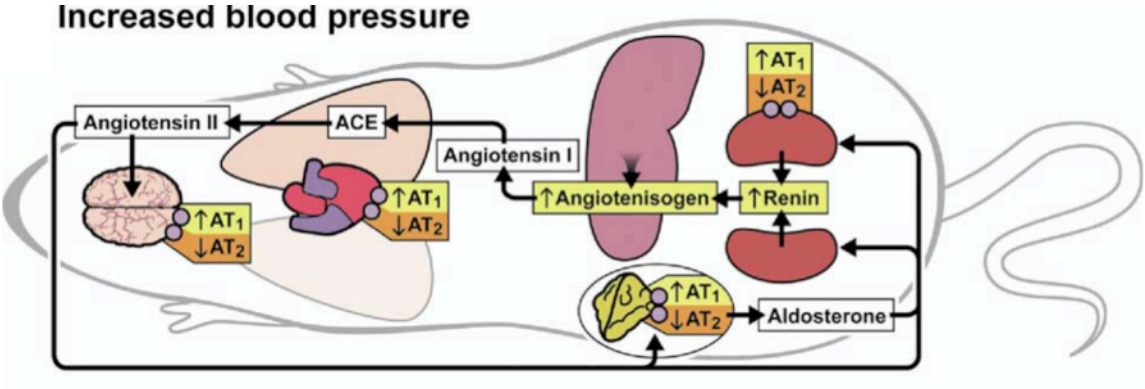

CHAPTER X

DISCUSSION

10.1 The Implications of Genome-wide MiRNA Profiling in Response to AngII

It has become increasingly apparent over time that the complexity of RAS is immense. Securing AngII through its interaction with the AT_1R as a powerful regulator of gene expression has given much insight into the potent role for this vasoactive hormone in cardiac biology and disease. Intracellular signaling mediated through AT_1R activation by AngII has a prominent place in vascular and endothelial physiology and dysfunction.

The unbiased miRNA profiles presented here may bridge the gap in our knowledge concerning the molecular basis of pathogenesis during chronic RAS activation, which increases angiotensinergic risk associated with morbidity and mortality from cardiovascular diseases. In many clinical settings, targeting RAS is an important therapeutic paradigm. Our study provides insights regarding how RAS-targeted therapies may affect miRNAs. This study was designed for global miRNA expression profiling in biological replicates following chronic AngII activation. Thirty-two miRNAs were AngII

regulated in most human and rodent samples. Expression of these miRNAs were antagonized following AT_2R activation by AngII and Losartan blockade of AT_1R in both VSMCs and HEK-AT_1R cells, suggesting that expression of these miRNAs is a hallmark of AngII action through the AT_1R, which is targeted in most clinical settings. The inclusion of RNA derived from tissue, primary cells and established cell lines in our analysis demonstrates that this miRNA fingerprint is not derived from complex heterotypic cell-cell interactions nor influenced by a multitude of endocrine, paracrine or autocrine and neuronal influences, a common confounding problem in many analyses.

The identified miRNA profile discussed in this study reflects common AngII-regulated changes in humans and rodents, a miRNA fingerprint of RAS action through the AT_1R. Though we did not determine how alterations in these miRNAs functionally affect the in vivo response to AngII, we propose that these miRNAs play a significant role in AngII mediated physiology and pathogenesis. If the miRNAs we identified can be shown to play a role in RAS function in vivo, they may represent new biomarkers of injury caused by RAS and should serve as useful prognostic markers during RAS targeted therapy.

10.2 Specificity of MiRNA Expression

Demonstrating miRNA specificity is important in elucidating the regulation of these small RNAs. Inclusion of losartan treated AT_1R as well as AngII treated AT_2R expressing control samples demonstrated specificity of the AngII effect through the AT_1R in our profiling experiments. The miRNA changes in individual comparisons showed a range between 60 and 234 miRNA genes per sample (Fig. 3.2 & 3.3).

This finding is consistent with the miRNA expression profiles characterized in complex tissues, sorted cells and individual cell lines, which demonstrated that on average ≈70-150 miRNA genes were expressed per sample (Landgraf et al., 2007, Chiang et al., 2010). Our finding of ≈30 miRNAs (Table IV.I) ubiquitously expressed in cell lines and tissue samples from rodents and human is also consistent with the observation in model studies for basic mechanisms of stem cell maintenance, hormonal differentiation, and malignant transformation to organ systems, in which the authors estimated ≈30-40 ubiquitously expressed miRNAs per sample (Chiang et al., 2010, Landgraf et al., 2007).

In addition, several miRNAs mapped to multicopy miRNA genes (Table III.VIII). Expression of a specific miRNA or a select few from the cluster suggests stimulus-specificity of processing of individual miRNAs from polycistronic pri-miRNA transcripts, as previously observed in human studies (Baskerville and Bartel, 2005). A third of the remaining miRNAs were expressed with a high degree of cell specificity (e.g., miRs-365, -699, -490, -434-3p, -675-3p are cardiomyocyte-specific).

Additionally, the expression of some miRNAs was only altered under one treatment condition (e.g., miRs-546, -100, -92a are strictly Losartan modulated) or only altered in one cell type (e.g., miRs- 376a*, -487b, -154*, -539, -376c* are expressed in HEK-AT_1R cells only). Tissue-specific factors might be essential for biogenesis of tissue-specific miRNAs, and therefore might be sensitive to the potential absence of such factors in some cells and tissues. Taken together, these findings are consistent with the

tissue and cell-type specific regulation of miRNAs in response to AngII and the potential role of these miRNAs in physiology and in various diseases.

As an important RAS hormone, AngII must play a wider role in regulating the relative abundance and specificity of expression of miRNAs in order to regulate a variety of physiological and adaptive tissue remodeling processes. Thus, the miRNA regulation is a critical aspect of effectiveness of hormones such as AngII in various cells.

10.3 A SMC-specific MiRNA Signature

Regulation of miRNAs in VSMCs by a local increase in AngII can adversely affect vessel functions due to the high density of the AT_1R on VSMCs. Distinct VSMC phenotypes accumulate within arteries of individuals with disorders such as systemic and pulmonary hypertension, atherosclerosis, and asthma. During insult, VSMCs switch to a proliferative phenotype of poor contractility/excitability, exhibit changes in lipid metabolism, and have high extracellular matrix production leading to vessel remodeling. In contrast, the phenotype of healthy adult VSMCs is restricted cellular plasticity, in which the cells are geared for contraction with a unique repertoire of contractile proteins, agonist-specific receptors, ion channels, and signaling molecules. Thus VSMCs are an interesting model system for studying miRNA-modulated mechanisms of cell maintenance, differentiation, and phenotypic modulation (Rensen et al., 2007, Daugherty and Cassis, 2004).

Regulation of specific miRNAs as contributors to vascular disease (e.g., miR-155, -143, -145, -21, -126) has been studied (Urbich et al., 2008), but a comprehensive analysis targeting AngII-regulation of miRNAs in VSMCs and its associated diseases is lacking. Our analysis of AngII-regulated miRNAs in rat and human VSMC cell lines (Table IV.III) indicated for the first time a unique fingerprint consisting of novel miRNAs and miRNAs with known functions. As shown in Table IV.III, a significant number of the AngII-regulated miRNAs have been implicated in pathogenesis of other organs and tissues, implying that a systematic study of their role in vasculature is important. Confirmation of the VSMC candidates identified miRNAs that were both up and downregulated by AngII signaling through the AT_1R.

10.4 Regulation of the AngII-induced MiRNA Pool

Our data indicate that AT_1R signaling through JAK2 and MEK1 regulate two completely independent miRNA pools (Figures 5.2 & 5.3). The amount of a specific miRNA that exists within a cell is determined by its biogenesis and decay. The biogenesis of miRNAs is critically regulated at the level of transcription similar to those of protein-coding genes. Regulation of miRNA expression through the MEK/ERK1/2 interaction with PEA-15 cascade is known. PEA-15 sequesters ERK1/2 in the cytoplasm, thereby inhibiting the ability of ERK1/2 to localize to the nucleus and modulate miRNA gene transcription (Romano et al., 2012). Many miRNA genes are transcribed by a transcription factor binding to upstream promoters. However, transcriptional regulation of miRNA pools by AngII appears unlikely to us for two reasons: (i) transcription of miR-483 and IGF2 (the gene that harbors miR-483) were not altered by AngII activation

of the RASMC-AT_1R cells (data not shown); and (ii) ERK1/2 phosphorylation leads to translocation into the nucleus, where gene transcription and pri-miRNA processing are regulated.

In our study, both MEK1 and JAK2 inhibitors inhibited ERK1/2 activation, but these inhibitors affected distinct miRNAs, suggesting that the AngII-activated JAK2 and MEK signaling alters non-canonical and perhaps miRNA-specific regulatory steps. Pri-miRNA sequence-specific recruitment of Smad proteins (Smad-1 and -5) to the p68–DROSHA complex in pulmonary artery smooth muscle cells has been reported (Davis et al., 2010, Davis-Dusenbery and Hata, 2011). The association between Smads and pri-miRNAs is primarily controlled by Smad nuclear localization upon TGF-β activation. This non-canonical pathway relies on the interaction of the Smad amino-terminus MH1 domain with R-SBE. R-SBE contains a consensus RNA binding sequence (5' – CAGAC – 3'), which is present in the stem region of miR-21, miR-100, miR-199a-5p, and miR-27a (Davis et al., 2010).

AngII regulation of distinct miRNAs may involve novel non-canonical pathways. Our results suggest a novel Tyr-kinase pathway in miRNA regulation. Kim *et al* showed that the proteins involved in miRNA biogenesis (e.g., Drosha, TRBP, Dicer, Ago 2) could be phosphorylated by protein kinases. Accordingly AngII-activated kinases may potentially target Drosha, TRBP, Dicer, or Ago 2 to regulate biogenesis or degradation of miRNAs (Kim et al., 2010). However, this type of regulation would be expected to alter

the miRNA pool in a cell not individual miRNAs, hence this may not be the mechanism in our model system.

10.5 MiR-483-3p is a Novel AngII-regulated MiRNA

In our unbiased genome-wide screen of miRNAs modulated by AngII, we identified a subset of 22 miRNAs differentially regulated in VSMCs by AngII activation of the AT_1R, including one whose predicted gene targets are involved in RAS homeostasis.

Identifying miR-483-3p as a novel AngII-regulated miRNA has given us some insight into the complexity of miRNA biology. Not only can many miRNA genes be expressed in any given cell type, but they also can regulate a multitude of cellular processes within a cell type (Bartel, 2004). Sequence alignment revealed that one of the VSMC candidate miRNAs, miR-483-3p, is encoded within intron 2 of IGF2, a gene that encodes a key mitogenic factor (Figure 6.3). Furthermore, the pri-miRNA is highly conserved in mammals (Figure 6.4), prompting us to select miR-483-3p for further characterization of its role in altering global gene networks, cellular metabolism, and VSMC phenotype.

We found that in VSMCs, miR-483-3p is downregulated, whereas, IGF2 expression is upregulated, suggesting that miR-483-3p is independently regulated by AngII signaling (Figure 6.2). Furthermore, VSMCs treated with the AT_1R-specific inverse agonist, Candesartan showed upregulation of miR-483-3p. Analysis of the

kinetics of miR-483-3p induction revealed that upon acute treatment with AngII (0.5 h), the miRNA levels increase, however with chronic AngII treatment (24 h), miR-483-3p levels are significantly decreased (Figure 7.1), pointing toward a role for this miRNA in tissue RAS, which is substantially involved in AngII-mediated vascular pathologies. We next determined whether miR-483-3p was expressed in any other cell types that are commonly and adversely affected by local action of AngII. Our observations demonstrated that miR-483-3p is expressed in various cell types of muscle cell lineage, in addition to a kidney and multiple carcinoma cells types (Figure 7.3), and to a lesser extent in epithelial cells (Figure 7.4). Taken together these data reveal that miR-483-3p could have a distinct role in mediating vascular abnormalities that arise as a result of tissue RAS activation.

10.6 Regulation of the RAS by miR-483-3p

To gain insight into the function of miR-483-3p, we analyzed its potential gene targets, using several miRNA target prediction algorithms (Brennecke et al., 2005). We identified putative binding sites for miR-483-3p in the 3′UTR of several genes involved in the RAS, including AGT, ACE-1, ACE-2 and the type II receptor, AGTR2, suggesting that miR-483-3p coordinates RAS homeostasis (Figure 6.1). To test this hypothesis, we determined the effect of miR-483-3p on the expression of AGT, ACE-1, ACE-2 and AGTR2 in HEK-293T cells and RASMCs. To assess the effects of miR-483-3p on the 3'-UTR of human AGT, ACE-1, ACE-2, and AGTR2, we used luciferase reporter constructs. Transfection of HEK-293T-miR483 cells with 3'-UTR constructs for the RAS target genes repressed luciferase activity of all 4 targets. These effects of miR-483-

3p were reversible by co-transfection with an antisense inhibitor of miR-483-3p (anti-miR-483) (Figure 7.7). MiR-483-3p also repressed AGT and to a lesser extent ACE-1 protein in RASMCs, indicating that its effects are robust on endogenous protein levels as well. Inhibition of miR-483-3p by anti-miR-483 increased the expression of AGT and ACE-1 in RASMCs (Figure 7.8), which is consistent with the hypothesis that miR-483-3p has a physiological role in regulating the expression of these components of the RAS.

Determining the molecular mechanism by which AngII, through receptor activation, can lead to a change in miR-483-3p expression was of importance in this study. We showed that miR-483-3p is regulated in part by the AngII-specific kinase MEK1. Levels of miR-483-3p were upregulated upon inhibition of MEK1, which was the opposite response seen with AngII stimulation (Figure 5.3). Additionally, under pharmacological inhibition of MEK1, the miR-483-3p target AGT was increased (Figure 7.9). Together, these results give us confidence that AGT is a direct target of miR-483-3p and that the regulation of this miRNA is in fact through MEK1 activation.

The ability of miR-483-3p to target multiple components of the RAS is profound. Most importantly, the effect of miR-483-3p on AGT is the most convincing and points to a third portion of the RAS that could be a potential therapeutic target. Both ACE-1 inhibitors and ARBs are utilized to date to effectively treat hypertension and related abnormalities caused by over activity of tissue RAS (Ritter, 2011); however, targeting AGT has not been shown until now. Suppressing angiotensinogen would ultimately

block production of AngII, similar to ACE-1 inhibitors, but may have fewer side effects. Without *in vivo* studies, however, we will not know the true capacity of targeting AGT.

10.7 Modulation of VSMC Phenotype

The RAS is known to be highly active during vascular insult. Specifically, AngII when over active plays a significant role in inducing a synthetic phenotype in adult VSMCs (Bader et al., 2001). In this state, cells synthesize growth factors and other proteins that enhance their proliferative and migratory potential. A critical aspect of this study was to determine the extent to which miR-483-3p could alter VSMC phenotype and thereby modify migration of VSMCs in the presence of AngII. Using a wound-healing assay, we demonstrated that RASMCs overexpressing miR-483-3p had the capability of suppressing AngII-mediated cell migration (Figure 8.2). In the presence of Candesartan the effect of miR-483-3p is maintained and cell migration is also slowed.

A single miRNA has the potential to orchestrate post-transcriptional regulation of approximately 100-200 genes in a cells, either by translational inhibition or degradation of the target mRNA (Bartel, 2009). We postulate that miR-483-3p targets VSMC-specific cytoskeletal proteins involved in cellular movement, thereby causing suppression of cell migration even in the presence of AngII. Characterizing miR-483-3p, as a causative agent in VSMC phenotypic switching is a significant aspect of AngII biology that will aid in understanding tissue RAS further.

10.8 Final Remarks

The results of the current work have shown that AT_1R activation by AngII produces signals that regulate specific miRNA expression. A distinct AngII-regulated miRNA signature emerged in VSMCs, which was validated in independent samples. Further insight into how miRNAs modulate phenotype of cells in different tissues will be valuable for a greater understanding of AngII biology, as well as in determining the intrinsic regulatory influence of RAS on cardiovascular disease.

Following our previous profiling study in human heart failure (Naga Prasad and Karnik, 2010, Naga Prasad et al., 2009) it was increasingly apparent that understanding the complex network involving miRNAs and their targets, which leads to a coordinated pattern of gene expression, will undoubtedly provide important tools to develop novel therapeutic strategies. This will enhance knowledge of physiological regulation, dysregulated vascular remodeling, and mechanism for atherosclerotic disease progression. In addition, selective regulation of particular miRNAs targeting vascular diseases is a promising prospect for future therapy. Much work remains to be accomplished to advance our knowledge of the involvement of miRNAs in RAS pathogenesis of cardiovascular disease and to develop therapeutic strategies to ultimately affect morbidity and mortality.

Although the pathways regulating the RAS are well characterized, AngII-induced miRNAs and the molecular mechanisms of their expression remain poorly defined. Having focused our efforts on understanding the functional role and mechanism by which miR-483-3p is regulated is only one example of an AngII-responsive miRNA having a

substantial impact. As we move forward with this work, we will be able to distinguish additional RAS regulated miRNA that could have an important function in cardiovascular biology. Our work identifies miR-483-3p as a potential regulator of tissue RAS homeostasis, which has an important impact on VSMC biology. Because tissue RAS is highly active in vascular disease, there has been intense interest in therapeutically targeting the RAS (Paul et al., 2006). Our study suggests that modulating endogenous levels of miR-483-3p may be a useful therapeutic strategy for regulating RAS and controlling VSMC phenotypic switching.

CHAPTER XI

FUTURE DIRECTIONS

11.1 Introduction

The results presented in this dissertation have shown a class of 32 miRNAs that are universally responsive to AngII in humans and rodents, a fingerprint of miRNA expression in VSMCs regulated by AngII, and evidence of unconventional regulation of miRNA levels in VSMCs through AT_1R signaling. This study as a whole has allowed us to appreciate the capacity of AngII signaling through the AT_1R in mediating the transcriptome and the miRNome. Further in-depth analyses of the AngII-responsive miRNAs will answer questions regarding the function of these miRNAs in modulating phenotype in other cell systems.

We also present our initial efforts of characterizing the biological function of a single AngII-regulated miRNA in VSMCs, as a means to understand its role in vascular physiology and progression of AngII-mediated pathologies. In addition to fully

characterizing miR-483-3p, in future studies we will examine whether additional miRNAs identified as differentially regulated in the genome-wide analysis are able to modulate VSMC phenotypes, such as vascular inflammation and remodeling in response to AngII.

11.2 Complete Transcriptional Characterization

With the more recent advent of techniques for direct sequencing of the transcriptional output of the genome, we can now begin to think about a complete transcriptional characterization of all the cells of an organism, following AngII stimulation. RNA sequencing (RNA-Seq) is direct high-throughput sequencing that enables researchers to examine transcriptome fine structure. Transcript sequences are mapped back to a reference genome and then counted to assess the level of gene expression, the number of mapped reads being the measure of expression level for that gene or genomic region (Malone and Oliver, 2011). Because RNA-Seq provides direct access to the sequence, junctions between exons can be assayed without prior knowledge of the gene structure, RNA editing events can be detected, and knowledge of polymorphisms can provide direct measurements of allele-specific expression (Malone and Oliver, 2011).

Since the completion of the Human Genome Project, our perception of our genome has dramatically shifted. That is, the number of protein-coding genes in our genome has been revised down, whereas the number of non-protein coding transcripts has significantly increased. Long non-coding RNAs (lncRNAs) are one group of non-

protein coding transcripts that were generally considered transcriptional 'noise' until the advent of RNA-Seq technologies. These RNAs are longer than 200 nucleotides, making them distinguishable from small regulatory RNAs such as miRNAs. The function and activity of these lncRNAs remain poorly understood; therefore, future studies must seek to examine their role within our genome. What is known is that these RNAs are involved in a variety of biological processes as regulatory molecules (Moran et al., 2012, Yan and Wang, 2012). Much like miRNAs, lncRNA expression profiles are altered in human disease states, including several types of cancer (Brunner et al., 2012). Deciphering the role of AngII in mediating expression of lncRNAs would be beneficial in elucidating the complete effect of AngII stimulation and AT_1R activation on regulating the cellular transcriptome.

The ability of the peptide hormone AngII to induce transcription by signaling through the AT_1R is an area of research that is constantly being expanded. Elucidating the full capacity of AngII as a cellular agonist in inducing gene expression of additional non-coding RNAs will likely provide further insight into the tissue-selective modulation of AngII effects in disease states.

BIBLIOGRAPHY

APLIN, M., CHRISTENSEN, G. L. & HANSEN, J. L. 2008. Pharmacologic perspectives of functional selectivity by the angiotensin II type 1 receptor. *Trends Cardiovasc Med,* 18**,** 305-12.

BADER, M. & GANTEN, D. 2008. Update on tissue renin-angiotensin systems. *J Mol Med (Berl),* 86**,** 615-21.

BADER, M., PETERS, J., BALTATU, O., MULLER, D. N., LUFT, F. C. & GANTEN, D. 2001. Tissue renin-angiotensin systems: new insights from experimental animal models in hypertension research. *J Mol Med (Berl),* 79**,** 76-102.

BARTEL, D. P. 2004. MicroRNAs: genomics, biogenesis, mechanism, and function. *Cell,* 116**,** 281-97.

BARTEL, D. P. 2009. MicroRNAs: target recognition and regulatory functions. *Cell,* 136**,** 215-33.

BASKERVILLE, S. & BARTEL, D. P. 2005. Microarray profiling of microRNAs reveals frequent coexpression with neighboring miRNAs and host genes. *RNA,* 11**,** 241-7.

BELL, L. & MADRI, J. A. 1990. Influence of the angiotensin system on endothelial and smooth muscle cell migration. *Am J Pathol,* 137**,** 7-12.

BERGMAN, D., HALJE, M., NORDIN, M. & ENGSTROM, W. 2012. Insulin-Like Growth Factor 2 in Development and Disease: A Mini-Review. *Gerontology*.

BERK, B. C. 2003. Angiotensin type 2 receptor (AT2R): a challenging twin. *Sci STKE,* 2003**,** PE16.

BERTERO, T., GASTALDI, C., BOURGET-PONZIO, I., IMBERT, V., LOUBAT, A., SELVA, E., BUSCA, R., MARI, B., HOFMAN, P., BARBRY, P., MENEGUZZI, G., PONZIO, G. & REZZONICO, R. 2011. miR-483-3p controls proliferation in wounded epithelial cells. *FASEB J,* 25**,** 3092-105.

BERTERO, T., GASTALDI, C., BOURGET-PONZIO, I., MARI, B., MENEGUZZI, G., BARBRY, P., PONZIO, G. & REZZONICO, R. 2013. CDC25A targeting by miR-483-3p decreases CCND-CDK4/6 assembly and contributes to cell cycle arrest. *Cell Death Differ*.

BHATNAGAR, A., UNAL, H., JAGANNATHAN, R., KAVETI, S., DUAN, Z. H., YONG, S., VASANJI, A., KINTER, M., DESNOYER, R. & KARNIK, S. S. 2013. Interaction of G-Protein betagamma Complex with Chromatin Modulates GPCR-Dependent Gene Regulation. *PLoS One,* 8**,** e52689.

BHATT, K., MI, Q. S. & DONG, Z. 2011. microRNAs in kidneys: biogenesis, regulation, and pathophysiological roles. *Am J Physiol Renal Physiol,* 300**,** F602-10.

BILLET, S., BARDIN, S., VERP, S., BAUDRIE, V., MICHAUD, A., CONCHON, S., MUFFAT-JOLY, M., ESCOUBET, B., SOUIL, E., HAMARD, G., BERNSTEIN, K. E., GASC, J. M., ELGHOZI, J. L., CORVOL, P. & CLAUSER, E. 2007. Gain-of-function mutant of angiotensin II receptor, type 1A, causes hypertension and cardiovascular fibrosis in mice. *J Clin Invest,* 117**,** 1914-25.

BLUME, A., KASCHINA, E. & UNGER, T. 2001. Angiotensin II type 2 receptors: signalling and pathophysiological role. *Curr Opin Nephrol Hypertens,* 10**,** 239-46.

BOETTGER, T., BEETZ, N., KOSTIN, S., SCHNEIDER, J., KRUGER, M., HEIN, L. & BRAUN, T. 2009. Acquisition of the contractile phenotype by murine arterial smooth muscle cells depends on the Mir143/145 gene cluster. *J Clin Invest,* 119**,** 2634-47.

BOOZ, G. W. & BAKER, K. M. 1996. Role of type 1 and type 2 angiotensin receptors in angiotensin II-induced cardiomyocyte hypertrophy. *Hypertension,* 28**,** 635-40.

BRENNECKE, J., STARK, A., RUSSELL, R. B. & COHEN, S. M. 2005. Principles of microRNA-target recognition. *PLoS Biol,* 3**,** e85.

BRODERICK, J. A. & ZAMORE, P. D. 2011. MicroRNA therapeutics. *Gene Ther,* 18**,** 1104-10.

BRUNNER, A. L., BECK, A. H., EDRIS, B., SWEENEY, R. T., ZHU, S. X., LI, R., MONTGOMERY, K., VARMA, S., GILKS, T., GUO, X., FOLEY, J. W., WITTEN, D. M., GIACOMINI, C. P., FLYNN, R. A., POLLACK, J. R., TIBSHIRANI, R., CHANG, H. Y., VAN DE RIJN, M. & WEST, R. B. 2012. Transcriptional profiling of long non-coding RNAs and novel transcribed regions across a diverse panel of archived human cancers. *Genome Biol,* 13**,** R75.

BUCHAN, J. R. & PARKER, R. 2007. Molecular biology. The two faces of miRNA. *Science,* 318**,** 1877-8.

BURNIER, M. 2001. Angiotensin II type 1 receptor blockers. *Circulation,* 103**,** 904-12.

CHEN, J., LOZACH, J., GARCIA, E. W., BARNES, B., LUO, S., MIKOULITCH, I., ZHOU, L., SCHROTH, G. & FAN, J. B. 2008. Highly sensitive and specific microRNA expression profiling using BeadArray technology. *Nucleic Acids Res,* 36**,** e87.

CHIANG, H. R., SCHOENFELD, L. W., RUBY, J. G., AUYEUNG, V. C., SPIES, N., BAEK, D., JOHNSTON, W. K., RUSS, C., LUO, S., BABIARZ, J. E., BLELLOCH, R.,

SCHROTH, G. P., NUSBAUM, C. & BARTEL, D. P. 2010. Mammalian microRNAs: experimental evaluation of novel and previously annotated genes. *Genes Dev,* 24**,** 992-1009.

DAUGHERTY, A. & CASSIS, L. 2004. Angiotensin II-mediated development of vascular diseases. *Trends Cardiovasc Med,* 14**,** 117-20.

DAVIS, B. N., HILYARD, A. C., NGUYEN, P. H., LAGNA, G. & HATA, A. 2010. Smad proteins bind a conserved RNA sequence to promote microRNA maturation by Drosha. *Mol Cell,* 39**,** 373-84.

DAVIS-DUSENBERY, B. N. & HATA, A. 2011. Smad-mediated miRNA processing: a critical role for a conserved RNA sequence. *RNA Biol,* 8**,** 71-6.

DE GASPARO, M., CATT, K. J., INAGAMI, T., WRIGHT, J. W. & UNGER, T. 2000. International union of pharmacology. XXIII. The angiotensin II receptors. *Pharmacol Rev,* 52**,** 415-72.

DINH, D. T., FRAUMAN, A. G., JOHNSTON, C. I. & FABIANI, M. E. 2001. Angiotensin receptors: distribution, signalling and function. *Clin Sci (Lond),* 100**,** 481-92.

DORN, G. W., 2ND 2011. MicroRNAs in cardiac disease. *Transl Res,* 157**,** 226-35.

DOULTON, T. W., HE, F. J. & MACGREGOR, G. A. 2005. Systematic review of combined angiotensin-converting enzyme inhibition and angiotensin receptor blockade in hypertension. *Hypertension,* 45**,** 880-6.

ELIA, L., QUINTAVALLE, M., ZHANG, J., CONTU, R., COSSU, L., LATRONICO, M. V., PETERSON, K. L., INDOLFI, C., CATALUCCI, D., CHEN, J., COURTNEIDGE, S. A. & CONDORELLI, G. 2009. The knockout of miR-143 and -145

alters smooth muscle cell maintenance and vascular homeostasis in mice: correlates with human disease. *Cell Death Differ,* 16**,** 1590-8.

ELTON, T. S. & MARTIN, M. M. 2007. Angiotensin II type 1 receptor gene regulation: transcriptional and posttranscriptional mechanisms. *Hypertension,* 49**,** 953-61.

ELTON, T. S., SANSOM, S. E. & MARTIN, M. M. 2010. Cardiovascular Disease, Single Nucleotide Polymorphisms; and the Renin Angiotensin System: Is There a MicroRNA Connection? *Int J Hypertens,* 2010.

ELTON, T. S. K., D. E.; MALANA, G. E.; MARTIN, M. M.; NUOVO, G. J.; PLEISTER, A. P.; FELDMAN, D. S. 2008. MiR-132 Regulates Angiotensin II Type 1 Receptor Expressiong Through a Protein Coding Region Binding Site. *Circulation.* 118: S_513.

ESQUELA-KERSCHER, A. & SLACK, F. J. 2006. Oncomirs - microRNAs with a role in cancer. *Nat Rev Cancer,* 6**,** 259-69.

FABIAN, M. R., SONENBERG, N. & FILIPOWICZ, W. 2010. Regulation of mRNA translation and stability by microRNAs. *Annu Rev Biochem,* 79**,** 351-79.

FAZI, F. & NERVI, C. 2008. MicroRNA: basic mechanisms and transcriptional regulatory networks for cell fate determination. *Cardiovasc Res,* 79**,** 553-61.

FERLAND-MCCOLLOUGH, D., FERNANDEZ-TWINN, D. S., CANNELL, I. G., DAVID, H., WARNER, M., VAAG, A. A., BORK-JENSEN, J., BRONS, C., GANT, T. W., WILLIS, A. E., SIDDLE, K., BUSHELL, M. & OZANNE, S. E. 2012. Programming of adipose tissue miR-483-3p and GDF-3 expression by maternal diet in type 2 diabetes. *Cell Death Differ,* 19**,** 1003-12.

FERNANDES, T., HASHIMOTO, N. Y., MAGALHAES, F. C., FERNANDES, F. B., CASARINI, D. E., CARMONA, A. K., KRIEGER, J. E., PHILLIPS, M. I. & OLIVEIRA, E. M. 2011. Aerobic exercise training-induced left ventricular hypertrophy involves regulatory MicroRNAs, decreased angiotensin-converting enzyme-angiotensin ii, and synergistic regulation of angiotensin-converting enzyme 2-angiotensin (1-7). *Hypertension,* 58**,** 182-9.

FICHTLSCHERER, S., DE ROSA, S., FOX, H., SCHWIETZ, T., FISCHER, A., LIEBETRAU, C., WEBER, M., HAMM, C. W., ROXE, T., MULLER-ARDOGAN, M., BONAUER, A., ZEIHER, A. M. & DIMMELER, S. 2010. Circulating microRNAs in patients with coronary artery disease. *Circ Res,* 107**,** 677-84.

FIRE, A., XU, S., MONTGOMERY, M. K., KOSTAS, S. A., DRIVER, S. E. & MELLO, C. C. 1998. Potent and specific genetic interference by double-stranded RNA in Caenorhabditis elegans. *Nature,* 391**,** 806-11.

FORBES, J. M. C., M. E. 2011. The Renin Angiotensin System. *In:* AL., T. M. E. (ed.) *Studies on Renal Disorders, Oxidative Stress in Applied Basic Research and Clinical Practice.* Springer Science.

FRIDDLE, C. J., KOGA, T., RUBIN, E. M. & BRISTOW, J. 2000. Expression profiling reveals distinct sets of genes altered during induction and regression of cardiac hypertrophy. *Proc Natl Acad Sci U S A,* 97**,** 6745-50.

GABBIANI, G., SCHMID, E., WINTER, S., CHAPONNIER, C., DE CKHASTONAY, C., VANDEKERCKHOVE, J., WEBER, K. & FRANKE, W. W. 1981. Vascular smooth muscle cells differ from other smooth muscle cells: predominance of vimentin filaments and a specific alpha-type actin. *Proc Natl Acad Sci U S A,* 78**,** 298-302.

GALLINAT, S., BUSCHE, S., RAIZADA, M. K. & SUMNERS, C. 2000. The angiotensin II type 2 receptor: an enigma with multiple variations. *Am J Physiol Endocrinol Metab,* 278**,** E357-74.

GRIFFITHS-JONES, S., GROCOCK, R. J., VAN DONGEN, S., BATEMAN, A. & ENRIGHT, A. J. 2006. miRBase: microRNA sequences, targets and gene nomenclature. *Nucleic Acids Res,* 34**,** D140-4.

HAO, J., ZHANG, S., ZHOU, Y., HU, X. & SHAO, C. 2011. MicroRNA 483-3p suppresses the expression of DPC4/Smad4 in pancreatic cancer. *FEBS Lett,* 585**,** 207-13.

HARRISON, D. G., CAI, H., LANDMESSER, U. & GRIENDLING, K. K. 2003. Interactions of angiotensin II with NAD(P)H oxidase, oxidant stress and cardiovascular disease. *J Renin Angiotensin Aldosterone Syst,* 4**,** 51-61.

HUNYADY, L. & CATT, K. J. 2006. Pleiotropic AT1 receptor signaling pathways mediating physiological and pathogenic actions of angiotensin II. *Mol Endocrinol,* 20**,** 953-70.

HUTVAGNER, G. & ZAMORE, P. D. 2002. A microRNA in a multiple-turnover RNAi enzyme complex. *Science,* 297**,** 2056-60.

IKEDA, S. & PU, W. T. 2010. Expression and function of microRNAs in heart disease. *Curr Drug Targets,* 11**,** 913-25.

IRANI, K. 2000. Oxidant signaling in vascular cell growth, death, and survival : a review of the roles of reactive oxygen species in smooth muscle and endothelial cell mitogenic and apoptotic signaling. *Circ Res,* 87**,** 179-83.

JEPPESEN, P. L., CHRISTENSEN, G. L., SCHNEIDER, M., NOSSENT, A. Y., JENSEN, H. B., ANDERSEN, D. C., ESKILDSEN, T., GAMMELTOFT, S., HANSEN,

J. L. & SHEIKH, S. P. 2011. Angiotensin II type 1 receptor signalling regulates microRNA differentially in cardiac fibroblasts and myocytes. *Br J Pharmacol,* 164**,** 394-404.

KADLECOVA, M., DOBESOVA, Z., ZICHA, J. & KUNES, J. 2008. Abnormal Igf2 gene in Prague hereditary hypertriglyceridemic rats: its relation to blood pressure and plasma lipids. *Mol Cell Biochem,* 314**,** 37-43.

KARNIK, S. S., GOGONEA, C., PATIL, S., SAAD, Y. & TAKEZAKO, T. 2003. Activation of G-protein-coupled receptors: a common molecular mechanism. *Trends Endocrinol Metab,* 14**,** 431-7.

KERTESZ, M., IOVINO, N., UNNERSTALL, U., GAUL, U. & SEGAL, E. 2007. The role of site accessibility in microRNA target recognition. *Nat Genet,* 39**,** 1278-84.

KIM, S. & IWAO, H. 2000. Molecular and cellular mechanisms of angiotensin II-mediated cardiovascular and renal diseases. *Pharmacol Rev,* 52**,** 11-34.

KIM, Y. K., HEO, I. & KIM, V. N. 2010. Modifications of small RNAs and their associated proteins. *Cell,* 143**,** 703-9.

KOBILKA, B. K. 2007. G protein coupled receptor structure and activation. *Biochim Biophys Acta,* 1768**,** 794-807.

LAGOS-QUINTANA, M., RAUHUT, R., LENDECKEL, W. & TUSCHL, T. 2001. Identification of novel genes coding for small expressed RNAs. *Science,* 294**,** 853-8.

LAGOS-QUINTANA, M., RAUHUT, R., YALCIN, A., MEYER, J., LENDECKEL, W. & TUSCHL, T. 2002. Identification of tissue-specific microRNAs from mouse. *Curr Biol,* 12**,** 735-9.

LANDGRAF, P., RUSU, M., SHERIDAN, R., SEWER, A., IOVINO, N., ARAVIN, A., PFEFFER, S., RICE, A., KAMPHORST, A. O., LANDTHALER, M., LIN, C., SOCCI, N. D., HERMIDA, L., FULCI, V., CHIARETTI, S., FOA, R., SCHLIWKA, J., FUCHS, U., NOVOSEL, A., MULLER, R. U., SCHERMER, B., BISSELS, U., INMAN, J., PHAN, Q., CHIEN, M., WEIR, D. B., CHOKSI, R., DE VITA, G., FREZZETTI, D., TROMPETER, H. I., HORNUNG, V., TENG, G., HARTMANN, G., PALKOVITS, M., DI LAURO, R., WERNET, P., MACINO, G., ROGLER, C. E., NAGLE, J. W., JU, J., PAPAVASILIOU, F. N., BENZING, T., LICHTER, P., TAM, W., BROWNSTEIN, M. J., BOSIO, A., BORKHARDT, A., RUSSO, J. J., SANDER, C., ZAVOLAN, M. & TUSCHL, T. 2007. A mammalian microRNA expression atlas based on small RNA library sequencing. *Cell,* 129**,** 1401-14.

LAU, N. C., LIM, L. P., WEINSTEIN, E. G. & BARTEL, D. P. 2001. An abundant class of tiny RNAs with probable regulatory roles in Caenorhabditis elegans. *Science,* 294**,** 858-62.

LAVOIE, J. L. & SIGMUND, C. D. 2003. Minireview: overview of the renin-angiotensin system--an endocrine and paracrine system. *Endocrinology,* 144**,** 2179-83.

LEE, R. C. & AMBROS, V. 2001. An extensive class of small RNAs in Caenorhabditis elegans. *Science,* 294**,** 862-4.

LEE, R. C., FEINBAUM, R. L. & AMBROS, V. 1993. The C. elegans heterochronic gene lin-4 encodes small RNAs with antisense complementarity to lin-14. *Cell,* 75**,** 843-54.

LEE, S. D., CHU, C. H., HUANG, E. J., LU, M. C., LIU, J. Y., LIU, C. J., HSU, H. H., LIN, J. A., KUO, W. W. & HUANG, C. Y. 2006. Roles of insulin-like growth factor II in

cardiomyoblast apoptosis and in hypertensive rat heart with abdominal aorta ligation. *Am J Physiol Endocrinol Metab,* 291**,** E306-14.

LEMARIE, C. A. & SCHIFFRIN, E. L. 2010. The angiotensin II type 2 receptor in cardiovascular disease. *J Renin Angiotensin Aldosterone Syst,* 11**,** 19-31.

LERMAN, L. O., CHADE, A. R., SICA, V. & NAPOLI, C. 2005. Animal models of hypertension: an overview. *J Lab Clin Med,* 146**,** 160-73.

LEWIS, B. P., BURGE, C. B. & BARTEL, D. P. 2005. Conserved seed pairing, often flanked by adenosines, indicates that thousands of human genes are microRNA targets. *Cell,* 120**,** 15-20.

LI, J. Y., YONG, T. Y., MICHAEL, M. Z. & GLEADLE, J. M. 2010. Review: The role of microRNAs in kidney disease. *Nephrology (Carlton),* 15**,** 599-608.

LIJNEN, P. & PETROV, V. 1999. Renin-angiotensin system, hypertrophy and gene expression in cardiac myocytes. *J Mol Cell Cardiol,* 31**,** 949-70.

LIU, X., SEMPERE, L. F., GUO, Y., KORC, M., KAUPPINEN, S., FREEMANTLE, S. J. & DMITROVSKY, E. 2011. Involvement of microRNAs in lung cancer biology and therapy. *Transl Res,* 157**,** 200-8.

MA, N., LI, F., LI, D., HUI, Y., WANG, X., QIAO, Y., ZHANG, Y., XIANG, Y., ZHOU, J., ZHOU, L., ZHENG, X. & GAO, X. 2012. Igf2-derived intronic miR-483 promotes mouse hepatocellular carcinoma cell proliferation. *Mol Cell Biochem,* 361**,** 337-43.

MAJORS, A. K., SENGUPTA, S., WILLARD, B., KINTER, M. T., PYERITZ, R. E. & JACOBSEN, D. W. 2002. Homocysteine binds to human plasma fibronectin and inhibits its interaction with fibrin. *Arterioscler Thromb Vasc Biol,* 22**,** 1354-9.

MALONE, J. H. & OLIVER, B. 2011. Microarrays, deep sequencing and the true measure of the transcriptome. *BMC Biol,* 9**,** 34.

MARAGKAKIS, M., ALEXIOU, P., PAPADOPOULOS, G. L., RECZKO, M., DALAMAGAS, T., GIANNOPOULOS, G., GOUMAS, G., KOUKIS, E., KOURTIS, K., SIMOSSIS, V. A., SETHUPATHY, P., VERGOULIS, T., KOZIRIS, N., SELLIS, T., TSANAKAS, P. & HATZIGEORGIOU, A. G. 2009. Accurate microRNA target prediction correlates with protein repression levels. *BMC Bioinformatics,* 10**,** 295.

MARGULIES, K. B., BEDNARIK, D. P. & DRIES, D. L. 2009. Genomics, transcriptional profiling, and heart failure. *J Am Coll Cardiol,* 53**,** 1752-9.

MARTIN, M. M., BUCKENBERGER, J. A., JIANG, J., MALANA, G. E., KNOELL, D. L., FELDMAN, D. S. & ELTON, T. S. 2007a. TGF-beta1 stimulates human AT1 receptor expression in lung fibroblasts by cross talk between the Smad, p38 MAPK, JNK, and PI3K signaling pathways. *Am J Physiol Lung Cell Mol Physiol,* 293**,** L790-9.

MARTIN, M. M., BUCKENBERGER, J. A., JIANG, J., MALANA, G. E., NUOVO, G. J., CHOTANI, M., FELDMAN, D. S., SCHMITTGEN, T. D. & ELTON, T. S. 2007b. The human angiotensin II type 1 receptor +1166 A/C polymorphism attenuates microrna-155 binding. *J Biol Chem,* 282**,** 24262-9.

MATSUBARA, H. 1998. Pathophysiological role of angiotensin II type 2 receptor in cardiovascular and renal diseases. *Circ Res,* 83**,** 1182-91.

MEHTA, P. K. & GRIENDLING, K. K. 2007. Angiotensin II cell signaling: physiological and pathological effects in the cardiovascular system. *Am J Physiol Cell Physiol,* 292**,** C82-97.

MISHRA, P. K., TYAGI, N., KUNDU, S. & TYAGI, S. C. 2009. MicroRNAs are involved in homocysteine-induced cardiac remodeling. *Cell Biochem Biophys,* 55**,** 153-62.

MISRA, S., FU, A. A., MISRA, K. D., SHERGILL, U. M., LEOF, E. B. & MUKHOPADHYAY, D. 2010. Hypoxia-induced phenotypic switch of fibroblasts to myofibroblasts through a matrix metalloproteinase 2/tissue inhibitor of metalloproteinase-mediated pathway: implications for venous neointimal hyperplasia in hemodialysis access. *J Vasc Interv Radiol,* 21**,** 896-902.

MIURA, S. & KARNIK, S. S. 1999. Angiotensin II type 1 and type 2 receptors bind angiotensin II through different types of epitope recognition. *J Hypertens,* 17**,** 397-404.

MIURA, S. & KARNIK, S. S. 2000. Ligand-independent signals from angiotensin II type 2 receptor induce apoptosis. *EMBO J,* 19**,** 4026-35.

MIURA, S., KARNIK, S. S. & SAKU, K. 2011. Review: angiotensin II type 1 receptor blockers: class effects versus molecular effects. *J Renin Angiotensin Aldosterone Syst,* 12**,** 1-7.

MIURA, S., MATSUO, Y., KIYA, Y., KARNIK, S. S. & SAKU, K. 2010. Molecular mechanisms of the antagonistic action between AT1 and AT2 receptors. *Biochem Biophys Res Commun,* 391**,** 85-90.

MIURA, S., ZHANG, J., MATSUO, Y., SAKU, K. & KARNIK, S. S. 2004. Activation of extracellular signal-activated kinase by angiotensin II-induced Gq-independent epidermal growth factor receptor transactivation. *Hypertens Res,* 27**,** 765-70.

MORAN, V. A., PERERA, R. J. & KHALIL, A. M. 2012. Emerging functional and mechanistic paradigms of mammalian long non-coding RNAs. *Nucleic Acids Res,* 40**,** 6391-400.

NAGA PRASAD, S. V., DUAN, Z. H., GUPTA, M. K., SURAMPUDI, V. S., VOLINIA, S., CALIN, G. A., LIU, C. G., KOTWAL, A., MORAVEC, C. S., STARLING, R. C., PEREZ, D. M., SEN, S., WU, Q., PLOW, E. F., CROCE, C. M. & KARNIK, S. 2009. Unique microRNA profile in end-stage heart failure indicates alterations in specific cardiovascular signaling networks. *J Biol Chem,* 284**,** 27487-99.

NAGA PRASAD, S. V. & KARNIK, S. S. 2010. MicroRNAs--regulators of signaling networks in dilated cardiomyopathy. *J Cardiovasc Transl Res,* 3**,** 225-34.

NAKASHIMA, H., SUZUKI, H., OHTSU, H., CHAO, J. Y., UTSUNOMIYA, H., FRANK, G. D. & EGUCHI, S. 2006. Angiotensin II regulates vascular and endothelial dysfunction: recent topics of Angiotensin II type-1 receptor signaling in the vasculature. *Curr Vasc Pharmacol,* 4**,** 67-78.

NANA-SINKAM, S. P. & CROCE, C. M. 2011. MicroRNAs as therapeutic targets in cancer. *Transl Res,* 157**,** 216-25.

OHTSU, H., SUZUKI, H., NAKASHIMA, H., DHOBALE, S., FRANK, G. D., MOTLEY, E. D. & EGUCHI, S. 2006. Angiotensin II signal transduction through small GTP-binding proteins: mechanism and significance in vascular smooth muscle cells. *Hypertension,* 48**,** 534-40.

OLIVERIO, M. I., KIM, H. S., ITO, M., LE, T., AUDOLY, L., BEST, C. F., HILLER, S., KLUCKMAN, K., MAEDA, N., SMITHIES, O. & COFFMAN, T. M. 1998. Reduced growth, abnormal kidney structure, and type 2 (AT2) angiotensin receptor-mediated

blood pressure regulation in mice lacking both AT1A and AT1B receptors for angiotensin II. *Proc Natl Acad Sci U S A,* 95**,** 15496-501.

PANDIT, K. V., MILOSEVIC, J. & KAMINSKI, N. 2011. MicroRNAs in idiopathic pulmonary fibrosis. *Transl Res,* 157**,** 191-9.

PARADIS, P. 2000. Overexpression of angiotensin II type I receptor in cardiomyocytes induces cardiac hypertrophy and remodeling. *Proceedings of the National Academy of Sciences,* 97**,** 931-936.

PASQUINELLI, A. E., REINHART, B. J., SLACK, F., MARTINDALE, M. Q., KURODA, M. I., MALLER, B., HAYWARD, D. C., BALL, E. E., DEGNAN, B., MULLER, P., SPRING, J., SRINIVASAN, A., FISHMAN, M., FINNERTY, J., CORBO, J., LEVINE, M., LEAHY, P., DAVIDSON, E. & RUVKUN, G. 2000. Conservation of the sequence and temporal expression of let-7 heterochronic regulatory RNA. *Nature,* 408**,** 86-9.

PAUL, M., POYAN MEHR, A. & KREUTZ, R. 2006. Physiology of local renin-angiotensin systems. *Physiol Rev,* 86**,** 747-803.

PIERCE, K. L., PREMONT, R. T. & LEFKOWITZ, R. J. 2002. Seven-transmembrane receptors. *Nat Rev Mol Cell Biol,* 3**,** 639-50.

PONTREMOLI, R., RAVERA, M., VIAZZI, F., NICOLELLA, C., BERRUTI, V., LEONCINI, G., GIACOPELLI, F., BEZANTE, G. P., SACCHI, G., RAVAZZOLO, R. & DEFERRARI, G. 2000. Genetic polymorphism of the renin-angiotensin system and organ damage in essential hypertension. *Kidney Int,* 57**,** 561-9.

RAMCHANDRAN, R., TAKEZAKO, T., SAAD, Y., STULL, L., FINK, B., YAMADA, H., DIKALOV, S., HARRISON, D. G., MORAVEC, C. & KARNIK, S. S. 2006.

Angiotensinergic stimulation of vascular endothelium in mice causes hypotension, bradycardia, and attenuated angiotensin response. *Proc Natl Acad Sci U S A,* 103**,** 19087-92.

RAYNER, K. J., SUAREZ, Y., DAVALOS, A., PARATHATH, S., FITZGERALD, M. L., TAMEHIRO, N., FISHER, E. A., MOORE, K. J. & FERNANDEZ-HERNANDO, C. 2010. MiR-33 contributes to the regulation of cholesterol homeostasis. *Science,* 328**,** 1570-3.

REINHART, B. J., SLACK, F. J., BASSON, M., PASQUINELLI, A. E., BETTINGER, J. C., ROUGVIE, A. E., HORVITZ, H. R. & RUVKUN, G. 2000. The 21-nucleotide let-7 RNA regulates developmental timing in Caenorhabditis elegans. *Nature,* 403**,** 901-6.

RENSEN, S. S., DOEVENDANS, P. A. & VAN EYS, G. J. 2007. Regulation and characteristics of vascular smooth muscle cell phenotypic diversity. *Neth Heart J,* 15**,** 100-8.

RITTER, J. M. 2011. Dual blockade of the renin-angiotensin system with angiotensin converting enzyme (ACE) inhibitors and angiotensin receptor blockers (ARBs). *Br J Clin Pharmacol,* 71**,** 313-5.

ROMANO, G., ACUNZO, M., GAROFALO, M., DI LEVA, G., CASCIONE, L., ZANCA, C., BOLON, B., CONDORELLI, G. & CROCE, C. M. 2012. MiR-494 is regulated by ERK1/2 and modulates TRAIL-induced apoptosis in non-small-cell lung cancer through BIM down-regulation. *Proc Natl Acad Sci U S A,* 109**,** 16570-5.

ROSENBAUM, D. M., RASMUSSEN, S. G. & KOBILKA, B. K. 2009. The structure and function of G-protein-coupled receptors. *Nature,* 459**,** 356-63.

ROSSI, G. P., SACCHETTO, A., CESARI, M. & PESSINA, A. C. 1999. Interactions between endothelin-1 and the renin-angiotensin-aldosterone system. *Cardiovasc Res,* 43**,** 300-7.

RUIZ-ORTEGA, M., LORENZO, O., RUPEREZ, M., ESTEBAN, V., SUZUKI, Y., MEZZANO, S., PLAZA, J. J. & EGIDO, J. 2001. Role of the renin-angiotensin system in vascular diseases: expanding the field. *Hypertension,* 38**,** 1382-7.

SAITO, Y. & BERK, B. C. 2002. Angiotensin II-mediated signal transduction pathways. *Curr Hypertens Rep,* 4**,** 167-71.

SANSOM, S. E., NUOVO, G. J., MARTIN, M. M., KOTHA, S. R., PARINANDI, N. L. & ELTON, T. S. 2010. miR-802 regulates human angiotensin II type 1 receptor expression in intestinal epithelial C2BBe1 cells. *Am J Physiol Gastrointest Liver Physiol,* 299**,** G632-42.

SANTOS, R. A., SIMOES E SILVA, A. C., MARIC, C., SILVA, D. M., MACHADO, R. P., DE BUHR, I., HERINGER-WALTHER, S., PINHEIRO, S. V., LOPES, M. T., BADER, M., MENDES, E. P., LEMOS, V. S., CAMPAGNOLE-SANTOS, M. J., SCHULTHEISS, H. P., SPETH, R. & WALTHER, T. 2003. Angiotensin-(1-7) is an endogenous ligand for the G protein-coupled receptor Mas. *Proc Natl Acad Sci U S A,* 100**,** 8258-63.

SCALBERT, E. & BRIL, A. 2008. Implication of microRNAs in the cardiovascular system. *Curr Opin Pharmacol,* 8**,** 181-8.

SHUKLA, G. C., SINGH, J. & BARIK, S. 2011. MicroRNAs: Processing, Maturation, Target Recognition and Regulatory Functions. *Mol Cell Pharmacol,* 3**,** 83-92.

SILVERSTEIN, R. L. & RAM, C. V. 2005. Angiotensin-receptor blockers: benefits beyond lowering blood pressure. *Cleve Clin J Med,* 72**,** 825-32.

SMALL, E. M. & OLSON, E. N. 2011. Pervasive roles of microRNAs in cardiovascular biology. *Nature,* 469**,** 336-42.

STAESSEN, J. A., LI, Y. & RICHART, T. 2006. Oral renin inhibitors. *Lancet,* 368**,** 1449-56.

TAUBMAN, M. B. 2003. Angiotensin II: a vasoactive hormone with ever-increasing biological roles. *Circ Res,* 92**,** 9-11.

TEERLINK, J. R. 1996. Neurohumoral mechanisms in heart failure: a central role for the renin-angiotensin system. *J Cardiovasc Pharmacol,* 27 Suppl 2**,** S1-8.

TOUYZ, R. M. & SCHIFFRIN, E. L. 2000. Signal transduction mechanisms mediating the physiological and pathophysiological actions of angiotensin II in vascular smooth muscle cells. *Pharmacol Rev,* 52**,** 639-72.

URBICH, C., KUEHBACHER, A. & DIMMELER, S. 2008. Role of microRNAs in vascular diseases, inflammation, and angiogenesis. *Cardiovasc Res,* 79**,** 581-8.

VAN ROOIJ, E., MARSHALL, W. S. & OLSON, E. N. 2008. Toward microRNA-based therapeutics for heart disease: the sense in antisense. *Circ Res,* 103**,** 919-28.

VAN ROOIJ, E., PURCELL, A. L. & LEVIN, A. A. 2012. Developing microRNA therapeutics. *Circ Res,* 110**,** 496-507.

VASUDEVAN, S., TONG, Y. & STEITZ, J. A. 2007. Switching from repression to activation: microRNAs can up-regulate translation. *Science,* 318**,** 1931-4.

VERDONK, K., DANSER, A. H. & VAN ESCH, J. H. 2012. Angiotensin II type 2 receptor agonists: where should they be applied? *Expert Opin Investig Drugs,* 21**,** 501-13.

VERONESE, A., LUPINI, L., CONSIGLIO, J., VISONE, R., FERRACIN, M., FORNARI, F., ZANESI, N., ALDER, H., D'ELIA, G., GRAMANTIERI, L., BOLONDI, L., LANZA, G., QUERZOLI, P., ANGIONI, A., CROCE, C. M. & NEGRINI, M. 2010. Oncogenic role of miR-483-3p at the IGF2/483 locus. *Cancer Res,* 70**,** 3140-9.

VERONESE, A., VISONE, R., CONSIGLIO, J., ACUNZO, M., LUPINI, L., KIM, T., FERRACIN, M., LOVAT, F., MIOTTO, E., BALATTI, V., D'ABUNDO, L., GRAMANTIERI, L., BOLONDI, L., PEKARSKY, Y., PERROTTI, D., NEGRINI, M. & CROCE, C. M. 2011. Mutated beta-catenin evades a microRNA-dependent regulatory loop. *Proc Natl Acad Sci U S A,* 108**,** 4840-5.

WANG, W. C., JUAN, A. H., PANEBRA, A. & LIGGETT, S. B. 2011. MicroRNA let-7 establishes expression of beta2-adrenergic receptors and dynamically down-regulates agonist-promoted down-regulation. *Proc Natl Acad Sci U S A,* 108**,** 6246-51.

WHITE, S. M., CONSTANTIN, P. E. & CLAYCOMB, W. C. 2004. Cardiac physiology at the cellular level: use of cultured HL-1 cardiomyocytes for studies of cardiac muscle cell structure and function. *Am J Physiol Heart Circ Physiol,* 286**,** H823-9.

WINTER, J., JUNG, S., KELLER, S., GREGORY, R. I. & DIEDERICHS, S. 2009. Many roads to maturity: microRNA biogenesis pathways and their regulation. *Nat Cell Biol,* 11**,** 228-34.

YAN, B. & WANG, Z. 2012. Long noncoding RNA: its physiological and pathological roles. *DNA Cell Biol,* 31 Suppl 1**,** S34-41.

YIN, G., YAN, C. & BERK, B. C. 2003. Angiotensin II signaling pathways mediated by tyrosine kinases. *Int J Biochem Cell Biol,* 35**,** 780-3.

YU, J., WANG, F., YANG, G. H., WANG, F. L., MA, Y. N., DU, Z. W. & ZHANG, J. W. 2006. Human microRNA clusters: genomic organization and expression profile in leukemia cell lines. *Biochem Biophys Res Commun,* 349**,** 59-68.

YUE, H., LI, W., DESNOYER, R. & KARNIK, S. S. 2010. Role of nuclear unphosphorylated STAT3 in angiotensin II type 1 receptor-induced cardiac hypertrophy. *Cardiovasc Res,* 85**,** 90-9.

ZAINA, S., PETTERSSON, L., THOMSEN, A. B., CHAI, C. M., QI, Z., THYBERG, J. & NILSSON, J. 2003. Shortened life span, bradycardia, and hypotension in mice with targeted expression of an Igf2 transgene in smooth muscle cells. *Endocrinology,* 144**,** 2695-703.

ZHANG, F., HU, Y., XU, Q. & YE, S. 2010. Different effects of angiotensin II and angiotensin-(1-7) on vascular smooth muscle cell proliferation and migration. *PLoS One,* 5**,** e12323.

ZHANG, X., AZHAR, G. & WEI, J. Y. 2012. The expression of microRNA and microRNA clusters in the aging heart. *PLoS One,* 7**,** e34688.